Dissertation

submitted to the
Combined Faculties for the Natural Sciences and for Mathematics
of the Ruperto-Carola University of Heidelberg, Germany
for the degree of
Doctor of Natural Sciences

presented by

Master of Science Hannah Katarina Schneider

born in Tübingen, Germany
Oral-examination:……

Quantitative analysis of proteins facilitating fatty acid uptake: CD36, Caveolin-1, FATP4 and ACSL1

Referees: Prof. Dr. Gert Fricker

Prof. Dr. Robert Ehehalt

To My Mother

We pushed on, impelled by our burning curiosity. What other marvels did this cavern contain? What new treasures lay here for science to unfold? I was prepared for any surprise, my imagination was ready for any astonishment however astounding.

Jules Verne – A journey to the center of the earth

Table of Contents

LIST OF ABBREVIATIONS VI

LIST OF UNITS VIII

1. SUMMARY 1

2. ZUSAMMENFASSUNG 3

3. INTRODUCTION 5

3.1 Fatty acid metabolism 5

3.1.1 Properties and functions of fatty acids 5

3.1.2 Cellular fatty acid uptake 6

3.2 Fatty acid translocase CD36 9

3.2.1 Structur and function of CD36 9

3.2.2 Role of caveolin-1 in CD36 signaling 11

3.3 Fatty acid activating enzymes 12

3.3.1 The acyl-CoA synthetase family 12

3.3.2 The catalyzed reaction 13

3.3.3 Fatty acid transport protein 4 (FATP4) 14

3.3.4 Long-chain acyl-CoA synthetase 1 (ACSL1) 15

3.4 Aim of study 17

4. MATERIAL AND METHODS 19

4.1 Equipment 19

4.1.1 Molecular biology equipment 19

4.1.2 Protein biochemistry equipment 20

4.1.3 Radioactive work equipment 20

4.1.4 Cell culture equipment 20

4.2 Chemicals 21

4.2.1 Molecular biology chemicals 21
4.2.2 Protein biochemistry chemicals 21
4.2.3 Radioactive work chemicals 21
4.2.4 Cell culture chemicals 22

4.3 Kits 22

4.4 Molecular biology material 23

4.4.1 Molecular weight standards 23
4.4.2 Antibodies 23
4.4.3 Enzymes 24
4.4.4 Oligonucleotides 24
4.4.5 Plasmids 25

4.5 Buffers and media 26

4.5.1 Media 26
4.5.2 Buffers 27

4.6 Cells, viruses, bacteria 28

4.6.1 Cells 28
4.6.2 Viruses 29
4.6.3 Bacteria 30

4.7 Software 30

4.8 Molecular biology techniques 31

4.8.1 Preparation of chemically competent *E. coli* 31
4.8.2 Heat shock transformation of *E. coli* 31
4.8.3 Electroporation of *E. coli* 32
4.8.4 Small and large scale preparation of plasmid DNA 32
4.8.5 Measurement of nucleic acid concentrations 34
4.8.6 Agarose gel electrophoresis 34
4.8.7 Polymerase chain reaction (PCR) 34
4.8.8 Restriction digest 35

4.8.9 Purification of DNA 35
4.8.10 Ligation 36
4.8.11 Cloning of adenoviral plasmids 37

4.9 Biochemistry techniques 39

4.9.1 Bradford protein assay 39
4.9.2 Sodium dodecyl sulfate polyacrylamide gel electrophoresis (SDS-PAGE) 39
4.9.3 Western blotting 41
4.9.4 SDS-PAGE analysis with ImageJ 42
4.9.5 Coomassie blue protein staining 43
4.9.6 Protein purification 43
4.9.7 Establishment of a $FATP4_{FLAG}$ protein standard 44
4.9.8 Protein quantification by western blotting 45
4.9.9 Radioactive oleate uptake assays 46

4.10 Cell culture techniques 48

4.10.1 Culture of immortalized cell lines 48
4.10.2 Freezing and thawing of cells 49
4.10.3 Counting cells 49
4.10.4 Production of cell pellets 50
4.10.5 Transient transfection of cells by lipofection 50
4.10.6 Generation of retroviruses 51
4.10.7 Production of stable cell lines by retroviral infection 52
4.10.8 Generation of adenoviruses 53
4.10.9 Infection of cells with adenovirus 55
4.10.10 Immunofluorescence 56

4.11 Statistical analysis 57

5. RESULTS 58

5.1 Generation of stable MDCK cell lines 58

5.1.1 ACSL1 overexpression in MDCK cells is achieved by retroviral infection 58

5.1.2 Cav-1 knock down diminishes protein expression levels by more than 80 % 59

5.2 CD36 overexpression increases oleate uptake 60

5.2.1 CD36 mediated oleate uptake is similarly enhanced independent from free oleate concentrations 60

5.2.2 CD36 overexpression increases oleate uptake over a range of different oleate concentrations 61

5.3 Quantification of CD36, FATP4 and ACSL1 protein amounts in correlation to oleate uptake 62

5.3.1 Preparation of recombinant $FATP4_{FLAG}$ protein standard 62

5.3.2 Oleate uptake is significantly enhanced by FATP4 overexpression and correlates with FATP4 protein quantities 63

5.3.3 Oleate uptake increases in correlation to the amount of overexpressed CD36 protein 64

5.3.4 At comparable protein expression levels CD36 increases oleate uptake more than FATP4 66

5.3.5 CD36 is expressed at significantly lower quantities than FATP4 but increases oleate uptake more than FATP4 when normalized to protein amounts 67

5.3.6 Co-expression of CD36 and FATP4 has a synergistic effect on oleate uptake 69

5.3.7 Simultaneous overexpression of ACSL1 and CD36 significantly increases oleate uptake in comparison to single protein overexpression 71

5.3.8 ACSL1 and FATP4 mediated increases in fatty acid uptake are not additive 72

5.3.9 Knock down of Cav-1 has no effect on oleate uptake independent from CD36 expression 74

5.3.10 Overexpression of CD36 and FATP4 increases short term oleate uptake in correlation to protein amounts 77

5.4 Analysis of CD36, FATP4 and ACSL1 localization by immunofluorescence microscopy 79

5.4.1 CD36 is expressed at the plasma membrane and intracellularly 79

5.4.2 FATP4 is located at the endoplasmic reticulum 80

5.4.3 Co-expression of CD36 and FATP4 does not change either protein localization 80

5.4.4 ACSL1 is expressed on mitochondria and does not alter the localization of CD36 or FATP4 81

5.4.5 Cav-1 knock down does not change CD36 localization 82

6. DISCUSSION 84

6.1 FATP4 overexpression increases fatty acid uptake more than CD36 overexpression – due to higher expression levels 84

6.2 Cav-1 does not influence CD36 mediated fatty acid uptake 86

6.3 CD36 and FATP4 are differentially localized and enhance fatty acid uptake by distinct mechanisms 88

6.4 Transport and metabolic trapping act synergistically to increase fatty acid uptake 90

6.5 Conclusion 91

6.6 Suggestion of a model for facilitated fatty acid uptake involving CD36, FATP4 and ACSL1 93

7. REFERENCES 95

8. APPENDIX 100

8.1 List of Figures 100

8.2 List of Tables 102

8.3 Publication and Oral Presentations 103

9. AFFIRMATION 104

10. ACKNOWLEDGEMENTS 105

List of Abbreviations

α	anti
a_	antisense
ACS	acyl-CoA synthetase
ACSL	long-chain acyl-CoA synthetase
ACSL1	long-chain acyl-CoA synthetase 1
AMP	adenosine monophosphate
APS	ammonium persulfate
ATP	adenosine triphosphate
bp	base pair
BSA	bovine serum albumin
Cav-1	caveolin-1
cDNA	complementary DNA
CoA	coenzyme A
DMEM	Dulbecco's modified Eagle's medium
DMSO	dimethyl sulfoxide
DNA	deoxyribonucleic acid
dNTP	deoxyribonucleoside triphosphate
dpi	dots per inch
dsRNA	doublestranded RNA
E_{260}	extinction at 260 nm
E. coli	*Escherichia coli*
ECL	enhanced chemiluminescence
EDTA	ethylenediaminetetraacetic acid
ER	endoplasmic reticulum
$FABP_{(PM)}$	(plasma membrane) fatty acid binding protein
FAT/CD36	fatty acid translocase/cluster of differentiation 36
FATP	fatty acid transport protein
FATP4	fatty acid transport protein 4
FBS	fetal bovine serum
GFP	green fluorescent protein
HBS	HEPES buffered saline
HEK	human embryonic kidney
HEPES	4-(2-hydroxyethyl)-1-piperazineethanesulfonic acid
HRP	horseradish peroxidase
IF	immunofluorescence
IgG	immunoglobulin G
ITB	Inoue Transformation Buffer
kb	kilobase(s)
LB	Luria Bertani
MDCK	Madin-Darby canine kidney
MEM	Eagle's minimum essential medium
MMLV	Moloney Murine Leukemia Virus
ms	mouse
NAFLD	non-alcoholic fatty liver disease
NASH	non-alcoholic steatohepatitis
OD	optical density

OD_{600}	optical density measured at a wavelength of 600 nm
PAGE	polyacrylamide gel electrophoresis
PBS	phosphate buffered saline
PCR	polymerase chain reaction
PIPES	piperazine-N,N′-bis(2-ethanesulfonic acid)
PFA	paraformaldehyde
rb	rabbit
RNA	ribonucleic acid
RNAi	RNA interference
rpm	rounds per minute
RT	room temperature
s_	sense
SD	standard deviation
SDS	sodium dodecyl sulfate
SG	saponin gelatine washing solution
SGB	saponin gelatine BSA washing/blocking solution
SSO	sulfo-*N*-succinimidyl oleate
TAE	Tris acetate EDTA
taq	*thermus aquaticus*
TBS	Tris buffered saline
TEMED	N,N,N',N'-tetramethylethylenediamine
Tm	melting temperature
TNE	Tris NaCl EDTA buffer
TNEX	Tris NaCl EDTA Triton X buffer
Tris	tris(hydroxymethyl)aminomethane
U	unit
UV	ultraviolet
VSV-G	glycoprotein G of the Vesicular stomatitis virus
WB	western blot

List of Units

time units	
s	second
min	minute
h	hour

physical/chemical units	
A	ampere
°C	degree Celcius
Ci	curie
Da	dalton
F	farad
g	gram
g	unit of gravity
l	litre
M	molar
N	normal
Ω	ohm
V	volt
W	watt

dimensions	
k	kilo
m	milli
µ	micro
n	nano
p	pico

1. Summary

Fatty acids are essential for the cellular metabolism but their uptake has to be tightly regulated to prevent fatty acid associated diseases. Proteins that facilitate fatty acid uptake include CD36, FATP4, ACSL1 and Caveolin-1. CD36, FATP4 and ACSL1 increase oleate uptake upon overexpression. CD36 is an integral transmembrane glycoprotein that directly facilitates fatty acid uptake across the plasma membrane. The structural protein Caveolin-1 binds fatty acids and is discussed as potential interaction partner for CD36. The acyl-CoA synthetases FATP4 and ACSL1 are localized intracellularly and activate fatty acids by esterification with coenzyme A, thus driving fatty acid uptake indirectly by metabolic trapping.

This study was designed to 1) quantify absolute protein amounts of CD36, FATP4 and ACSL1 proteins in overexpressing cell lines and calculate protein specific oleate uptake 2) test CD36, FATP4, ACSL1 and Caveolin-1 for cooperativity in facilitating fatty acid uptake.

MDCK cells were chosen as an unspecialized and unbiased model system and overexpressing cells were generated by retroviral and adenoviral infection. Infection of MDCK cells with increasing amounts of CD36 or FATP4 adenovirus resulted in enhanced fatty acid uptake as measured by incubation with radiolabeled oleic acid for three hours. Protein amounts of CD36 and FATP4 were analyzed by western blotting and absolute protein quantities were calculated by correlation to a recombinant protein standard. Increases in fatty acid uptake correlated to rising protein amounts of CD36 and FATP4 in accordance with rising adenovirus quantities used for infection.

Comparison of CD36 and FATP4 expression showed a significant difference in protein quantities whereas the difference in oleate uptake was much smaller: 13 ng CD36 protein increased oleate uptake by 20 % whereas 701 ng FATP4 protein resulted in 37 % enhancement. When CD36 and FATP4 were expressed at equal quantities, oleate uptake was still enhanced more by 10 ng CD36 protein as by 10 ng FATP4 protein (27 % versus 4 %, respectively), indicating that CD36 is more efficient in increasing fatty acid uptake than FATP4. The function of CD36 in fatty acid transport of MDCK cells was independent from Caveolin-1, as an 80 % knock down of Caveolin-1 did not alter CD36 dependent oleate uptake.

Immunofluorescence analysis confirmed the localization of CD36 to the plasma membrane whereas FATP4 localized to the endoplasmic reticulum and ACSL1 was expressed at mitochondria. Co-expression of CD36 and FATP4 enhanced oleate uptake significantly more than calculated from single protein overexpression, resulting in an increase by 49 pmol oleate/µg total protein for co-expressing cells as compared to 10 pmol oleate/µg total protein for CD36 and 21 pmol oleate/µg total protein for FATP4 overexpressing cells. Oleate uptake was similarly increased in CD36 and ACSL1 co-expressing cells whereas FATP4 and ACSL1 together enhanced fatty acid uptake less than calculated from single protein overexpression: oleate uptake was increased by 30 pmol oleate/µg total protein in co-expressing cells as compared to 26 pmol oleate/µg total protein in FATP4 and 15 pmol oleate/µg total protein in ACSL1 cells.

In conclusion, CD36, FATP1 and ACSL1 enhance fatty acid uptake by two different mechanisms: CD36 directly facilitates fatty acid transport across the plasma membrane whereas FATP4 and ACSL1 indirectly mediate fatty acid uptake by metabolic trapping of intracellular fatty acids. CD36 is expressed at significantly lower protein amounts than FATP4 but increases fatty acid uptake more than FATP4 when expressed at similar quantities. The two acyl-CoA synthetases FATP4 and ACSL1 target similar metabolic processes and therefore show no cooperativity in fatty acid uptake. As both enzyme act intracellularly, their impact on fatty acid uptake is limited by the transport rate of fatty acids across the plasma membrane. CD36 cooperates with FATP4 and ACSL1 in enhancing oleate uptake, probably due to an efficient combination of facilitated fatty acid transport across the plasma membrane by CD36 followed by immediate intracellular fatty acid activation by FATP4 and ACSL1.

2. Zusammenfassung

Fettsäuren sind essentiell für den zellulären Stoffwechsel jedoch muss ihre Aufnahme streng reguliert werden, um Erkrankungen zu vermeiden. Die Aufnahme von Fettsäuren in Zellen wird durch Proteine wie CD36, FATP4, ACSL1 und Caveolin-1 vermittelt, von denen CD36, FATP4 und ACSL1 die Fettsäureaufnahme nach Proteinüberexpression steigern. CD36 ist ein glykosyliertes Transmembranprotein, welches direkt die Aufnahme von Fettsäuren über die Plasmamembran fördert. Als potentieller Interaktionspartner für CD36 wird das Strukturprotein Caveolin-1 diskutiert, welches Fettsäuren bindet. Die Acyl-CoA-Synthetasen FATP4 und ACSL1 sind intrazellulär lokalisiert und aktivieren Fettsäuren durch Veresterung mit Coenzym A, wodurch die Fettsäureaufnahme indirekt durch *metabolic trapping* gesteigert wird.

Ziele dieser Arbeit waren 1) die Quantifizierung absoluter Proteinmengen von CD36, FATP4 und ACSL1 in überexprimierenden Zelllinien und die Berechnung der Protein-spezifischen Oleataufnahme 2) die Untersuchung von CD36, FATP4, ACSL1 und Caveolin-1 auf Kooperativität bei der Vermittlung der Fettsäureaufnahme.

Als Modelsystem wurden MDCK Zellen gewählt und überexprimierende Zellen durch retrovirale und adenovirale Infektion generiert. Die Infektion von MDCK Zellen mit steigenden Mengen von CD36 und FATP4 Adenovirus resultierte nach Inkubation mit radioaktiv markierter Ölsäure über drei Stunden in einer gesteigerten Fettsäureaufnahme. Die Proteinmengen von CD36 und FATP4 wurden mittels Western Blot analysiert und absolute Proteinmengen durch Korrelation mit einem rekombinanten Proteinstandard berechnet. Der Anstieg der Fettsäureaufnahme korrelierte mit den zunehmenden Proteinmengen von CD36 und FATP4 in Übereinstimmung mit den für die Infektion genutzten ansteigenden Adenovirusmengen.

Ein Vergleich der Proteinexpression von CD36 und FATP4 ergab eine signifikante Differenz der Proteinmengen wohingegen die Unterschiede in der Oleataufnahme deutlich geringer waren: 13 ng CD36 Protein erhöhten die Oleataufnahme um 20 % wohingegen 701 ng FATP4 Protein in einer Steigerung der Oleataufnahme um 37 % resultierten. Bei der Expression gleicher Mengen von CD36 und FATP4 Protein wurde die Oleataufnahme durch 10 ng CD36 Protein mehr gesteigert als durch 10 ng

FATP4 Protein (27 % im Vergleich zu 4 %). Dies deutet darauf hin, dass CD36 die Fettsäureaufnahme effizienter erhöht als FATP4. Die Funktion von CD36 im Fettsäuretransport von MDCK Zellen war unabhängig von Caveolin-1, da ein 80 %iger *knock down* des Caveolin-1 Proteins die CD36 vermittelte Oleataufnahme nicht beeinflusste.

Durch Immunfluoreszenzanalyse wurde die Lokalisation von CD36 an der Plasmamembran bestätigt wohingegen FATP4 auf dem Endoplasmatischen Retikulum und ACSL1 auf den Mitochondrien exprimiert wurden. Die Koexpression von CD36 und FATP4 steigerte die Oleataufnahme signifikant mehr als basierend auf der Überexpression der einzelnen Proteine berechnet und resultierte in einem Anstieg um 49 pmol Oleat/µg Gesamtprotein für koexprimierende Zellen verglichen mit einer Steigerung um 10 pmol Oleat/µg Gesamtprotein für CD36 und 21 pmol Oleat/µg Gesamtprotein für FATP4 überexprimierende Zellen. Die Oleataufnahme war in ähnlicher Weise in CD36 und ACSL1 koexprimierenden Zellen erhöht. Die gemeinsame Expression von FATP4 und ACSL1 hingegen steigerte die Fettsäureaufnahme weniger als ausgehend von der Überexpression der einzelnen Proteine berechnet, sodass in koexprimierenden Zellen die Oleataufnahme um 30 pmol Oleat/µg Gesamtprotein erhöht wurde verglichen mit einem Anstieg um 26 pmol Oleat/µg Gesamtprotein in FATP4 und 15 pmol Oleat/µg Gesamtprotein in ACSL1 überexprimierenden Zellen.

Es lässt sich schlussfolgern, dass CD36, FATP4 und ACSL1 die Fettsäureaufnahme durch zwei verschiedene Mechanismen steigern: CD36 vermittelt direkt den Fettsäuretransport über die Plasmamembran während FATP4 und ACSL1 die Fettsäureaufnahme indirekt durch *metabolic trapping* intrazellulärer Fettsäuren beeinflussen. CD36 wird in signifikant geringeren Proteinmengen exprimiert als FATP4 aber steigert die Fettsäureaufnahme mehr als FATP4 bei vergleichbarer Proteinexpression. Die beiden Acyl-CoA-Synthetasen FATP4 und ACSL1 wirken auf ähnliche metabolische Prozesse. Da beide Enzyme intrazellulär agieren, ist ihr Einfluss auf die Fettsäureaufnahme durch die Transportrate von Fettsäuren über die Plasmamembran limitiert, so dass sie keine Kooperativität in der Fettsäureaufnahme zeigen. CD36 kooperiert mit FATP4 und ACSL1 in der Erhöhung der Fettsäureaufnahme, vermutlich aufgrund einer effizienten Kombination von erleichterter Fettsäureaufnahme über die Plasmamembran durch CD36 gefolgt von einer unmittelbaren intrazellulären Aktivierung der Fettsäuren durch FATP4 und ACSL1.

3. Introduction

3.1 Fatty acid metabolism

3.1.1 Properties and functions of fatty acids

Lipids are essential for life. Together with proteins and carbohydrates they make up the most important components of mammalian nutrition, thus enabling and sustaining animal and human life. The term lipid describes various subgroups of hydrophobic or amphiphilic molecules which are important for energy supply, needed as building blocks for cellular membranes and play a role in intracellular signaling.

The hydrophobic properties of many lipids are caused by fatty acids. All fatty acids are composed of a hydrocarbon chain coupled to a carboxylic acid group at one end. Although fatty acids vary in chain length and degree of saturation, most naturally occurring fatty acids have an even number of carbon atoms, including long-chain and very long-chain fatty acids with 14 – 24 carbon atoms. Short chain fatty acids play a role especially in the intestine where they may modulate colonic health (Wong *et al.*, 2006). The hydrocarbon chains of fatty acids are typically unbranched and can include one or more double bonds, usually in *cis* conformation. In polyunsaturated fatty acids double bonds are set apart by at least one methylen group. Most commonly occurring are the saturated fatty acids palmitic acid (16:0) and stearic acid (18:0) as well as their unsaturated counterparts palmitoleic acid (16:1) and oleic acid (18:1) (Berg JM, 2003). Some fatty acids cannot be synthesized by the human organism itself and must be taken up by nutrition. These essential fatty acids are linoleic (18:2) and linolenic (18:3) acid.

The tasks performed by fatty acids are diverse and range from energy supply over cellular signaling and posttranslational modification to membrane synthesis. Lipid droplets serve as intracellular, specialized storage organelles: a neutral lipid core, mainly consisting of triglycerides and cholesterol esters, is surrounded by a phospholipid monolayer covered with perilipin family proteins. If energy is required, e.g. during physical exercise, triglycerides are split into glycerol and free fatty acids which are released in the bloodstream and transported to the peripheral target tissues (Ducharme and Bickel, 2008). Fatty acids are also involved in regulating cellullar processes by functioning as signaling molecules, such as eicosanoids (reviewed by (Funk, 2001)). The eicosanoids include three different subgroups, prostaglandins,

leukotrienes and thromboxanes that are mostly derived from one common precursor molecule, the arachidonic acid. Eicosanoids have an influence on various processes, including inflammation, antilipolytic activity and platelet aggregation. One of the most prominent features of fatty acids is their contribution to the construction of cellular membranes. Lipid membranes are essential for cell viability and enable the establishment of separate functional units within a cell or between different cells. Glycerophospholipids like phosphatidylcholine, phosphatidylethanolamine, phosphatidylserine, phosphatidylinositol and phosphatidic acid are the major components of cell membranes, with phosphatidylcholine contributing to over 50 % to eukaryotic membrane phospholipids. Cholesterol is the predominant sterol of mammalian membranes and together with phosphatiylcholine has a strong impact on membrane fluidity. Sphingolipids with saturated or unsaturated fatty acid side chains make up the third group of membrane lipids (reviewed by (van Meer *et al.*, 2008)).
Imbalances in fatty acid metabolism can have severe consequences. An excess of fatty acids may result in accumulation of triacylglycerol in various organs, such as liver, heart, muscle and pancreas. In consequence, normal cellular functions are disturbed, resulting in apoptosis and impaired insulin signaling, caused by lipotoxicity (reviewed by (Li *et al.*, 2010)). Furthermore, irregulations in lipid homeostasis were linked to the onset and progression of non-alcoholic fatty liver disease (NAFLD) and non-alcoholic steatohepatitis (NASH). Elevated serum amounts of free fatty acids have been identified in liver biopsies from obese NASH patients (Bechmann *et al.*, 2010), correlating excess fatty acids with a pathological inflammation of the liver. Starting with an obese condition, excess in fatty acids may also contribute to the development of the metabolic syndrome, type 2 diabetes, artherosclerosis and cardiovascular disease, thus emphasizing the importance of careful regulation of lipid metabolism.

3.1.2 Cellular fatty acid uptake

The uptake of fatty acids is a general process found in many cell types. Fatty acids are bound to albumin and transported in the blood to their target tissues. In order to be further utilized, fatty acids dissociate from their carrier protein and are taken up into the cells. Intracellular fatty acids are then activated by esterification with coenzyme A (CoA) and submitted to further downstream metabolism. Two different

mechanism are considered for cellular fatty acid uptake: 1) passive diffusion 2) protein mediated uptake (Abumrad *et al.*, 1998; Hamilton *et al.*, 2002). At a high fatty acid to albumin ratio passive diffusion is described to be the predominant mechanism whereas at low fatty acid to albumin ratios a facilitated and saturable uptake by specialized proteins is suggested (reviewed by (Abumrad *et al.*, 1999)).

Different models and candidate proteins have been discussed in the context of cellular fatty acid uptake so far. Black and DiRusso argued for vectorial acylation, linking the fatty acid transport across the plasma membrane to intracellular fatty acid activation. Thereby, fatty acids would be trapped inside the cells, thus rendering the uptake process unidirectional (Black and DiRusso, 2003). For vectorial acylation, a functional and spatial coupling at the plasma membrane of a fatty acid transporter with a fatty acid activating enzyme is suggested (Zou *et al.*, 2003; Kampf and Kleinfeld, 2007) whereas another model argues for metabolic trapping of fatty acids at intracellular organelles rather than at the plasma membrane. Within this model, intracellular acyl-CoA synthetases would be sufficient to drive fatty acid uptake metabolically: fatty acid activation would imbalance the equilibrium of intracellular and extracellular free fatty acids and result in a driving force for fatty acid uptake (Fullekrug *et al.*, 2012).

There are three likely candidates for protein mediated cellular fatty acid uptake: fatty acid translocase (FAT)/cluster of differentiation 36 (CD36), the family of fatty acid transport proteins (FATPs) as well as plasma membrane fatty acid binding protein ($FABP_{PM}$). CD36, an integral transmembrane protein, is highly expressed in adipose tissue, heart, skeletal muscle and intestine (reviewed by (Abumrad *et al.*, 1999)). Alterations in fatty acid metabolism influence CD36 expression, corresponding to a suggested function in fatty acid uptake. Caveolin-1 (Cav-1), a structural protein, has been proposed as possible interaction partner for CD36 in mediating fatty acid uptake. A whole family of conserved proteins, the FATPs, are equally considered as mediators of fatty acid uptake. Two different functions have been proposed for FATPs (reviewed by (Gimeno, 2007)), implying that they possess an acyl-CoA synthetase activity: direct transport of fatty acids across the cell membrane versus intracellular esterification of fatty acids. FABPs bind long-chain fatty acids and are suggested to have tissue-specific functions. For plasma membrane fatty acid binding protein ($FABP_{pm}$) various evidence has been obtained for a potential involvement in fatty acid metabolism. Changes in fatty acid transport conditions were accompanied

by alterations in $FABP_{pm}$ expression levels, including the differentiation of 3T3-L1 fibroblasts into adipocytes which went along with a rise in fatty acid uptake as well as an induction of $FABP_{pm}$ (reviewed by (Brinkmann *et al.*, 2002)). An antibody directed against $FABP_{PM}$ inhibited oleate uptake in the hepatocytes (Stremmel *et al.*, 1986), indicating a role for $FABP_{PM}$ in liver fatty acid uptake.

A potential interplay of plasma membrane proteins and intracellular proteins has been suggested, thus making fatty acid uptake a highly coordinated, multistep process. A possible model would implicate the mediation of fatty acid uptake by CD36, maybe in interaction with Cav-1. Fatty acids could then be transported by FABPs to various organelles for activation by intracellular proteins such as FATP4 and long-chain acyl-CoA synthetase 1 (ACSL1) (Figure 1).

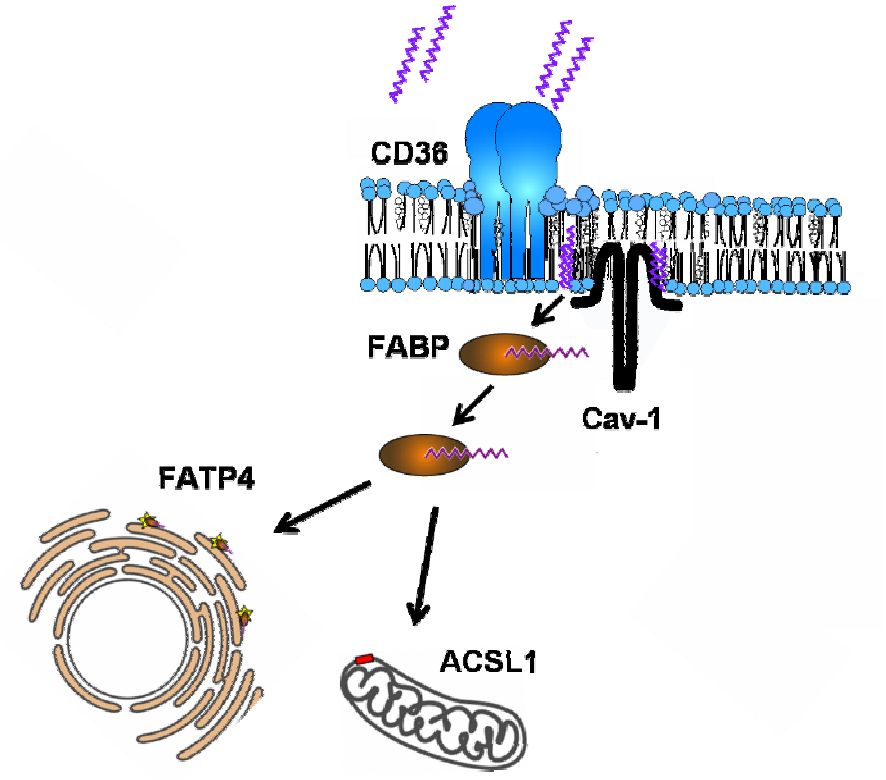

Figure 1: Model of fatty acid uptake.
CD36 is localized in the plasma membrane where it mediates the uptake of extracellular fatty acids into the cell, possibly in cooperation with Cav-1. FABPs transport the fatty acids to intracellular organelles like the ER or mitochondria, followed by fatty acid activation by intracellular enzyme such as FATP4 and ACSL1 (adapted from (Ehehalt *et al.*, 2006).

3.2 Fatty acid translocase CD36

3.2.1 Structur and function of CD36

The fatty acid translocase (FAT) or cluster of differentiation 36 (CD36), is an integral transmembrane glycoprotein with a molecular weight of 88 kDa. The protein is expressed on a variety of different cell types, including adipocytes, hepatocytes, myocytes, platelets, mononuclear phagocytes and some epithelia (reviewed by (Silverstein and Febbraio, 2009)). In line with its extensive expression pattern, CD36 has been described to contain multiple functions within the mammalian organism, ranging from its action as a pattern recognition receptor over taste perception for fat and involvement in inflammatory responses to the uptake of long-chain fatty acids. CD36 represents a gene family together with two other proteins, lysosomal integral membrane protein-2 (LIMP-2) as well as CD36 and LIMP-2 analogous (CLA-1), equally named scavenger receptor B-1 (SRB-1). Orthologs of CD36 were identified in insects, nematodes, sponges and slime mold, thereby indicating that the common ancestral gene dates back more than 300 million years.

The protein structure is conserved in mammals and characterized by a prominent extracellular domain ending in two short cytoplasmic tails. The extracellular loop is heavily glycosylated and features three disulfide bonds at conserved cysteines (Cys243- Cys311, Cys272-Cys333, and Cys313-Cys322) together with at least two ligand binding domains, one for proteins with thrombospondin repeat (TSR) domain and one for oxidized lipids. The C- and the N-terminal part are located intracellularly and contain two palmitoylated cysteine residues each (reviewed by (Silverstein and Febbraio, 2009), Figure 2). The C-terminal part of CD36 was shown to be required for proper localization at the cell surface, as a truncation of the final 10 amino acids caused intracellular retention of the protein (Eyre *et al.*, 2007). Furthermore, inhibition of cysteine palmitoylation interfered with CD36 processing at the endoplasmic reticulum as well as with trafficking through secretory pathways, indicating a regulatory function for palmitoylation in the translocation of CD36 to the plasma membrane (Thorne *et al.*, 2010). Although CD36 has been investigated for decades, only little light has been shed on its intracellular signaling so far.

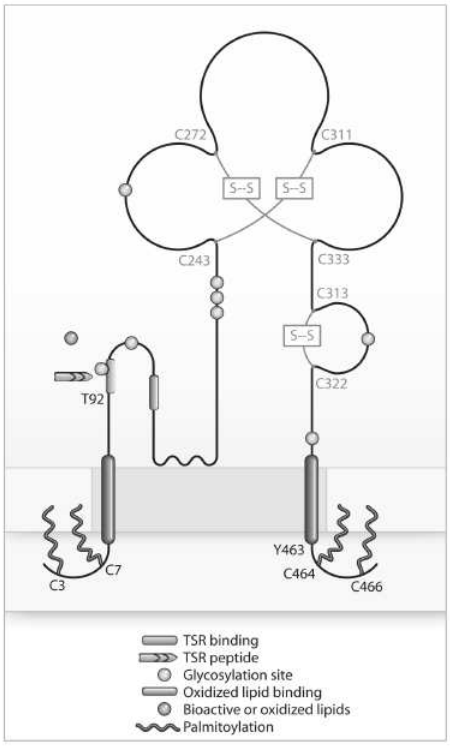

Figure 2: Structure of CD36
The transmembrane protein CD36 is characterized by a prominent extracelluar loop that is heavily glyosylated. The C- and N-terminus are short, intracellularly located tails that each feature two palmitoylated cysteines. The extracellular part of the protein contains three disulfid bonds linking conserved cysteine residues as well as ligand binding domains for proteins with TSR domain and oxidized lipids (adapted from (Silverstein and Febbraio, 2009)).

Suggestions have been made as to linking CD36 signaling to the activation of Src kinases and nitric-oxide synthase (reviewed by (Abumrad, 2005)). During lipid absorption, CD36 function is regulated by ubiquitination and subsequent degradation which is initiated by digestion products (Tran *et al.*, 2011).

Many publications have so far assigned a role in long-chain fatty acid uptake to the CD36 protein (reviewed by (Su and Abumrad, 2009)). CD36 overexpression increased oleate uptake in COS cells while the expression of CD36 in the plasma membrane was confirmed (Ehehalt *et al.*, 2008). Bonen and co-workers suggested a translocation of CD36 from intracellular stores to the sarcolemma upon muscle contraction, thereby linking the function of CD36 in fatty acid uptake to its localization at the plasma membrane (Bonen *et al.*, 2000). The relevance of CD36 for long-chain fatty acid uptake was further confirmed by animal studies: the intestinal uptake of very long-chain fatty acids was strongly impaired in CD36 null mice after feeding a high fat diet (Drover *et al.*, 2008). Likewise, CD36 null mice displayed a reduction in fatty acid uptake in the muscle and adipose tissue (Coburn *et al.*, 2000).

In accordance with its relevance for fatty acid uptake CD36 has been implicated in the onset and progression of pathologic conditions like obesity, type 2 diabetes, the metabolic syndrome and atherosclerosis (Koonen *et al.*, 2007; Love-Gregory *et al.*, 2008).

3.2.2 Role of caveolin-1 in CD36 signaling

CD36 function in fatty acid uptake was hypothesized to be influenced by its localization within the plasma membrane. The cellular membrane is an inhomogeneous structure that is subdivided in liquid ordered and liquid disordered domains. Tightly packed subdomains, predominantly consisting of cholesterol and sphingolipids, float freely within the liquid disordered phase, thus generating a subcompartmentalization which spotlights and coordinates the bioactivity of membrane components (Lingwood and Simons, 2010). These so termed lipid rafts play an important role as signaling platforms involved in various cellular processes by concentrating receptors and signaling molecules in one place.

Caveolae are a special subset of lipid rafts. They are small cell membrane invaginations which are involved in cell signaling and transport processes. They are composed of the coat proteins caveolin-1, -2 and -3 (Cav-1, -2, -3), with Cav-1 and Cav-3 being essential for proper caveolae construction. Also caveolae do occur in different cell types they are most often found in adipocytes as well as in vascular endothelial cells, fibroblasts and epithelial cells (reviewed by (Chidlow and Sessa, 2010)). Cav-1 binds long-chain fatty acids with high affinity and has been suggested to play role in lipid traffic (Liu *et al.*, 2002) and to modulate fatty acid transport across the plasma membrane (Meshulam *et al.*, 2006).

When Cav-1 was investigated for its function in fatty acid metabolism, Cav-1 null mice developed hyperinsulinemia when nourished with a high fat diet (Cohen *et al.*, 2003). Another study showed normal serum insulin in Cav-1 null mice but increased levels of free fatty acids and triglycerides (Razani *et al.*, 2002) hinting at a role for Cav-1 in fatty acid metabolism.

For CD36, the existence of two pools within the plasma membrane was suggested: inside and outside lipid rafts, with raft association leading to an increase in fatty acid uptake (Ehehalt *et al.*, 2008). A possible functional relationship of CD36 and Cav-1 in fatty acid uptake is still a matter of debate. As discussed by Su and Abumrad,

caveolin function is regulated by Src kinases which have also been linked to CD36 signaling (reviewed by (Su and Abumrad, 2009)), indicating a possible interaction. Due to the high expression rate of Cav-1 in adipocytes together with the localization of CD36 to lipid rafts and its role in fatty acid uptake Cav-1 is a worthwhile target for investigation in the context of CD36 function.

3.3 Fatty acid activating enzymes

3.3.1 The acyl-CoA synthetase family

Fatty acids need to be activated before they can be used by cells for energy production, signaling and further downstream metabolic pathways. The activation of fatty acids by esterification with coenzyme A is a highly conserved process that is performed in organisms from archea to man (reviewed by (Watkins, 2008)). In mammals, this reaction is catalyzed by the family of acyl-CoA synthetases (ACS) which can activate fatty acids with various chain lengths, mostly between 12 – 20 carbon atoms. Depending on their preferred substrates, acyl-CoA synthetase are subdivided into short-chain (C_2 - C_4), medium-chain (C_4 – C_{12}), long-chain (C_{12} – C_{20}), very long-chain (C_{18} – C_{26}) and bubblegum (C_{14} – C_{24}) acyl-CoA synthetases (reviewed by (Soupene and Kuypers, 2008)). There are 26 different acyl-CoA synthetases expressed in mammals, including 13 enzymes for the activation of long-chain fatty acids only. Physiologically of highest importance are the five long-chain acyl-CoA synthetases (ACSL1, 3 - 6) as well as the six very long-chain acyl-CoA synthetase (ACSVL) or fatty acid transport proteins (FATP1-6), which activate intracellular fatty acids including oleate and palmitate.

Acyl-CoA synthetases play an important role in lipid metabolism and are required to ensure lipid homeostasis. The described functions are manifold and include substrate provision for energy production and lipid synthesis but also enzyme regulation, protein acylation, modulation of ion channels and membrane potential as well as protein trafficking (reviewed by (Li *et al.*, 2010)). The localization of the different acyl-CoA synthetase family members remains a matter of debate and includes the controversy whether the respective proteins are localized at the plasma membrane or at intracellular organelles, such as the endoplasmic reticulum, lipid droplets or mitochondria.

3.3.2 The catalyzed reaction

The acyl-CoA synthetase family members catalyze the esterification of intracellular fatty acids with coenzyme A in order to activate fatty acids for further downstream metabolism. During the reaction, an acyl-AMP intermediate is produced under consumption of adenosine triphosphate (ATP) (Mashek *et al.*, 2004). In a two-step reaction, a thioester bond is formed between the carboxyl group of a fatty acid and the sulfhydryl group of coenzyme A. Initially, a fatty acid is converted to an acyl-adenylate under energy consumption, thereby metabolizing ATP to pyrophosphate. In a second step, the sulfhydryl group of coenzyme A reacts with the intermediate acyl-adenylate in order to produce acyl-CoA and adenosine monophosphate (AMP) (Figure 3). Both reaction steps are completely reversible. The equilibrium of the reaction is shifted towards the production of acyl-CoA by fast hydrolysis of the intermediate pyrophosphate (Berg JM, 2003).

.

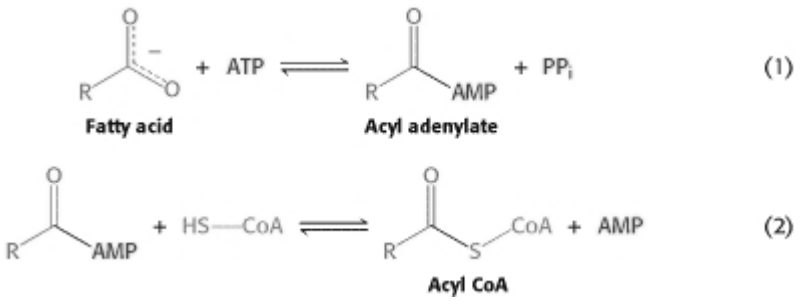

Figure 3: Activation of fatty acids by esterification with coenzyme A.
Free fatty acids are activated by esterification with coenzyme A in a two-step process. At first, a fatty acid reacts with ATP in order to form an acyl-adenylate intermediate under energy consumption. The resulting pyrophosphate is rapidly hydrolyzed, thereby driving the reaction. Secondly, coenzyme A is bound to the acyl-adenylate by a thioester bond in order to generate acyl-CoA and AMP (adapted from (Berg JM, 2003)).

Although its catalyzed reaction has been characterized, the mammalian acyl-CoA synthetase structure remains yet to be identified. Homologies to the bacterial isoform indicate a similar mode of action for the mammalian version. In bacteria, acyl-CoA synthetases act as dimers. Their structure features a conserved fatty acid Gate domain which defines substrate specificity (reviewed by (Forneris and Mattevi, 2008; Soupene and Kuypers, 2008)). One main obstacle that has to be overcome by acyl-CoA synthetases is the simultaneous interaction with hydrophilic as well as hydrophobic substrates. The bacterial acyl-CoA synthetase FACS is an elegant example of how molecules derived from the aqueous cellular environment together

with molecules originating from the lipid bilayer can be introduced in a common reaction that is catalyzed by one single enzyme. FACS dimers are located close to the lipid bilayer from which fatty acid substrates are directly obtained. A hydrophobic cavity is formed between the two monomeric parts which binds fatty acids in a position that makes the carboxyl group accessible for the hydrophilic substrates. ATP and coenzyme A are taken up through a hydrophilic entrance facing the aqueous environment. After completing the reaction, the acyl-CoA product is released through the hydrophilic opening (Figure 4). In conclusion, by action of the bacterial acyl-CoA synthetase FACS a hydrophilic fatty acid has been made accessible to cellular metabolic pathways by coupling to hydrophilic coenzyme A (reviewed by (Forneris and Mattevi, 2008)).

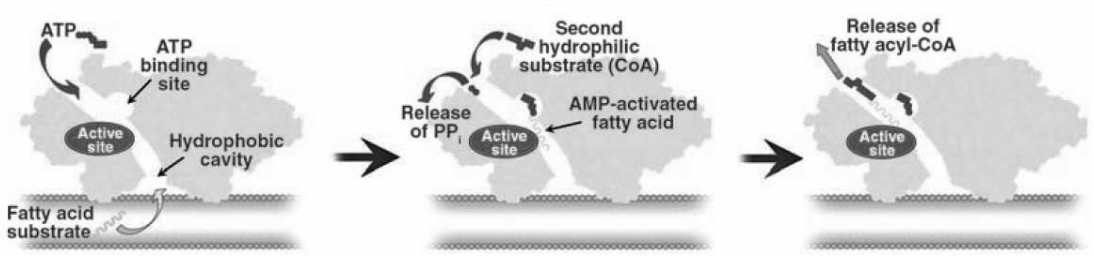

Figure 4: Mechanism of fatty acid activation by the bacterial acyl-CoA synthetase FACS.
FACS acts as a dimer which is closely associated with cellular membranes. Hydrophobic fatty acid substrates originiate from lipid membranes and are transported to the enzymatically active site through a hydrophobic cavity. The hydrophilic substrates ATP and coenzyme A are derived from the aqueous environment through a hydrophilic opening. After coupling coenzyme A to the fatty acid the resulting hydrophilic product is released via the hydrophilic channel (adapted from (Forneris and Mattevi, 2008)).

3.3.3 Fatty acid transport protein 4 (FATP4)

In 1994, the first FATP was identified from a murine adipocyte cDNA library as a protein that increased long-chain fatty acid uptake when overexpressed in adipocytes. The protein, which was subsequently termed FATP1, showed an increased expression during the differentiation of 3T3-L1 adipocytes, corresponding to a formerly described rise in long-chain fatty acid uptake (Schaffer and Lodish, 1994). In the following years, six human FATPs (FATP1-6) were identified as transmembrane proteins with a common, highly conserved FATP signature sequence. The different family members are expressed in various cell types, all of which are involved in fatty acid metabolism (reviewed by (Stahl *et al.*, 2001)). Although there is congruency about the involvement of FATPs in fatty acid uptake, the underlying mechanism as well as the subcellular localization are still under debate.

The family member FATP4 is expressed in adipose tissue, brain, skeletal muscle, heart and intestine. FATP4-null mice display severe skin defects, including hyperproliferative hyperkeratosis, defective barrier function and restrictive dermopathy. In consequence, animals die before or closely after birth. The epidermis of FATP4-null mice is characterized by altered lipid levels, with a decrease in phosphatidylcholine, phosphatidylethanolamine and cholesterol ester content, hinting at a profound influence of FATP4 on lipid metabolism (reviewed by (Watkins, 2008)).

Stahl and co-workers described FATP4 as a plasma membrane localized fatty acid transporter, that is expressed on the apical site of enterocytes (Stahl *et al.*, 1999), thus facilitating fatty acid uptake. This view was contradicted by studies clearly showing an intracellular localization of FATP4 at the endoplasmic reticulum. Although a function of FATP4 as fatty acid transporter was thus excluded, a positive correlation was shown between protein expression and fatty acid uptake (Milger *et al.*, 2006). In accordance with increased FATP4 expression levels, acyl-CoA synthetase activity and fatty acid uptake were enhanced in hepatoma cell lines HuH7 and HepG2 (Krammer *et al.*, 2011) as well as in 3T3-L1 adipocytes (Zhan *et al.*, 2012). FATP4 mediated fatty acid uptake was further increased by short term insulin treatment, hinting at a new target in insulin dependent metabolic modulation (Digel *et al.*, 2011). These results reverse the view of FATP4 as a plasma membrane located fatty acid transport protein. It was rather shown that intracellular activation of fatty acids by acyl-CoA synthetases is sufficient to drive cellular fatty acid uptake.

3.3.4 Long-chain acyl-CoA synthetase 1 (ACSL1)

Mammalian long-chain acyl-CoA synthetases play an important role in lipid metabolism by generation of long-chain acyl-CoA esters that have regulatory functions. To date, five long-chain acyl-CoA synthetase genes have been identified in humans, with each gene having different transcript variants. In 1990, the first cDNA encoding an long-chain acyl-CoA synthetase was isolated from rat liver and subsequently termed ACSL1. Indications for a relevance in fatty acid metabolism were obtained by observation of an increase in ACSL1 mRNA in rat liver after feeding a high fat diet (Suzuki *et al.*, 1990).

The intracellular localization of long-chain acyl-CoA synthetase proteins is controversial as different studies place them either in the plasma membrane or at various intracellular locations. ACSL1 has been detected on mitochondria, lipid droplets and the plasma membrane (reviewed by (Soupene and Kuypers, 2008)). Upon overexpression in primary rat hepatocytes, ACSL1 was found on the endoplasmic reticulum and acyl-CoA synthetase activity was increased. Alterations in fatty acid metabolism included the enhanced incorporation of oleate into diacylglycerol and phospholipids, whereas less oleate was integrated into cholesterol esters. It was suggested, that ACSL1 channeled its substrate fatty acids towards different metabolic fates depending on enzyme localization and protein interaction (Li *et al.*, 2006). Another study localized overexpressed ACSL1 to mitochondria in Ptk2 cells. Oleate uptake was enhanced upon ACSL1 overexpression, verifying that the intracellular localization of a fatty acid metabolizing enzyme is sufficient to increase fatty acid uptake (Milger *et al.*, 2006).

ACSL1 accounts for 80 % of total acyl-CoA synthetase activity in adipose tissues and represents the predominant long-chain acyl-CoA synthetase isoform in the liver. Following a specific knock out of ACSL1 in adipose tissue of mice, animals displayed significantly decreased rates of fatty acid oxidation. The results hinted at a specific function for ACSL1 in directing fatty acids towards ß-oxidation in adipocytes (Ellis *et al.*, 2010). Impaired ß-oxidation was also observed in a liver specific ACSL1 knock out mouse model together with a decreased acyl-CoA synthetase activity and acyl-CoA amount in the liver (Li *et al.*, 2009). Accordingly, ACSL1 is involved in regulating lipid metabolism by directing fatty acids towards ß-oxidation.

3.4 Aim of study

Lipids are essential components of life and have multiple functions in cellular metabolism. They contribute to the construction of cellular membranes, serve as signaling molecules and are needed for energy storage and supply. Imbalances of lipid homeostasis can contribute to onset and progression of diseases like the metabolic syndrome, diabetes type 2, atherosclerosis and cardiovascular illnesses. Therefore, cellular fatty acid uptake has to be carefully regulated.

Proteins implicated in fatty acid transport are the gylcoprotein CD36, the acyl-CoA synthetases FATP4 and ACSL1 and the structural protein Cav-1. CD36, FATP4 and ACSL1 were described to increase cellular fatty acid uptake upon overexpression, mediated by different mechanisms. CD36 is a plasma membrane localized protein that directly facilitates fatty acid transport whereas FATP4 and ACSL1 are localized intracellularly. They indirectly drive fatty acid uptake by depleting the level of intracellular fatty acids through fatty acid activation, thus making them available for downstream metabolic pathways. Cav-1 is a structural protein of membrane invaginations, termed caveolae. It possesses a lipid binding site and has been linked to mediating intra- and extracellular lipid transport.

CD36, FATP4 and ACSL1 localization and their function in fatty acid uptake have been a topic of interest for several years. But to date, no analysis was performed in which the amounts of overexpressed proteins were quantified and then related to their specific effect on fatty acid uptake. Accordingly, this study addressed two main topics:

1) the molecular stoichiometry of fatty acid uptake

- absolute quantification of CD36, FATP4 and ACSL1 protein amounts in overexpressing cell lines
- calculation of protein-specific fatty acid uptake by relating protein quantities to the respective increase in oleate uptake

2) the potential cooperativity of proteins regulating fatty acid uptake

- investigation of whether CD36, FATP4 and ACSL1 cooperate in facilitating fatty acid uptake
- analysis of the influence of Cav-1 on CD36 mediated fatty acid transport

MDCK cells were chosen as a model system because they are not specialized in lipid transport, unlike adipocytes, muscle cells or cardiac cells, and thus permitted an unbiased quantitiative analysis. For experiments, it was required to generate MDCK cells with stable protein overexpression (FATP4, ACSL1) or knock down (Cav-1) as well as MDCK cells with adjustable protein overexpression (CD36 or FATP4 adenovirus infected cells).

Absolute protein amounts of CD36, FATP4 and ACSL1 should be quantified by western blotting and calculated by densitometric analysis by comparison to a recombinant protein standard. Cells should be incubated with ^{3}H-oleic acid for 3 h and fatty acid uptake should be determined by radiolabeled measurement. Finally, the specific alteration in fatty acid uptake should be calculated for the assessed amount of overexpressed protein. Cellular localization as described in the scientific literature should be verified for each protein by immunofluorescene.

4. Material and Methods

If not otherwise noted disposable and non-disposable materials were manufactured by Eppendorf (Hamburg), Greiner Bio-One (Frickenhausen) and Schott (Mainz). Chemicals were purchased from the Chemikalienlager Zentralbereich Neuenheimer Feld 367 (Heidelberg), AppliChem (Darmstadt), Merck (Darmstadt), Carl Roth (Karlsruhe) and Sigma-Aldrich (Steinheim).

4.1 Equipment

4.1.1 Molecular biology equipment

Table 1: Molecular biology equipment used in this study.

equipment	manufacturer
agarose gel chamber	cti, Idstein
agarose gel documentation system	Peqlab, Erlangen
BioPhotometer	Eppendorf, Hamburg
centrifuges refrigerated bench-top centrifuge 5804 R rotors: A 4-44, F 34-6-38 refrigerated microcentrifuge 5415 R rotor: F 45-24-11 ultracentrifuge Optima XL-90 Rotor: SW 41-Ti	 Eppendorf, Hamburg Eppendorf, Hamburg Beckman Coulter, Krefeld
Electroporator Gene Pulser Xcell	Bio-Rad, München
electroporation cuvettes	Peqlab, Erlangen
GeneAmp PCR System 2400	Perkin Elmer, Waltham (USA)
microplate reader PHOmo	Anthos Mikrosysteme, Krefeld
microscopes fluorescence microscope BX41 laser scanning spectral confocal microscope TCS SP2	 Olympus, Hamburg Leica, Wetzlar
pH meter SevenEasy	Mettler-Toledo, Schwerzenbach (Schweiz)
polyclear tubes for ultracentrifugation (14 mm x 89 mm)	Beranek, Weinheim

4.1.2 Protein biochemistry equipment

Table 2: Protein biochemistry equipment used in this study.

equipment	manufacturer
Amersham Hyperfilm ECL	GE Healthcare, München
autoradiography hypercassette	Amersham Biosciences, Little Chalfont (UK)
blotting paper	Schleicher und Schüll/Whatman, Dassel
developer machine Agfa Curix 60	Christiansen, München
Protran nitrocellulose membrane	Whatman, Dassel
sodium dodecyl sulfate polyacrylamide gel electrophoresis (SDS-PAGE) chamber	Bio-Rad, München
semi-dry blotting chamber	cti, Idstein

4.1.3 Radioactive work equipment

Table 3: Radioactive work equipment used in this study.

equipment	manufacturer
liquid scintillation counter LS 6500	Beckman Coulter, Krefeld
polyethylene vials for liquid scintillation counting Minis 2000	Zinsser Analytic, Frankfurt am Main
Safe-Lock tubes (1.5 ml)	Eppendorf, Hamburg
Ultima Gold	Perkin Elmer, Waltham (USA)

4.1.4 Cell culture equipment

Table 4: Cell culture equipment used in this study.

equipment	manufacturer
cell culture dishes (60 cm^2, 145 cm^2)	Cellstar/Greiner Bio-One, Frickenhausen
cell culture flasks (T25, T75, T175)	Cellstar/Greiner Bio-One, Frickenhausen
cell culture multiwell plates (6-well, 12-well, 96-well)	Cellstar/Greiner Bio-One, Frickenhausen
cover slips (10 mm in diameter)	Marienfeld, Lauda-Königshofen
Microscope slides	Marienfeld, Lauda-Königshofen
Neubauer improved counting chamber	Assistent, Sondheim/Rhön
sterile syringe filters, nitrocellulose free (0.45 µm)	Millipore, Schwalbach/Ts

4.2 Chemicals

4.2.1 Molecular biology chemicals

Table 5: Molecular biology chemicals used in this study.

chemical	manufacturer
bovine serum albumin (BSA) (A6003)	Sigma-Aldrich, Steinheim
fatty acid free BSA (A3803)	Sigma-Aldrich, Steinheim
6 x DNA Loading Dye	Fermentas, St. Leon-Rot
Deoxyribonucleoside triphosphate (dNTP) mix (10 mM each)	Fermentas, St. Leon-Rot
Kanamycin	Sigma-Aldrich, Steinheim

4.2.2 Protein biochemistry chemicals

Table 6: Protein biochemistry chemicals used in this study.

chemical	manufacturer
acrylamide/bis solution (30 %)	Bio-Rad, München
ammonium persulfate (APS)	Sigma-Aldrich, Steinheim
ANTI-FLAG M2 affinity gel	Sigma-Aldrich, Steinheim
ß-mercaptoethanol	AppliChem, Darmstadt
blotting grade blocker nonfat dry milk	Bio-Rad, München
Bradford protein assay dye	Bio-Rad, München
bromphenolblue	Merck, Darmstadt
Coomassie brilliant blue R-250	Merck, Darmstadt
$FATP4_{FLAG}$ protein standard	S. Staudacher, AG J. Füllekrug, University Hospital Heidelberg
N,N,N',N'-tetramethylethylenediamine (TEMED)	AppliChem, Darmstadt
Ponceau Red	Serva Electrophoresis, Heidelberg
sodium dodecyl sulfate (SDS)	Sigma-Aldrich, Steinheim
Western Lightning Plus enhanced chemiluminescence (ECL)	Perkin Elmer, Waltham (USA)

4.2.3 Radioactive work chemicals

Table 7: Radioactive work chemicals used in this study.

chemical	manufacturer
oleic acid	Sigma-Aldrich, Steinheim
^{3}H-oleic acid	Perkin Elmer, Waltham (USA)

4.2.4 Cell culture chemicals

Table 8: Cell culture chemicals used in this study.

chemical	manufacturer
ampicillin sodium salt	Sigma-Aldrich, Steinheim
calcium chloride ($CaCl_2$)	Sigma-Aldrich, Steinheim
cesium chloride (CsCl)	Boehringer-Mannheim, Mannheim
Collagen R solution	Serva, Heidelberg
culture medium DMEM/MEM/OptiMEM	Gibco/Invitrogen, Carlsbad (USA)
dimethyl sulfoxide (DMSO)	Sigma-Aldrich, Steinheim
fetal bovine serum (FBS)	Gibco/Invitrogen, Carlsbad (USA)
GlutaMAX-I (200 mM, 100 x)	Gibco/Invitrogen, Carlsbad (USA)
Hoechst 33342	Invitrogen, Carlsbad (USA)
Lipofectamine 2000	Invitrogen, Carlsbad (USA)
Mowiol mounting medium	Calbiochem, La Jolla (USA)
paraformaldehyde (PFA)	Riedel-de Haën, Seelze
penicillin (10 U/µl)/streptomycin (10 g/l)	Gibco/Invitrogen, Carlsbad (USA)
Polybrene (hexadimethrine bromide)	Sigma-Aldrich, Steinheim
Puromycin	Clontech, Mountain View (USA)
Saponin Quillaja Bark	Sigma-Aldrich, Steinheim
Teleostan gelatin	Sigma-Aldrich, Steinheim
trypsin	Gibco/Invitrogen, Carlsbad (USA)

4.3 Kits

Table 9: Kits used in this study.

kit	manufacturer
Marligen PowerPrep® HP Plasmid Purification System	OriGene, Rockville (USA)
Nucleo Spin® Extract Kit II	Macherey-Nagel, Düren
Nucleo Spin® Plasmid Kit	Macherey-Nagel, Düren
QIAquick Gel Extraction Kit	Qiagen, Hilden

4.4 Molecular biology material

4.4.1 Molecular weight standards

Table 10: Molecular weight standards used in this study.

weight standard	range	manufacturer
GeneRuler™ 1 kilobase (kb) DNA Ladder	250-10,000 base pairs (bp)	Fermentas, St. Leon-Rot
Page Ruler™ Prestained Protein Ladder	10-170 kilodalton (kDa)	Fermentas, St. Leon-Rot

4.4.2 Antibodies

Table 11: Antibodies used in this study.

antibody	incubation conditions		characteristics	manufacturer
	WB	IF		
primary antibodies				
ms-α-β-actin	1:200,000 (over night, 4 °C)	-	monoclonal antibody	A5441 Sigma-Aldrich, Steinheim
ms-α-CD36	-	1:200 (1 h, RT)	monoclonal antibody, raised against human CD36	sc-70642 Santa Cruz Biotechnology Heidelberg
ms-α-FLAG M2	-	1:1,000 (1 h, RT)	monoclonal antibody, affinity purified	F1804 Sigma-Aldrich, Steinheim
rb-α-Cav1 (N20)	1:20,000 (1 h, RT)	1:200 (1 h, RT)	polyclonal antibody, affinity purified, raised against human Cav-1	sc-894 Santa Cruz Biotechnology Heidelberg
rb-α-FATP4 (C3/5)	1:5,000 (over night, 4 °C)	1:1,000 (1 h, RT)	-	J. Füllekrug, University Hospital Heidelberg (Milger *et al.*, 2006)
rb-α-FLAG	1:10,000 (over night, 4 °C)	1:500 (1 h, RT)	polyclonal antibody, affinity purified	F7425 Sigma-Aldrich, Steinheim
secondary antibodies				
α-ms-Cy2	-	1:200 (1 h, RT)	Cy2-conjugated anti-mouse IgG	715-225-151 Dianova, Hamburg
α-ms-Cy3	-	1:1,000 (1 h, RT)	Cy3-conjugated anti-mouse IgG	715-165-151 Dianova, Hamburg
α-rb-Cy2	-	1:200 (1 h, RT)	Cy2-conjugated anti-rabbit IgG	711-225-152 Dianova, Hamburg
α-rb-Cy3	-	1:1,000 (1 h, RT)	Cy3-conjugated anti-rabbit IgG	711-165-152 Dianova, Hamburg
α-ms-HRP	1:10,000 (1 h, RT)	-	peroxidase-conjugated anti-mouse IgG	711-035-003 Dianova, Hamburg
α-rb-HRP	1:10,000 (1 h, RT)	-	peroxidase-conjugated anti-rabbit IgG	711-035-152 Dianova, Hamburg
western blot (WB), immunofluorescence (IF), mouse (ms), rabbit (rb), anti (α), room temperature (RT), horseradish peroxidase (HRP), immunoglobulin G (IgG)				

4.4.3 Enzymes

Table 12: Enzymes used in this study.

enzyme	activity [units (U)/ml]	manufacturer
general enzymes		
Antarctic Phosphatase	-	New England Biolabs, Frankfurt am Main
Quick T4 DNA Ligase	-	New England Biolabs, Frankfurt am Main
thermus aquaticus (*taq*) DNA Polymerase	-	Qiagen, Hilden
restriction enzymes		
AgeI	5,000 U/ml	New England Biolabs, Frankfurt am Main
BglII	10,000 U/ml	New England Biolabs, Frankfurt am Main
KpnI	10,000 U/ml	Fermentas, St. Leon-Rot
NdeI	20,000 U/ml	New England Biolabs, Frankfurt am Main
PacI	10,000 U/ml	New England Biolabs, Frankfurt am Main
PmeI	10,000 U/ml	New England Biolabs, Frankfurt am Main
XbaI	20,000 U/ml	New England Biolabs, Frankfurt am Main
XhoI	20,000 U/ml	New England Biolabs, Frankfurt am Main

4.4.4 Oligonucleotides

Oligonucleotides were purchased from Sigma-Aldrich (Steinheim) and adjusted to a working concentration of 100 µM in sterile H_2O.

Table 13: Oligonucleotides used in this study.

primer	Tm	length	sequence (5` - 3`)
s_CD36-1_LC	65.7 °C	21	TTGATGTGCAAAATCCACAGG
s_CD36-2_LC	65.1 °C	19	AAAACGGCTGCAGGTCAAC
a_CD36-2_LC	65.0 °C	20	TCACCAATGGTCCCAGTCTC
s_CD36.FLAG (adeno)	79.7 °C	33	GGTACCAGATCTACCATGGGCTGTGACCGGAAC
a_CD36.FLAG (adeno)	74.1 °C	31	AAGCTTCTCGAGTTACTTGTCATCGTCGTCC
CMV forward	76.8 °C	21	CGCAAATGGGCGGTAGGCGTG
EGFP-C	62.0 °C	20	ATGGTCCTGCTGGAGTTCGT
antisense (a_), sense (s_), melting temperature (Tm), green fluorescent protein (GFP)			

4.4.5 Plasmids

Table 14: Plasmids for cloning used in this study.

plasmid	characteristics	tag	resistence	reference	internal number
plasmids for cloning					
pcDNA3	mammalian expression vector	-	ampicillin, neomycin	Stratagene, Santa Clara (USA)	JF 001
GFP -CD36. pNice	plasmid for subcloning, ligation of GFP-$CD36_{FLAG}$ into pEGFP-N1, green fluorescence	FLAG	kanamycin	this work	JF 782
GFP -CD36-FLAG	expression vector for human CD36 with N-terminal GFP and C-terminal FLAG, green fluorescence	FLAG	kanamycin, neomycin	D. Lublin, St. Louis (USA)	JF 664
pEGFP-N1	enhanced green fluorescent protein expression	-	kanamycin, neomycin	Clontech, Mountain View (USA)	JF 067
CD36-FLAG.pcDNA3	expression vector for human CD36 with C-terminal FLAG	FLAG	ampicillin, neomycin	D. Lublin, St. Louis (USA)	JF 502

Table 15: Retroviral plasmids used in this study.

plasmid	characteristics	tag	resistence	reference	internal number
retroviral plasmids					
pQCXIP-J (pQ)	retroviral expression vector, based on pQCXIP (BD Biosciences, Clontech, Heidelberg)	-	ampicillin, puromycin	J. Füllekrug, University Hospital Heidelberg	JF 596
cav1-ko.pRVH1puro	retroviral expression vector for stable Cav-1 knock down by RNA interference	-	ampicillin, puromycin	MPI-CBG, Dresden (Schuck *et al.*, 2004)	JF 383
ACSL1.pRJ	retroviral expression vector for stable overexpression of rat ACSL1 with C-terminal FLAG	FLAG	ampicillin, puromycin	T. Zhan, AG J. Füllekrug, University Hospital Heidelberg	JF 659
pVSV-G	expression vector for the Vesicular Stomatitis Virus glycoprotein	-	ampicillin	MPI-CBG, Dresden (Schuck *et al.*, 2004)	JF 380

Table 16: Adenoviral plasmids used in this study.

plasmid	characteristics	tag	resistence	reference	internal number
adenoviral plasmids					
pAda/pshuttle-CMV	basic transfer plasmid for recombinant adeno-virus construction	-	kanamycin	P. Keller, MPI-CBG, Dresden	JF 101
CD36.pAda	adenoviral shuttle plasmid for human CD36 with C-terminal FLAG	FLAG	ampicillin	this work	JF 780
GFP -CD36.pAda	adenoviral shuttle plasmid for human CD36 with N-terminal GFP and C-terminal FLAG, green fluores-cence	FLAG	ampicillin	this work	JF 781
FATP4. pAdTrack-CMV	adenoviral expression plasmid for murine FATP4, cytosolic green fluorescence	-	kanamycin	C. Becker, AG J. Füllekrug, University Hos-pital Heidelberg	JF 430
pAdEasy-1	adenoviral backbone plasmid with E1/E3 deletion for recombinant adenovirus contruction	-	kanamycin	P. Keller, MPI-CBG, Dresden	JF 109
CD36.pAdv	adenoviral expression plasmid for human CD36 with C-terminal FLAG	FLAG	ampicillin	this work	JF 790
GFP -CD36.pAdv	adenoviral expression plasmid for human CD36 with N-terminal GFP and C-terminal FLAG, green fluores-cence	FLAG	ampicillin	this work	JF 791

4.5 Buffers and media

4.5.1 Media

Luria Bertani (LB) media for cultivation of bacteria were autoclaved before use. Cell culture media and supplements were sterile at delivery and subsequently handled under sterile conditions.

Table 17: Media used in this study.

medium	components	purpose
molecular biology		
LB medium	10 g/l tryptone, 5 g/l yeast extract, 10 g/l NaCl, pH 7.0, for plates: 30 g Select agar/l (100 µg/ml ampicillin, 30 µg/ml kanamycin)	*E. coli*

cell culture		
DMEM	DMEM 4.5 g/l glucose + GlutaMAX + 10 % (v/v) FBS + 1 % (v/v) pen/strep	HEK 239 cells phoenix gp cells
DMEM low glucose	DMEM 1 g/l glucose + GlutaMAX + 10 % (v/v) FBS	retrovirus production
MEM	MEM 4.5 g/l glucose + GlutaMAX + 10 % (v/v) FBS + 1 % (v/v) pen/strep	MDCK cells
OptiMEM	reduced serum medium	adenoviral infection lipofection
Dulbecco's modified Eagle's medium (DMEM), Eagle's minimum essential medium (MEM)		

4.5.2 Buffers

If not otherwise stated buffers were prepared in Millipore-H_2O. The appropriate pH was adjusted at room temperature whenever required.

Table 18: Buffers used in this study.

buffer	**components**
molecular biology	
6 x DNA loading dye	38 % (w/v) glycerol, 0.08 % (w/v) bromphenolblue, 0.08 % (w/v) xylencyanol
Inoue Transformation Buffer (ITB)	10 mM piperazine-N,N′-bis(2-ethanesulfonic acid) (PIPES) (pH 6.7 with KOH), 15 mM $CaCl_2$, 250 mM KCl, 55 mM $MnCl_2$
phosphate buffered saline (PBS)	137 mM NaCl, 10 mM Na_2HPO_4, 2.7 mM KCl, 2 mM KH_2PO_4, pH 7.4
2 x adenovirus storage buffer	10 mM tris(hydroxymethyl)aminomethane (Tris) (pH 8.0), 100 mM NaCl, 0.1 % (w/v) BSA, 50 % (w/v) glycerol
10 x Tris acetate EDTA (TAE)	400 mM Tris/acetate, 10 mM ethylenediaminetetraacetic acid (EDTA)/NaOH, pH 8.0
western blot	
blotting buffer	25 mM Tris, 190 mM glycin, 20 % (v/v) MeOH
0.1 % coomassie blue	1 g Coomassie brilliant blue R-250, 300 ml MeOH, 200 ml H_2O, dissolved at RT, 400 ml H_2O, 100 ml (glacial) acetic acid
destain solution	10 % (v/v) acetic acid, 30 % (v/v) MeOH
4 x Laemmli buffer	250 mM Tris/HCl (pH 6.8), 50 % (w/v) glycerol , 8 % (w/v) SDS, 0.02 % (w/v) bromphenolblue, 5 % (v/v) β-mercaptoethanol
running buffer	25 mM Tris, 190 mM glycin, 0.1 % (w/v) SDS
SDS-PAGE special sample buffer	62 mM Tris/HCl (pH 6.8), 2 % (w/v) SDS, 10 % (w/v) glycerol
20 x Tris buffered saline (TBS) Tween	200 mM Tris/HCl, 3 M NaCl (pH 7.4), 2 % (v/v) Tween-20
Tris NaCl EDTA (TNE) buffer	150 mM NaCl, 20 mM Tris/HCl (pH 7.4), 1 mM EDTA
Tris NaCl EDTA Triton X (TNEX) buffer	150 mM NaCl, 20 mM Tris/HCl (pH 7.4), 1 mM EDTA, 0.2 % (v/v) Triton X-100

radioactive assay	
STOP-mix	0.5 % (w/v) BSA with fatty acids in 1x PBS
cell culture	
2 x HEPES buffered saline (HBS)	280 mM NaCl, 50 mM 4-(2-hydroxyethyl)-1-piperazineethanesulfonic acid (HEPES), 12 mM glucose, 10 mM KCl, 1.5 mM Na_2HPO_4, pH 6.95
immunofluorescence	
Mowiol pH 8,5	4.8 g Mowiol, 12 g glycerol, 12 ml H_2O, dissolve at RT, 24 ml 0.2 M Tris/HCl (pH 8.5), dissolve at < 50 °C, centrifugation at 5,000 g for 15 min, use supernatant
4 % PFA	40 g PFA dissolved in 1 l 1 x PBS at < 80°C, 100 µl 1 M $CaCl_2$, 100 µl 1 M $MgCl_2$, pH 7.4
saponin gelatine (SG) washing solution	0.01 % (w/v) saponin, 0.2 % (w/v) gelatin, 0.02 % (v/v) sodium azide, in 1 x PBS
saponin gelatine BSA (SGB) washing/ blocking solution	0.1 % (w/v) saponin, 0.5 % (w/v) gelatin, 5 mg/ml BSA, 0.02 % (v/v) sodium azide, in 1 x PBS

4.6 Cells, viruses, bacteria

4.6.1 Cells

All cell lines were maintained under sterile conditions at 37 °C and 5 % CO_2. Stocks were stored in liquid nitrogen.

Table 19: Cells used in this study.

cell line	characteristics	ATCC	reference	medium	passaging
for assays					
wt MDCK	canine kidney cells	CCL-34	MPI-CBG, Dresden	MEM	at post-confluency, 1/2 for assays, 1/8 for propagation
$ACSL1_{FLAG}$ MDCK	canine kidney cells stably overexpressing rat $ACSL1_{FLAG}$	-	this work	MEM	at post-confluency, 1/2 for assays, 1/8 for propagation
Cav-1 KD MDCK	canine kidney cells with stable Cav-1 knock down	-	this work	MEM	at post-confluency, 1/2 for assays, 1/8 for propagation
FATP4 MDCK	canine kidney cells stably over-expressing mouse FATP4	-	M. Poppelreuther AG J. Füllekrug, University Hospital Heidelberg	MEM	at post-confluency, 1/2 for assays, 1/8 for propagation
pQCXIP-J MDCK	canine kidney cells stably infec-ted with a retro-viral expression plasmid	-	this work	MEM	at post-confluency, 1/2 for assays, 1/8 for propagation

for protein standards					
$FATP4_{FLAG}$ MDCK	canine kidney cells stably over-expressing mouse $FATP4_{FLAG}$	-	M. Poppelreuther, AG J. Füllekrug, University Hospital Heidelberg	MEM	at post-confluency, 1/8 for propagation
$_{FLAG}FATP4$ MDCK	canine kidney cells stably over-expressing shortened human $_{FLAG}$ FATP4	-	S. Staudacher, AG J. Füllekrug, University Hospital Heidelberg	MEM	at post-confluency, 1/8 for propagation
for retrovirus production					
Phoenix gp	gag pol expressing human embryonic kidney cells	SD-3514	MPI-CBG, Dresden	DMEM	at sub-confluency, 1/6 for propagation
for adenovirus production					
Hek293	human embryonic kidney cells containing adenovirus 5 DNA	CRL-1573	MPI-CBG, Dresden	DMEM	at sub-confluency, 1/6 for propagation
human embryonic kidney (HEK), Madin-Darby canine kidney (MDCK)					

4.6.2 Viruses

Retroviral stocks were kept frozen at -80 °C. Adenoviruses were stored in 50 % storage buffer at -20 °C.

Table 20: Viruses used in this study.

virus	characteristics	based on	reference
retroviruses			
$ACSL1_{FLAG}$	retroviral rat $ACSL1_{FLAG}$ overexpression	ACSL1.pRJ (JF 659)	this work
Cav-1	Cav-1 knock down by RNA interference	cav1-ko.pRVH1 puro (JF 383)	this work
pQCXIP-J	generated from retroviral expression vector (used as control in retroviral infection)	pQCXIP-J (JF 596)	this work
adenoviruses			
$CD36_{FLAG}$	adenoviral human $CD36_{FLAG}$ overexpression	CD36.pAdv (JF 790)	this work
FATP4	adenoviral murine FATP4 overexpression, cytosolic GFP expression	FATP4.pAdTrack-CMV (JF 430)	J. Füllekrug, University Hospital Heidelberg/this work

4.6.3 Bacteria

For propagation and cloning procedures *Escherichia coli (E. coli)* bacteria were cultured in liquid LB medium or on LB plates at 37 °C. Antibiotics were added at a concentration of 100 µg/ml for ampicillin and 30 µg/ml for kanamycin for selection purposes.

Table 21: Bacteria used in this study.

strain	characteristics/genotype	reference
Escherichia coli DH5α	Dam- and Dcm-methylation positive bacterial cells for standard cloning procedures, high yield and purity of produced plasmid DNA	Invitrogen, Frankfurt am Main
	fhuA2 Δ(argF-lacZ)U169 phoA glnV44 Φ80 Δ(lacZ)M15 gyrA96 recA1 relA1 endA1 thi-1 hsdR17	
Escherichia coli K12 ER2925	Dam- and Dcm-methylation negative bacterial cells, used in cloning procedures with Dam/Dcm-sensitive restriction enzymes	New England Biolabs, Frankfurt am Main
	ara-14 leuB6 fhuA31 lacY1 tsx78 glnV44 galK2 galT22 mcrA dcm-6 hisG4 rfbD1 R(zgb210::Tn10)TetS endA1 rpsL136 dam13::Tn9 xylA-5 mtl-1 thi-1 mcrB1 hsdR2	
Escherichia coli BJ5183-AD-1	streptomycin and ampicillin resistant electroporation competent bacterial cells, predestined for homologous recombination events aiming at the generation of adenoviral expression plasmids	Stratagene/Agilent Technologies, Waldbronn
	*end*A1 *sbc*BC *rec*BC *gal*K *met thi*-1 *bio*T *hsd*R (Strr) [pAdEasy-1 (Ampr)]	

4.7 Software

Table 22: Software used in this study.

software	reference
Adobe Photoshop 6.0.1	Adobe Systems Incorporated (USA)
AUTOsoft version 2.3.2	Autobio Co. LTD, Zhengzhou (China)
BioEdit version 5.0.9	Tom Hall, Ibis Biosciences, Carlsbad (USA) http://www.mbio.ncsu.edu/BioEdit/bioedit.html
cell^D 2.5	Olympus, Hamburg
Clone Manager 5.01	Scientific & Educational Software, Cary (USA)
ClustalW2	European Bioinformatics Institute, Cambridge (UK) http://www.ebi.ac.uk/Tools/msa/clustalw2/
EndNote X2	Thomson Reuters Corporation, New York (USA)
ImageJ 1.45s	Wayne Rasband, National Institutes of Health, Bethesda (USA) http://imagej.nih.gov/ij
Inkscape 0.48	Inkscape Community http://inkscape.org/
Leica Confocal Software LCS Lite	Leica, Wetzlar
Microsoft® Office Excel 2003 SP3	Microsoft Corporation, Redmond (USA)

4.8 Molecular biology techniques

4.8.1 Preparation of chemically competent *E. coli*

One commonly used method in molecular biology is the amplification of plasmid DNA by its introduction and subsequent expression in bacteria. Typically, competent *E. coli* are used due to their increased susceptibility to the uptake of exogenous DNA. There are two kinds of competent *E. coli* present that are either suitable for heat shock transformation (chemically competent cells) or electroporation (electrocompetent cells). Most often, *E. coli* DH5α are employed as the standard bacterial strain as they give a high yield and purity of plasmid DNA. In case of cloning procedures including the use of Dam/Dcm-sensitive restriction enzymes *E. coli* K12 ER2925 can be used alternatively. The following protocol for the preparation of chemically competent *E. coli* is based on the publication of Inoue *et al.* (Inoue *et al.*, 1990).

Chemically competent *E. coli* DH5α were plated on a LB plate without antibiotics and grown at 37 °C over night. The following day, a pre-culture was inoculated from a single colony in 50 ml LB without antibiotics and incubated at 37 °C and 230 rounds per minute (rpm) on a shaker for approximately 8 h. Different dilutions of the pre-culture were prepared in 250 ml LB ranging from 1:25 to 1:1,000 for an optical density measured at a wavelength of 600 nm (OD_{600}) < 1. Bacteria were cultured at RT and 230 rpm over night and during the next day until reaching an OD_{600} = 0.55 – 0.6. The suspension was chilled on ice for 10 min, followed by centrifugation at 2,500 g and 4 °C for 10 min. The remaining pellet was resuspended in 80 ml ice-cold ITB, chilled on ice for another 10 min and again centrifuged at 2,500 *g* and 4 °C for 10 min. Once more the pellet was resuspended in 20 ml ice-cold ITB and incubated on ice for 10 min. 1.5 ml DMSO were added to achieve a final concentration of 7 %, mixed gently and the suspension aliquoted on ice. The competent cells were flash frozen in liquid nitrogen and stored at -80 °C.

4.8.2 Heat shock transformation of *E. coli*

Heat shock transformation is a frequently used method for enhancing the introduction of exogenous plasmid DNA into competent bacterial cells. For this purpose, 0.5 µl DNA were mixed with 19 µl of chemically competent *E. coli* and

incubated on ice for 10 min. The heat shock was performed in a pre-heated thermal mixer at 42 °C for 1 min, followed by chilling the bacteria on ice for another 2 min. *E. coli* were afterwards spread on LB plates and incubated at 37 °C over night.
Depending on the introduced plasmid LB plates typically contained either 100 µg/ml ampicillin or 30 µg/ml kanamycin for selection purposes. Bacteria being selected for ampicillin could be immediately spread on the respective LB plates. On the contrary, bacteria that were expected to be resistant to kanamycin were incubated in 1 ml LB medium without antibiotics at 37 °C and 500 rpm on a shaker for 40 min. Afterwards, *E. coli* were pelleted by centrifugation at 3,350 g for 2 min, resuspended in 100 µl LB medium and finally spread on LB plates. The day after transformation, results were evaluated by counting the newly formed bacterial colonies.

4.8.3 Electroporation of *E. coli*

An alternative tool utilized for the transformation of bacterial cells is the short application of an external electric field. Thus, holes are created within the cell membrane thereby facilitating the uptake of plasmid DNA for a transient period of time. In this study, the electroporation of *E. coli* was exclusively conducted when performing homologous recombination events as part of the cloning procedure of adenoviral plasmids. For this purpose, electrocompetent *E. coli* BJ5183-AD-1 were used.
Hence, 5 µg of adenoviral vector DNA were mixed with 20 µl of electrocompetent *E. coli*, transferred into an electroporation cuvette and chilled on ice. The electric shock was performed in an electroporator by applying 2,500 V, 200 Ω and 250 µF. Afterwards, bacteria were resuspended in 500 µl LB medium without antibiotics and, in the case of adenoviral recombinants, immediately spread on LB plates containing 30 µg/ml kanamycin for selection.

4.8.4 Small and large scale preparation of plasmid DNA

Plasmid DNA was extracted and purified from *E. coli* by using commercially available systems.
The function of the Nucleo Spin Plasmid Kit, which is suitable for small scale plasmid preparation, is based on the principle of plasmid DNA liberation from

bacteria by alkaline lysis. The DNA is subsequently bound to a silica membrane, purified by washing and finally eluted in low salt buffer. Briefly, bacterial cells from 1 - 5 ml over night culture were harvested by centrifugation at 11,000 g for 30 s. The pellet was resuspended in 250 µl Buffer A1 by vortexing followed by addition of 250 µl Buffer A2 for cell lysis. After incubation at RT for 5 min genomic DNA and proteins were precipitated by using 300 µl Buffer A3. Samples were centrifuged at 11,000 *g* for 5 min and the supernatant transferred to a plasmid column to which DNA was bound during a centrifugation step at 11,000 g for 1 min. The DNA was afterwards purified by washing with 600 µl ethanolic Buffer A4 and centrifugation at 11,000 g for 1 min, followed by a second round of centrifugation at 11,000 g for 2 min in order to dry the silica membrane. Finally, the purified plasmid DNA was eluted in 50 µl of AE buffer by incubation at RT for 1 min followed by centrifugation at 11,000 g for 1 min.

For large scale plasmid preparation the Marligen PowerPrep HP Plasmid Purification System was used. Its working principle is equally based on alkaline lysis followed by a precipitation step. Purification of the released DNA is performed with help of an anion exchange resin with subsequent elution of the plasmid DNA under high salt conditions followed by isopropanol precipitation for desalting. In preparation, columns were equilibrated with 30 ml of equilibration buffer. Bacteria from 100 ml over night culture were harvested by centrifugation at 6,000 g for 10 min and resuspended in 10 ml Cell Suspension Buffer, followed by alkaline lysis in 10 ml Cell Lysis Solution at RT for 5 min. Proteins and genomic DNA were precipitated with 10 ml Neutralization Buffer and samples centrifuged at 15,000 *g* for 10 min. The supernatant was then transferred to an equilibrated column and the bound plasmid DNA subsequently washed with 60 ml Washing Buffer. In the following, the plasmid DNA was eluted with 15 ml Elution Buffer and precipitated by addition of 10.5 ml isopropanol and centrifugation at 15,000 g and 4 °C for 30 min. After washing the pellet in 5 ml 70 % ethanol and one final round of centrifugation at 15,000 g and 4 °C for 5 min the air-dried pellet was dissolved in 500 µl TE Buffer. Obtained DNA yields ranged from 0.4 – 2.8 µg/µl.

4.8.5 Measurement of nucleic acid concentrations

Optical density (OD) measurement was performed in order to assess the concentration and purity of nucleic acids in solution. Hence, the respective samples were diluted in sterile H_2O at a final volume of 100 µl and measured in an ultraviolet (UV) cuvette at a wavelength of 260 nm. Multiplication of the obtained extinction value (E_{260}) with 50 (DNA samples) or 40 (RNA samples) under consideration of the dilution factor gave the overall nucleic acid concentration in ng/µl. By additional OD measurement at a wavelength of 280 nm, respectively 230 nm, information could be obtained concerning the purity of the analyzed samples. Accordingly, contamination with proteins gave an $E_{260/280} < 1.8$ for DNA and $E_{260/280} < 2$ for RNA. Impurity due to salt or solvents showed as $E_{260/230} < 2$ for DNA and RNA samples. Typically, DNA samples used in cloning procedures displayed an $E_{260/280} \geq 1.8$ and $E_{260/230} \geq 2$.

4.8.6 Agarose gel electrophoresis

During cloning procedures DNA fragments were analyzed according to their molecular size by agarose gel electrophoresis. Therefore, 0.4 % or 1 % agarose was dissolved in 1 x TAE buffer by microwave heating. For later visualization of the DNA samples under UV light 3.5 µl 10 mg/ml ethidiumbromide were added before pouring the mixture into a sealed gel casting tray. Samples were mixed with 6 x DNA loading dye and filled into the gel pockets. 5 µl of a 1 kb molecular weight standard were loaded on each gel, thus allowing the identification of DNA samples in a range of 250 – 10,000 bp by comparison with the utilized standard marker. Agarose gels were run at 100 – 120 V for 30 – 60 min and results documented by photography.

4.8.7 Polymerase chain reaction (PCR)

The method of PCR was first described by Mullis *et al.* (Mullis *et al.*, 1986) and within this work used in order to generate DNA fragments to which restriction sites for later cloning steps were added. Thus, preparative PCR was performed as indicated below. Results were analyzed by agarose gel electrophoresis.

Table 23: Standard conditions for performing a preparative PCR.

1 x PCR reaction mix		**program**		
1 µl	DNA (1 µg/µl)	5 min	94 °C	
33 µl	H_2O			
5 µl	10 x reaction buffer	30 s	94 °C	20 cycles
6 µl	$MgCl_2$ (25 mM)	30 s	59 °C	
2 µl	dNTP mix (10 mM each)	30 s	72 °C	
1 µl	forward primer (100 pmol)			
1 µl	reverse primer (100 pmol)	7 min	72 °C	
1 µl	Taq DNA Polymerase	hold	4 °C	

4.8.8 Restriction digest

The preparative specific cleavage of DNA fragments by restriction enzymes was used during cloning procedures in order to generate fragments needed for ligation or to linearize adenoviral plasmids for homologous recombination events. In addition, analytical restriction digests were performed to control the outcome of cloning procedures.

A typical reaction mix was composed of 1 – 5 µg DNA, the appropriate restriction enzyme in 2 – 10 x excess as well as 3 - 5 µl 10 x reaction buffer and was adjusted to a final volume of 30 – 50 µl for preparative digests or 10 µl for analytical purposes with H_2O. If required, 100 ng/µl BSA were included in the mixture. The amount of utilized enzyme was calculated in reference to the specific enzyme activity, considering that 1 unit of enzyme would digest 1 µg of DNA within 1 h. Reactions were carried out at 37 °C for 1.5 – 3.5 h, followed by heat inactivation of the enzyme at 80 °C for 20 min if necessary.

4.8.9 Purification of DNA

The purification of DNA samples was performed by using the Nucleo Spin Extract Kit II, a system which is based on the binding of DNA to a silica membrane followed by washing with ethanolic buffer. The pure DNA is subsequently eluted in low salt buffer.

Typically, DNA purification was necessary during cloning procedures either in order to clean up samples after restriction digest or PCR or following agarose gel

electrophoresis so as to extract DNA samples from the respective agarose gel. In the latter case, fragments were excised from the agarose gel and the weight was determined. 200 µl of Binding Buffer NT were added per each 100 mg agarose and samples incubated at 50 °C for 5 – 10 min to completely dissolve the agarose. Alternatively, one volume of sample obtained from PCR or restriction digest was mixed with two volumes of Binding Buffer NT. Subsequently, the individual samples were loaded onto columns and the contained DNA bound to the silica membrane by centrifugation at 11,000 g for 1 min. Samples were washed with 700 µl Washing Buffer NT3 and again centrifuged at 11,000 *g* for 1 min, followed by a second centrifugation step at 11,000 g for 2 min in order to dry the silica membrane. Purified DNA was afterwards eluted in 15 – 50 µl Elution Buffer NE by incubation at RT for 1 min and subsequent centrifugation at 11,000 g for 1 min.

4.8.10 Ligation

Ligation reactions were carried out in order to clone a gene of interest into an appropriate expression vector during the generation of adenoviral plasmids, typically using restriction digests and purified DNA fragments. Due to the use of a quick ligation systems reactions could be carried out in a minimum time and at RT. For every ligation approach two controls were prepared, containing either only vector or insert DNA whereas the specific ligation sample possessed both parts. Reaction mixtures were prepared as shown in Table 24 and incubated for 10 – 15 min at RT, followed by heat shock transformation in *E. coli*.

Table 24: Reaction mixtures and conditions for standard ligation procedures.

vector control	insert control	ligation sample	chemical
1.0 µl	-	1.0 µl	vector
-	1.0 µl	1.0 µl	insert
2.5 µl	2.5 µl	2.5 µl	2 x Quick ligation buffer
1.0 µl	1.0 µl	-	H_2O
0.5 µl	0.5 µl	0.5 µl	Quick T4 DNA Ligase
10 - 15 min, RT			

The next day, the outcome of the ligation reaction was evaluated by counting the bacterial colonies. In case of a successful ligation no colonies were to be expected for the insert control, whereas colonies obtained from the vector control indicated self ligation of the vector and allowed for the estimation of the percentage of positive colonies for the ligation approach.

4.8.11 Cloning of adenoviral plasmids

Adenoviral plasmids were generated in order to produce adenoviruses for transient infection of target cell lines. Therefore, the AdEasy cloning system was used following the protocol described by He *et al.* (He *et al.*, 1998) as well as Luo *et al.* (Luo *et al.*, 2007). In general, the procedure is based on a two-vector-system consisting of shuttle plasmids as well as adenoviral backbone plasmids. The specific gene of interest is first cloned into a shuttle-vector by standard cloning procedures. There are different shuttle vectors available which usually harbour the 5' end of the adenoviral genome with early gene E1 and other genes, such as E2, E3 or E4, being deleted in order to generate space for transgene incorporation and prevent adenoviral replication. Expression of the gene of interest is driven by a CMV promoter. As a special feature, pAdTrack shuttle vectors contain a transgene independent GFP cassette which can be used as a control for successful infection of the various target cells. Shuttle vectors expressing the respective gene of interest are subsequently linearized and recombined into adenoviral backbone vectors by homologous recombination in *E. coli*. The resulting vector contains all genes required for virus production in a specialized packaging cell line but lacks genes essential for adenovirus production in naturally occurring cells.

In this work two different adenoviral expression plasmids were cloned, CD36.pAdv and GFP-CD36.pAdv, aiming to achieve an overexpression of FLAG tagged human CD36 in the respective target MDCK cell lines.

CD36.pAdv

Human $CD36_{FLAG}$ was amplified by PCR from template CD36-FLAG.pcDNA3, thereby adding restriction sites for later cloning steps to the $CD36_{FLAG}$ sequence. For PCR, s_CD36.FLAG(adeno) was used as sense primer and a_CD36.FLAG(adeno) as antisense primer. The resulting PCR product was run on an agarose gel, purified and subsequently cut using the restriction enzymes BglII and XhoI. Vector pAda/pshuttle-CMV was equally digested with BglII and XhoI, followed by agarose gel electrophoresis. The DNA band of the appropriate size was extracted from the gel and purified. A standard ligation procedure was performed in order to generate adenoviral shuttle plasmid CD36.pAda and resulting clones screened by restriction digest with NdeI. Successful cloning of CD36.pAda was confirmed by sequencing. Shuttle plasmid CD36.pAda was subsequently linearized by digestion with PmeI, purified and introduced into BJ5183-AD-1 electroporation competent *E. coli*. Thereby, homologous recombination events were triggered aiming at the incorporation of CD36.pAda into the adenoviral backbone vector pAdEasy-1, thus generating CD36.pAdv. Resulting clones were analyzed by restriction digest with PacI and positive clones identified due to their characteristic appearance on an agarose gel with DNA bands being evident at 30 kb and 3 kb, alternatively 30 kb and 4.5 kb.

GFP-CD36.pAdv

During the cloning of GFP-CD36.pAdv XbaI was used. Depending on the flanking sequences of the restriction site the enzyme may be sensitive to methylation by Dam methylases. This required part of the cloning process to take part in Dam negative bacterial cells. Hence, the appropriate plasmids primarily had to be transformed into Dam negative *E. coli* and the respective plasmid DNA prepared in order to enable successful cloning.

Vector plasmid pEGFP-N1 and insert plasmid GFP-CD36-FLAG were initially digested with AgeI and XbaI, run on an agarose gel and the specific products purified. A standard ligation reaction was performed to create subcloning plasmid GFP-CD36.pNice. Resulting bacterial colonies were screened for positive clones by restriction digest with KpnI and XbaI. The newly created plasmid GFP-CD36.pNice as well as the adenoviral vector pAda/pshuttle-CMV were subsequently cut with KpnI and XbaI, ran on an agarose gel and the specific DNA bands purified. After

performing a standard ligation procedure clones were analyzed by restriction digest with BglII and results verified by sequencing. The newly cloned adenoviral shuttle plasmid GFP-CD36.pAda was afterwards linearized with PmeI, purified and transformed into BJ5183-AD-1 *E. coli* by electroporation. By homologous recombination of GFP-CD36.pAda and the adenoviral backbone vector pAdEasy-1 the adenoviral expression plasmid GFP-CD36.pAdv was created. Again, successful cloning was verified by digestion with PacI.

4.9 Biochemistry techniques

4.9.1 Bradford protein assay

The total protein concentration in a solution was determined by a colorimetric assay based on the protocol of Bradford (Bradford, 1976). The Bradford protein assay dye contains Coomassie brilliant blue R-250 which can display either red or blue coloring. Protein binding stabilizes the blue form of the dye with an absorption maximum of 595 nm. Thus, the increase in absorption is directly proportional to the amount of blue dye in the solution and therefore can be used as a measure for protein content.

Cells were lysed in 1 N NaOH, therefore BSA was dissolved at 1 mg/ml in 1 N NaOH in order to establish a calibration curve samples could be compared to. A BSA dilution series from 2 – 12 ng in 1 N NaOH was prepared and adjusted to a final volume of 25 µl. For protein measurement, cells were harvested by incubation in 1 N NaOH for 60 min. 25 µl of each BSA dilution as well as different amounts of the respective sample were loaded in triplicates on a 96-well cell culture plate. The Bradford protein assay dye stock solution was diluted 1:5 in H_2O and 200 µl thereof added to each well. Absorption was measured in a microplate reader at 595 nm and sample values analyzed by reference to values obtained from the BSA standard curve.

4.9.2 Sodium dodecyl sulfate polyacrylamide gel electrophoresis (SDS-PAGE)

The method of SDS-PAGE allows the separation of proteins depending on their specific chain length. SDS, an anionic detergent, linearizes proteins and charges

them negatively thus allowing a separation by size depending on the electrophoretic mobility of the respective proteins in a polyacrylamide gel.

Gels were cast in two steps, starting with the preparation of the 8 % resolving gel. Components were used in amounts as indicated below (Table 25) and mixed by vortexing before and after addition of TEMED which initiated the polymerization of the gel. The mixture was applied to a gel caster system and isopropanol added on top of the gel in order to smoothen the surface and prevent formation of bubbles. In a second step, the 5 % stacking gel was prepared under the same conditions and poured on top of the resolving gel after the isopropanol had been discarded. For better visualization of the gel pockets a small amount of bromphenolblue was added. Gel pockets for sample application were formed by insertion of a comb in the gel caster system. Hardened gels were either stored in moist paper at 4 °C or immediately used for gel electrophoresis.

Table 25: Composition of stacking and resolving gels as used in SDS-PAGE.

Stacking gel (5 %)		**resolving gel (8 %)**	
1.7 ml	H_2O	2.55 ml	H_2O
312.5 µl	0.5 M Tris/HCl pH 6.8	1.00 ml	2 M Tris/HCl pH 8.8
425.0 µl	30 % acrylamide/bis solution	1.35 ml	30 % acrylamide/bis solution
25.0 µl	10 % APS	50 µl	10 % APS
25.0 µl	10 % SDS	50 µl	10 % SDS
vortex		**vortex**	
2.5 µl	TEMED	4 µl	TEMED

For sample preparation, cell pellets were dissolved in 2 x Laemmli buffer and heated at 95 °C and 1,400 rpm on a shaker for 5 min thus leading to the denaturation of proteins. When loading the gel, 5 µl of a protein molecular weight marker were applied to one of the gel pockets in order to later serve as size standard to which sample signals could be compared to. 15 – 30 µl of the respective samples were applied to the remaining gel pockets and the gel was run at 120 V, 200 mA and 50 W for 70 min in running buffer. The progress of the gel electrophoresis could be monitored by observation of the tracking dye bromphenolblue which was included in the Laemmli buffer and due to its low molecular weight moved ahead of most of the negatively charged proteins towards the positively charged anode.

4.9.3 Western blotting

By using the Western blotting technique proteins that have been separated by gel electrophoresis are transferred to a nitrocellulose membrane and afterwards detected by incubation with specific antibodies. Consequently, this process makes proteins available for subsequent densitometric quantification.

Proteins were transferred from the respective SDS gel to nitrocellulose membranes by the semi-dry blotting procedure. Therefore, for every gel to be blotted two stacks of three blotting papers cut to approximate gel size were soaked in blotting buffer. A nitrocellulose membrane was cut to gel size and shortly soaked in blotting buffer. The SDS gel was equally incubated in blotting buffer before being transferred onto one blotting paper stack sitting in a semi-dry blotting chamber. The equilibrated nitrocellulose membrane and the second blotting paper stack were piled on top and potential air bubbles removed by gently applying pressure onto the stack from the middle towards the border. Electroblotting was performed by administering 100 mA/blotted gel at 120 V and 50 W for 1 h, thus pulling the negatively charged proteins from the SDS gel onto the nitrocellulose membrane towards the positively charged electrode of the blotting chamber.

The efficiency of the protein transfer was controlled by subsequent staining of the nitrocellulose membrane in Ponceau Red, a dye with a detection limit of protein amounts around 0.5 – 1 µg. Its water solubility enables an intense, non-permanent and unspecific protein staining with low background signal. Results were documented by scanning of the stained membranes.

In order to prevent unspecific antibody binding during following incubation steps membranes were first of all blocked in 2 % nonfat dry milk dissolved in TBS-Tween. Incubation was carried out under gentle agitation for 30 min at RT. For specific labeling of a given protein the respective primary antibody was diluted in 2 % nonfat dry milk dissolved in TBS-Tween and applied to the blocked membrane. Samples were then incubated at RT for 1 h or at 4 °C over night on a rocker. Thereafter, membranes were washed several times in TBS-Tween to eliminate unbound antibody residues and subsequently incubated with the respective species-specific secondary antibody equally diluted in 2 % nonfat dry milk dissolved in TBS-Tween. After incubation at RT for 1 h blots were again rinsed several times in TBS-Tween for residual antibody removal.

All utilized secondary antibodies are linked to the reporter enzyme horseradish peroxidase which under cleavage of a chemiluminescent agent produces a luminescent signal that can be detected by exposure to a photographic film. The obtained signal is proportional to the amount of bound protein and can thus be used as a measure for protein quantity. Hence, the readily probed and washed membranes were air-dried, covered with ECL solution and incubated at RT for 1 min. Membranes were then exposed to photographic Amersham Hyperfilm ECL films in a darkroom. Films were afterwards developed by using a commercial developer machine and signals quantified with ImageJ.

4.9.4 SDS-PAGE analysis with ImageJ

ImageJ is an open source program for image processing that has been developed at the National Institute of Health with one of its potential applications including the densitometric quantification of western blot signals.

Results obtained by western blotting were digitalized by scanning the developed photographic films and saving them as jpg.files at 300 dots per inch (dpi). The single protein bands were measured using ImageJ, resulting in one profile blot for each captured signal. Profile blots showed the relative density of the respective lanes, with darker signals giving higher peaks and broader signals resulting in wider peaks. Background signals were substracted from the final quantification value by drawing a baseline on the bottom of each peak, thereby excluding the underlying area from the measurement. The obtained numbers for the measured areas under the peaks showed arbitrary units and could thus only be compared within the context of one single blot. In order to calculate absolute amounts of specific proteins the dilution series of an appropriate purified protein was loaded on each gel together with the respective samples. During the quantification process a standard curve was established using the arbitrary units obtained from the signals of the dilution series. Afterwards, the absolute amount of a specific protein on a western blot was calculated by referring its arbitrary units to the appropriate standard curve. Hence it was possible to quantify ng protein of any given protein signal.

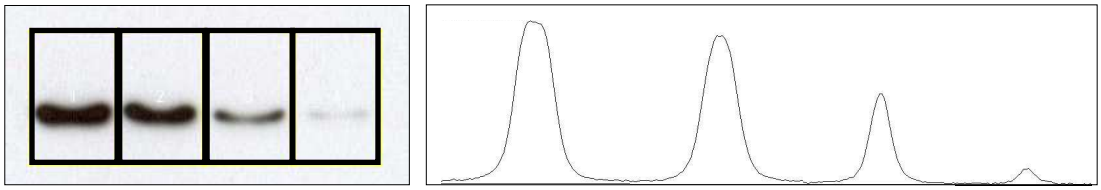

Figure 5: Quantification of western blot signals by using ImageJ.
Western blot lanes were quantified using ImageJ with obtaining a profile blot for each measured lane. Darker signals resulted in higher peaks, thus indicating a higher amount of detected protein on the blot.

4.9.5 Coomassie blue protein staining

Coomassie brilliant blue, an anionic dye, is commonly used for the unspecific staining of proteins and allows the visualization of protein bands in a SDS gel.

After finishing the SDS-PAGE process gels were incubated in 0.1 % comassie blue staining solution under gentle agitation for at least 2 h on a rocker. Due to the contained acetic acid proteins were simultaneously fixed. In order to reduce the background signal, gels were subsequently washed for several hours in destain solution which was identical to the staining mixture but lacking the dye. If the destaining process was not completely finished after several hours a final destain step was performed at 4 °C over night. The following day, stained gels were digitalized by scanning and signals quantified using ImageJ.

4.9.6 Protein purification

In order to generate protein standards for western blot analysis the ANTI-FLAG M2 affinity gel system from Sigma-Aldrich was used. Its functional principle is based on mouse IgG monoclonal antibodies that are covalently bound to agarose beads which allow for the purification of FLAG fusion proteins.

Thus, MDCK cells stably overexpressing FLAG-tagged FATP4 protein were seeded on 145 cm^2 cell culture dishes and grown to confluence. Cells were harvested with a rubber scraper and pelleted by centrifugation at 100 g and 4 °C for 5 min, followed by washing in 1 x PBS and repetition of the centrifugation step. The resulting pellet was either stored at –80 °C or immediately used for protein purification.

In preparation, the agarose beads were washed in order to eliminate the glycerol contained in the storage solution and to resuspend the beads in the respective working buffer. For each three 145 cm^2 cell culture dishes 25 µl agarose gel beads were taken up in 500 µl TNEX buffer, mixed by vortexing and centrifuged at 1,000 *g*

and 4 °C for 5 min. This step was repeated twice, finally discarding all but 50 µl of residual buffer volume containing the washed agarose beads.

A cell pellet harvested from three 145 cm^2 cell culture dishes was resuspended in 1.5 ml TNEX buffer and incubated on ice for 30 min with pipetting the mixture up and down after 10 min and 20 min. The Triton X-100 contained in the TNEX buffer was used to disrupt cell membranes and solubilize proteins for further purification steps. The sample was then centrifuged at 1,000 *g* and 4 °C for 5 min in order to separate cell debris and solubilized components. The supernatant was transferred into a new reaction tube and again centrifuged, this time at a higher speed of 13,000 *g* at 4 °C and for a prolonged time of 15 min to eliminate remaining debris. The resulting supernatant was carried over into the reaction tube containing the washed agarose beads. FLAG fusion proteins were bound to the IgG covered beads over night at 4 °C while rotating at slow speed. The following day, beads were sedimented by centrifugation at 1,000 g and 4 °C for 5 min. The bead-bound proteins were washed twice in 1 ml TNEX buffer and twice in 1 ml TNE buffer in order to eliminate the Triton X-100, always followed by centrifugation under the above conditions. After the final round of centrifugation all supernatant was carefully discarded, the remaining sample resuspended in 60 µl SDS-PAGE special sample buffer and incubated at 95 °C for 5 min at 1,400 rpm on a shaker. For later western blot analysis 0.6 µl ß-mercaptoethanol were added for protein denaturation and samples again incubated at 95 °C for 5 min at 1,400 rpm on a shaker. The purified proteins were subsequently stored at -20 °C until further use. Purification of FLAG-tagged FATP4 protein was performed at two different time points, yielding samples with 18,7 ng/µl and 47,5 ng/µl, respectively.

4.9.7 Establishment of a $FATP4_{FLAG}$ protein standard

For quantification of the specific amount of overexpressed $CD36_{FLAG}$, FATP4 or $ACSL1_{FLAG}$ protein within a given cell pellet the purified protein standard $FATP4_{FLAG}$ was used. Briefly, results were obtained by comparing different amounts of the specific sample to a $FATP4_{FLAG}$ standard curve via western blotting.

First of all, purified $FATP4_{FLAG}$ protein was quantified. Therefore, 1/4 - 1/3 of the total protein amount was loaded on a SDS gel together with a dilution series of BSA in 1 x PBS, ranging from 0.25 – 10 µg. Western blotting was performed and the

obtained protein bands analyzed by using ImageJ, thereby assessing the specific amount of $FATP4_{FLAG}$ protein in ng/µl. For subsequent analysis, two different amounts of the respective protein sample were applied to a SDS gel together with defined amounts of $FATP4_{FLAG}$ protein, thus yielding a standard curve to which sample signals could be compared to. Quantification of $CD36_{FLAG}$ and $ACSL1_{FLAG}$ protein was performed by using the rb-α-FLAG antibody whereas for analysis of FATP4 protein the rb-α-FATP4 (C3/5) antibody was applied.

During the course of this work three different $FATP4_{FLAG}$ protein standards were prepared which differed in their specific concentration. In order to obtain reliable results, one of the three standards was chosen as reference to which the remaining two standards could be referred to. Accordingly, the same protein samples were quantified once by using the reference standard and once by using one of the remaining standards. Results were analyzed by ImageJ and if necessary a correction factor calculated for the analyzed standard.

For production and purification of protein standards two different versions of the FLAG-tagged FATP4 protein were used, including full length FATP4 ($FATP4_{FLAG}$) as well as a shortened version of FATP4 ($_{FLAG}$ FATP4), running at 72 kDa and 33 kDa respectively. The latter protein was lacking its membrane anchor for facilitation of the purification process und had a FLAG-tag attached to the N-terminus (as opposed to the C-terminal FLAG-tag of the full length protein). Western blot analysis revealed that the localization of the FLAG-tag had an influence on the signal strength obtained by application of the rb-α-FLAG antibody. Accordingly, the C-terminal FLAG accounted for a stronger signal than the N-terminally located FLAG-tag. Thus, when comparing the shortened $_{FLAG}$FATP4 standard protein to the reference standard two independent correction factors had to be calculated: one for the rb-α-FLAG antibody and a second one for the rb-α-FATP4 (C3/5) antibody.

4.9.8 Protein quantification by western blotting

To quantify protein expression levels, 22 h after seeding MDCK cells were harvested by trypsinization from 12-well cell culture plates (1 well/sample). Cell pellets were taken up in 100 µl 2 x Laemmli buffer and further diluted up to 1:100 in 2 x Laemmli

buffer for FATP4 and ACSL1 samples if the specific protein amounts were very high.

Two different quantities of each sample were loaded on a SDS gel together with a dilution series of $FATP4_{FLAG}$ protein standard to establish a standard curve. The range of the dilution series was adapted depending on the amount of loaded protein samples, reaching from 0.125 – 15 ng. After western blotting, protein bands were quantified by densitometric analysis. Absolute quantities of $CD36_{FLAG}$, FATP4 and $ACSL1_{FLAG}$ protein were calculated by reference to the $FATP4_{FLAG}$ standard curve. For each sample, the respective mean was assessed. An exemplary quantification is shown in Figure 6.

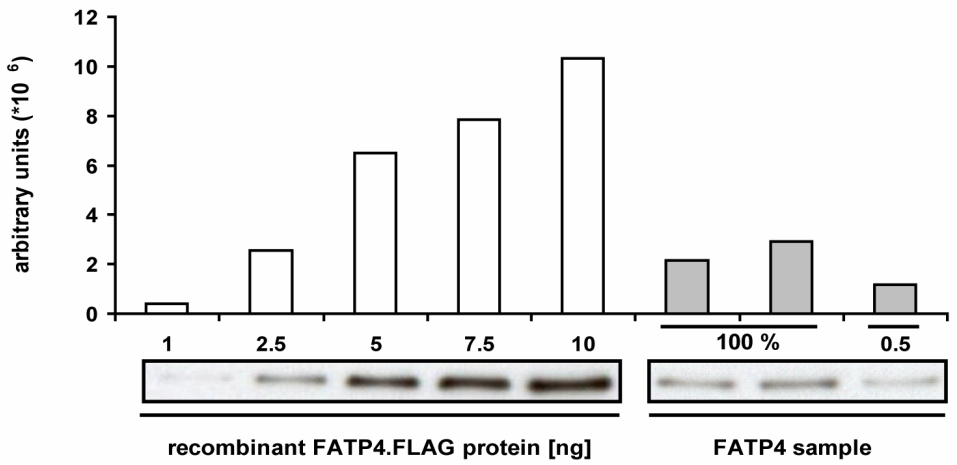

Figure 6: Quantification of FATP4 protein amounts by western blotting.
Wildtype MDCK cells infected with FATP4 adenovirus were harvested from 12-well cell culture plates by trypsinization. Two different protein amounts of the same sample were loaded on a SDS gel, with the higher amount loaded in duplicates. A $FATP4_{FLAG}$ protein standard dilution series was applied to the same gel. Protein bands obtained from western blotting were analyzed densitometrically with ImageJ and sample values related to the $FATP4_{FLAG}$ standard curve.

4.9.9 Radioactive oleate uptake assays

In order to determine the capacity of different kinds of cells to take up fatty acids under various conditions radioactive oleate uptake assays were performed. Cells were incubated with ^{3}H-oleic acid mixed with non-radioactive oleate. With reference to the incorporated amount of radioactivity the overall oleate uptake was calculated.

In preparation of performing the assay MDCK cells were seeded the previous day at a density of 400,000 cells/well on 12-well cell culture plates. For all experiments cells were cultured in triplicates. Whenever necessary MDCK cells were infected with the appropriate adenovirus 6 h after seeding and incubated over night. The following day, a radioactive labeling mix was prepared immediately before starting

the assay. A typical labeling mix was composed of 200 µM oleate and 100 µM BSA with 0.5 Ci/mol. The appropriate amounts of non-radioactive oleic acid stock and ^{3}H-oleic acid were mixed and the respective solvents evaporated under a weak nitrogen flow. In the following, the remaining fatty acids were taken up in 25 mM NaOH and subsequently bound to 800 µM fatty acid free BSA by vortexing. Culture medium without FBS was added up to the final volume, again mixed by vortexing and until further use stored at 37 °C.

Table 26: Composition of a labeling mix as used in radioactive uptake assays.

labeling mix		
amount	**concentration**	**chemical**
45.2 µl	20 µg/µl	oleic acid stock
1.6 µl	1 µCi/µl	^{3}H-oleic acid (50 µM)
evaporation of solvent under nitrogen flow		
153.6 µl	25 mM	NaOH
2,000 µl	800 µM	BSA without fatty acids
13,846 µl	-	culture medium without FBS

Approximately 22 h after seeding 800 µl of prewarmed labeling mix were applied to each well and incubated for either 5 min or 3 hours, the latter taking place at 37 °C and 5 % CO_2. To stop the reaction and prevent further fatty acid uptake, cells were washed twice with ice-cold STOP-mix after the indicated time followed by two washing steps with ice-cold PBS. Remaining fatty acids were thus bound by the BSA contained in the STOP-mix, whereas the PBS removed residual BSA in order to prevent falsification of the results later obtained in the Bradford protein assay. Cells were subsequently lysed by incubation in 500 µl 1 N NaOH per well for 1 h at RT. Lysates were afterwards transferred to Safe-Lock tubes and vortexed vigorously. 250 µl of lysate were used for the quantification of the contained radioactivity in a liquid scintillation counter while part of the remaining sample served for determination of the total protein amount by using the Bradford protein assay.

For final analysis, the overall amount of incorporated fatty acids was calculated by referring to the respective radioactive proportion of utilized oleic acid. This value was subsequently related to the measured protein amount of the given samples, stating the quantity of oleate taken up in reference to the amount of protein [pmol oleate/µg protein].

4.10 Cell culture techniques

4.10.1 Culture of immortalized cell lines

All cell culture experiments were carried out by using immortalized, adherently growing cell lines. According to their specific properties, cells were utilized for radioactive uptake assays, sample collection for western blots, immunofluorescence or virus production.

MDCK cells

MDCK cells are epithelial, immortalized cells that were derived from the kidney of a female adult cocker spaniel in 1958. This cell line is frequently used in order to study transport processes as the cells show a clear apico-basolateral polarity and can be easily polarized in cell culture. In this study, all analytical experiments were carried out by utilizing MDCK cells.

Hek293 cells

Hek293 cells originate from human embryonic kidney cells which have been transformed with adenovirus 5 DNA. When growing in cell culture the cells show rather weak adherence which allows easy harvesting. This cell line provides proteins that are lacking in commonly used adenoviral vectors, thus enabling the replication of adenoviruses in a cell culture system.

Phoenix gp cells

Phoenix gp cells are a packaging cell line suitable for the production of retroviruses. They originate from a human embryonic kidney cell line and are highly transfectable with calcium phosphate. In comparison to other packaging cell lines, Phoenix gp cells exclusively express the retroviral proteins gag and pol and therefore allow for virion pseudotyping.

All cells were kept in an incubator at 37 °C and 5 % CO_2 and during propagation procedures exclusively handled under sterile conditions. For passaging, the respective culture medium was discarded and cells were washed once with 1 x PBS in order to remove medium residues. For resuspension of cells, 2 ml trypsin/T75 flask were applied and incubated at 37 °C and 5 % CO_2 for 5 min (Phoenix gp, Hek293) to 30 min (MDCK). Trypsin, a serine protease, cleaves protein bounds between adherent cells and the surface of cell culture dishes thus allowing the gentle

removal of adherent cells. Subsequently, cells were resuspended in fresh culture medium and transferred to new flasks in proportions of 1/2 to 1/8 as indicated below.

Table 27: Culture conditions for immortalized, adherently growing cell lines.

cell line	characteristics	medium	passaging
MDCK	canine kidney cells	MEM	at post-confluency, 1/2 for assays, 1/8 for propagation
Hek293	human embryonic kidney cells containing adenovirus 5 DNA	DMEM	at sub-confluency, 1/6 for propagation
Phoenix gp	gag pol expressing human embryonic kidney cells	DMEM	at sub-confluency, 1/6 for propagation

4.10.2 Freezing and thawing of cells

For long-time storage cells were kept frozen in sterile cryotubes and stocked in liquid nitrogen. Typically, cells were grown to subconfluency in a T175 cell culture flask and harvested by trypsinization. 20 ml ice-cold standard culture medium were used for resuspension and cells were sedimented by centrifugation at 4 °C and 100 g for 5 min. The supernatant was discarded and cells were taken up in 5 ml ice-cold culture medium containing 10 % DMSO. 1 ml cell stock aliquots were initially cooled down at a rate of 1 °C/h by sitting in an isopropanol filled freezing device at -80 °C. After several days, stocks were transferred to liquid nitrogen for extended storage periods.

To start a new cell culture batch stocks were thawed rapidly either at RT or in a 37 °C preheated water bath. In order to dispose of the DMSO cells were taken up in 20 ml ice-cold fresh culture medium and sedimented by centrifugation at 100 g for 5 min. The supernatant was discarded, cells were resuspended in 15 ml prewarmed medium and cultured under standard conditions.

4.10.3 Counting cells

In order to maintain comparable conditions between different experiments cells were counted before seeding. Hence, trypsinized cells were resuspended in fresh culture medium and an aliquot of several µl was counted by using a Neubauer improved counting chamber. Four independent quadrants covered by the cell suspension were counted and the mean value was calculated. Finally, the number of cells per ml was determined by multiplication of the obtained value with 10,000.

4.10.4 Production of cell pellets

For western blot analysis cells were grown in 12-well cell culture plates and at the appropriate time point harvested by trypsinization as usual. Cells were resuspended in culture medium, transferred to 1.5 ml Eppendorf Safe-Lock tubes and sedimented by centrifugation at RT and 200 g for 5 min. The supernatant was discarded and the remaining pellets were washed once in 1 x PBS, followed by centrifugation at RT and 200 g for 5 min. The PBS was again discarded and pellets were stored at -80 °C until further use.

4.10.5 Transient transfection of cells by lipofection

Lipofection is a method of introducing plasmid DNA into cells in order to obtain a transient overexpression of the inserted genetic material. Lipofection reagents form liposomes in an aqueous environment which contain the respective plasmid DNA. By fusion of the phospholipid liposome with the phospholipid cellular membrane an efficient introduction of the genetic material into the cell is enabled. In this study Lipofectamine 2000 was used as lipofection reagent.

For standard procedures cells were seeded the previous day, preferably reaching a density of 60 - 80 % at the time point of transfection. 1 h prior to transfection the culture medium was replaced by medium without antibiotics and cells kept again at 37 °C and 5 % CO_2. Two different master mixes were prepared, incubated at RT for 5 min, mixed and incubated for another 20 min at RT. 200 µl lipofection mix/12-well were added dropwise to the medium and cells were cultured for at least 4 h under standard conditions. The transfection medium was then replaced by medium without antibiotics.

Table 28: Master mix preparation for Lipofectamine transfection.

1 x master mix for lipofection (12-well)			
master mix 1		**master mix 2**	
2 µg	DNA		
add 4 µl	H_2O	4 µl	Lipofectamine 2000
100 µl	OptiMEM	100 µl	OptiMEM

4.10.6 Generation of retroviruses

The retroviral system is a powerful means for the delivery of genetic material into a variety of mammalian cell lines, resulting in an efficient and stable overexpression of a given gene. Although often utilized to achieve increased gene expression retroviruses can as well be used in order to obtain a gene knock down by RNA interference (RNAi), a mechanism that is based on the degradation of mRNA initiated by a corresponding doublestranded RNA (dsRNA).

The amphotropic Phoenix system is based on the Moloney Murine Leukemia Virus (MMLV) and allows for the retroviral infection of most mammalian dividing cells. The Phoenix-gp producer cell line encodes the viral proteins gag (core proteins) and pol (reverse transcriptase). It can thus be pseudotyped with alternative viral envelope proteins by co-expression with a retroviral coding plasmid, thereby altering the host tropism of the respective virus. A commonly used variant for this purpose is the glycoprotein G of the Vesicular stomatitis virus (VSV-G) which promotes fusion of retroviral with cellular membranes and allows for the infection of a high variety of different mammalian cell types.

For generation of retroviral particles the packaging cell line Phoenix-gp has to be co-transfected with a plasmid encoding the gene of interest and the VSV-G plasmid, resulting in the production of infectious but replication deficient retroviral particles. The respective viral proteins gag, pol and env are therefore only expressed during culture of the packaging cell line. The produced retroviral particles can subsequently be used for the infection of various target cell lines, leading to the stable integration of the gene of interest into the cellular genome.

The herein described protocol for the generation of retroviruses goes back to the publication by Schuck *et al.* (Schuck *et al.*, 2004). In preparation, a 60 cm^2 dish was covered with Collagen R solution and incubated at 37 °C for 1 h. Afterwards, remaining collagen was removed and collagen coated dishes stored at 4 °C. Two days before transfection 1.2 x 10^6 Phoenix-gp cells were seeded in a 60 cm^2 dish. When reaching a confluency of 70 – 80 % 10 ml of fresh culture medium was applied and a master mix for $CaPO_4$ transfection was prepared as indicated in Table 29 and incubated for 5 min at RT.

Table 29: Master mix preparation for $CaPO_4$ transfection.

1 x master mix for $CaPO_4$ transfection (60 cm^2)	
add 540 µl	H_2O
4.5 µg	pVSV-G
13.5 µg	retroviral plasmid
132 µl	1 M $CaCl_2$
add 2 x HBS dropwise while vortexing	
540 µl	2 x HBS pH 6.95

The transfection mix was added dropwise to the cells and incubation was carried out at 37 °C and 5 % CO_2 for 16 h. 10 ml of fresh culture medium were then applied and incubated for another 8 h under the same conditions. For harvesting of retroviral particles 24 h after transfection medium was changed to 5 ml of DMEM low glucose and cells subsequently incubated at 32 °C and 5 % CO_2. Every 24 h the supernatant containing the freshly produced retroviral particles was collected and another 5 ml of DMEM low glucose were added to the Phoenix-gp packaging cells. Retroviral supernatants were passed through a sterile nitrocellulose free 0.45 µm syringe filter, shock frozen in liquid nitrogen and stored at –80 °C until further use. Collection of the retroviral particles was carried on for up to 8 days post transfection.

4.10.7 Production of stable cell lines by retroviral infection

For the generation of stable cell lines MDCK cells were seeded on 6-well cell culture plates aiming to reach subconfluency at the time point of infection. 24 h after seeding 500 µl of sterile filtered retroviral supernatant together with 4 µg/ml Polybrene in 1 x PBS were added to each well and incubated for 24 h at 32 °C and 5 % CO_2. Typically, approaches were performed in duplicates and cultured in parallel to uninfected control cells. In order to increase the efficiency of the retroviral infection process cells were cultured with retroviral supernatants on two consecutive days, followed by incubation in standard medium for another 24 h at 37 °C and 5 % CO_2.
Only cells with successful incorporation of the gene of interest had equally integrated a puromycin resistance gene which allowed for the antibiotic selection of stably expressing cells. Thus, samples were trypsinized, seeded again in new medium containing 8 µg/ml puromycin in 1 x PBS and cultured at 37 °C and 5 % CO_2.

During the following days, each day medium was changed to fresh medium containing 4 µg/ml puromycin until all control cells had died. The remaining cells were cultured to confluence and stocks prepared for further experiments.

4.10.8 Generation of adenoviruses

Replication deficient adenoviruses are a powerful tool for obtaining high levels of transient transgene expression in a variety of different mammalian cell lines. Within the AdEasy system pAdEasy-1 is a commonly used adenoviral vector which has been deleted for the early genes E1 and E3, thus making the use of an E1-expressing packaging cell line such as Hek293 necessary for adenovirus production and propagation. The resulting recombinant adenovirus possesses the ability to infect dividing as well as non-dividing cells without being able to further replicate within the respective target cell line.

Hek293 cells were seeded 24 h prior to transfection at a density of 1.5 x 10^6 cells per T25 cell culture flask. The following day, 10 µg of adenoviral recombinant DNA were digested with PacI in order to linearize the plasmid. Incubation was carried out at 37 °C for 4 h, followed by heat inactivation of the enzyme at 65 °C for 20 min.

Table 30: Linearization of adenoviral plasmid DNA.

restriction digest mix	
10 µl	DNA (10 µg)
3 µl	PacI (10 U/µl)
5 µl	NEB buffer 1
5 µl	10 x BSA
27 µl	H_2O

When reaching a confluency of 50 – 70 % Hek293 cells were washed once with 4 ml of OptiMEM and 2.5 ml of fresh OptiMEM were applied per T25 cell culture flask. The packaging cells were subsequently transfected with the linearized adenoviral plasmid DNA using Lipofectamine 2000 as the transfection reagent and incubated for 4 hours under standard cell culture conditions. The medium-transfection-mix was afterwards discarded and 6 ml of fresh medium added. Alternatively, if cells did not respond well to this protocol, DMEM without antibiotics was used instead of OptiMEM for incubation.

Table 31: Lipofection of Hek293 packaging cells using adenoviral plasmid DNA.

1 x master mix for lipofection (T25)			
master mix 1		**master mix 2**	
50 µl	digest product	25 µl	Lipofectamine 2000
625 µl	OptiMEM	625 µl	OptiMEM

Adenoviral generation follows a cycle of virus attachment to the cell surface, uptake by receptor-mediated endocytosis and translocation into the nucleus where the viral replication takes place. Finally, viruses are released from the cell by inducing cell death. Lysis of the packaging cell line can therefore be used as a measure for proceeding adenoviral replication and is typically seen 7 – 10 days post transfection. At that time point the remaining cells were harvested by simply rinsing them off the flask wall as they detached very easily. Samples were pelleted by centrifugation at 3,200 g and 4 °C for 5 min and resuspended in 1 ml ice-cold 1 x PBS. Viruses were subsequently released from the cellular nuclei by performing four freeze-thaw-cycles in order to disrupt the pelleted cells. Therefore, pellets were frozen in a dry ice-MeOH-bath, thawed again in a 37 °C water bath and vortexed three times for 10 s with being chilled in between for 10 s on ice. Four rounds of freeze-thaw-cycles were performed, followed by centrifugation at 3,200 g and 4 °C for 1 min. The supernatant containing the recombinant adenovirus was stored at -20 °C until further use.

As to increase the amount of produced adenovirus the harvested viral supernatants were subsequently used to infect increasing numbers of T75 and T175 cell culture flasks seeded with Hek293 cells. As soon as a third to half of the cells were detached adenoviruses were harvested as described above. For preparing a high titre stock packaging cells from 8 – 12 T175 cell culture flasks were infected with adenoviral supernatant and harvested when lysis became evident. After centrifugation at 1,000 g and 4 °C for 5 min the pellet was taken up in 8 ml ice-cold 1 x PBS and four rounds of freeze-thaw-cycles were performed. The sample was centrifuged at 3,200 *g* and 4 °C for 1 min and the resulting supernatant mixed with 4.4 g CsCl by vortexing. The suspension was transferred to a polyclear ultracentrifugation tube, covered with 2 ml of mineral oil and centrifuged in an ultracentrifuge with SW 41-Ti rotor at 32,000 rpm and 10 °C for 20 h over night. The following day the virus fraction was evident as a cloudy white band within the clear CsCl solution and could thus be

collected by using a syringe with an 18G needle attached. The high titre adenovirus stock was mixed to 50 % with 2 x storage buffer and stored at -20 °C.
The adenoviral titre of the respective stock was assessed by infection of mammalian target cells with various dilutions of adenovirus and infection efficiency evaluated by immunofluorescent staining.

4.10.9 Infection of cells with adenovirus

Recombinant adenoviruses are capable of infecting dividing as well as non-dividing cells, therefore making the consideration of confluency much less important for infection rates as opposed to the methods of lipofection and retroviral infection.
For adenoviral infection, cells were seeded at the desired density and incubated for 6 h at 37 °C and 5 % CO_2. The majority of experiments were performed using 12-well cell culture plates with 400,000 MDCK cells being seeded in each well. Different conditions were tested for the process of adenoviral infection, including incubation in OptiMEM only as opposed to OptiMEM with additional standard medium as well as discarding the adenovirus after 1 h of infection or incubation of the cells with adenovirus over night. The respective infection efficiencies were evaluated by western blotting and radioactive oleate uptake assays and the most suitable protocol was used for all further experiments as described below.
After 6 h of growth the culture medium was replaced by 200 µl OptiMEM containing the respective amount of adenovirus and incubated for 1 h at 37 °C and 5 % CO_2. Adenovirus amounts were strongly dependent on the individual titre of each stock as well as on the particular protein expression rate and ranged from several nl to several µl per 12-well. Subsequently, 800 µl of standard cell culture medium were added to each well and incubation was carried out over night. Typically, cells were used for further analysis by radioactive oleate uptake assays or immunofluorescence approximately 16 h post infection.

4.10.10 Immunofluorescence

Immunofluorescent staining allows the examination of the localization and expression of a particular protein within a cell by targeting it with a specific antibody. Subsequent binding of a species-specific secondary antibody which is coupled to a fluorophore enables the analysis of special distribution and intensity of expression by visualization under a fluorescence microscope.

Cells were seeded the previous day at different densities on 10 mm cover slips, typically in a 12-well cell culture plate. If required, adenoviral infection was performed at the day of seeding and cells incubated over night. The following day, samples were washed twice in 1 x PBS followed by fixation in 4 % PFA for 20 min at RT. In order to remove the remaining PFA cells were again rinsed twice with 1 x PBS and either directly used for immunofluorescent staining or stored at 4 °C in 1 x PBS until further use.

During the process of staining all incubation steps were performed by placing the cell covered side of the individual cover slips on a 30 µl droplet of SGB solution in a humidity chamber to prevent samples from running dry. In order to avoid unspecific binding of the utilized antibodies cells were initially blocked by incubation in SGB for 10 min at RT. The primary antibody was diluted in SGB, cover slips transferred to the appropriate antibody droplets and incubated at RT for 1 h. The appropriate species-specific secondary antibody was equally diluted in SGB. Cover slips were rinsed three times in SG solution to remove unbound antibody residues and transferred to the respective antibody droplets, followed by incubation in the dark at RT for 1h. If required, a co-staining of two antibodies diluted together in SGB could be performed under the same conditions.

After finishing the second incubation step cover slips were washed twice in SG and 1 x PBS each and embedded on a microscope slide using Mowiol as mounting medium. For unspecific staining of DNA the dye Hoechst 33342 was diluted 1:2,000 in Mowiol, thus staining nuclear DNA during the mounting process. Samples were air-dried for several hours and afterwards stored at -20 °C. Analysis was performed by fluorescence microscopy.

4.11 Statistical analysis

If not otherwise noted, radioactive oleate uptake assays were performed in triplicates and conducted three times under independent conditions. Each protein sample used for western blot analysis was quantified mostly in triplicates but at least in duplicates. Values are given as mean with standard deviation (SD). Statistical analysis was performed using the analysis function of Microsoft Office Excel by applying the two-sample *t*-test under the assumption of unequal variance.

5. Results

Fatty acid uptake is facilitated by plasma membrane as well as intracellularly localized proteins like CD36, FATP4, ACSL1 and Cav-1 through different mechanisms. During this study, protein amounts of CD36, FATP4 and ACSL1 were quantified by comparison to a recombinant protein standard and related to respective alterations in oleate uptake. CD36, FATP4, ACSL1 and Cav-1 were tested for cooperative acting in mediating fatty acid uptake and their cellular localizations verified by immunofluorescence.

5.1 Generation of stable MDCK cell lines

Stable protein overexpressing and knock down MDCK cell lines were generated by retroviral infection of the respective wildtype strain. During this study, three different stable cell lines were used:

- MDCK cells stably overexpressing $ACSL1_{FLAG}$ ($ACSL1_{FLAG}$ MDCK)
- MDCK cells stably overexpressing FATP4 (FATP4 MDCK)
- MDCK cells with stable knock down of Cav-1 (Cav-1 KD MDCK)

$ACSL1_{FLAG}$ MDCK as well as Cav-1 KD MDCK cells were generated as part of this work whereas the FATP4 MDCK cell line was kindly provided by Margarete Poppelreuther (AG J. Füllekrug, University Hospital Heidelberg).

5.1.1 ACSL1 overexpression in MDCK cells is achieved by retroviral infection

Stable $ACSL1_{FLAG}$ protein overexpressing MDCK cells were generated by retroviral infection with subsequent puromycin selection. A second stable MDCK cell line was generated based on the retroviral expression vector pQCXIP-J and served as control. Puromycin selection of both cell lines was successfully performed as assessed by the killing of uninfected wildtype MDCK cells that were used for growth control. The effective overexpression of $ACSL1_{FLAG}$ protein was evidenced by protein quantification by western blotting and correlated with enhanced oleate uptake (see sections 5.3.7 and 5.3.8).

5.1.2 Cav-1 knock down diminishes protein expression levels by more than 80 %

A Cav-1 KD MDCK cell line was generated by retroviral infection to determine the influence of Cav-1 on oleate uptake in wildtype and CD36 overexpressing cells. Knock down of Cav-1 expression was performed very efficiently as evidenced by western blotting (Figure 7 A).

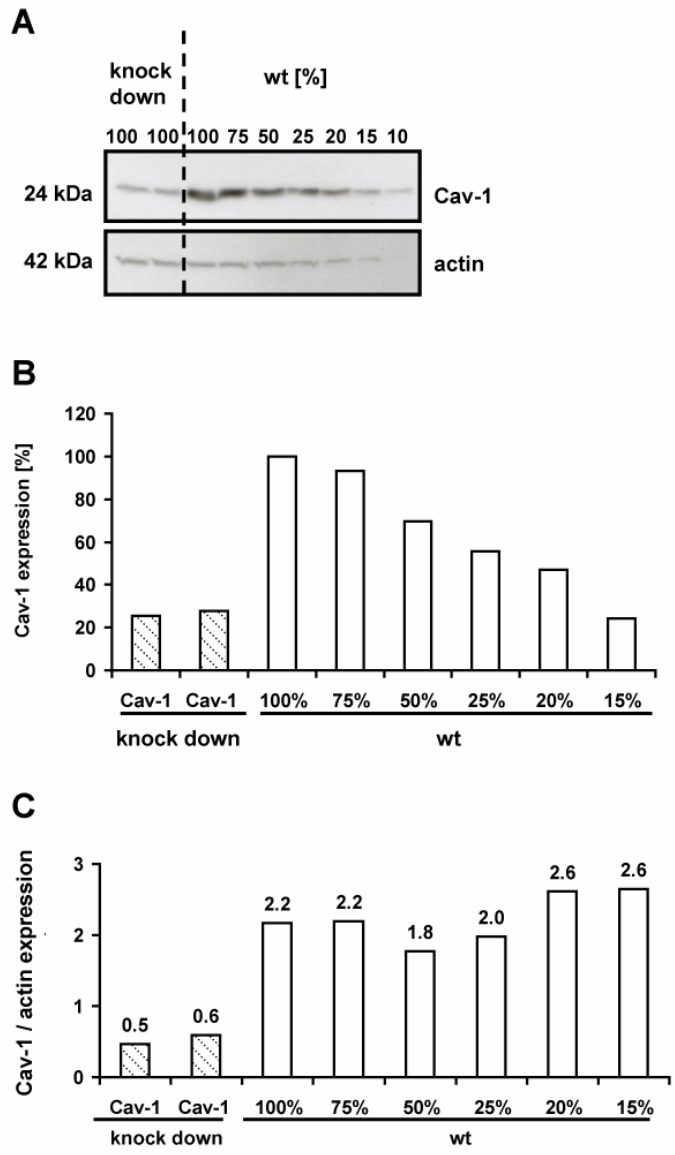

Figure 7: Quantification of Cav-1 knock down in MDCK cells.

A) Western blot showing protein expression levels of Cav-1 in knock down and wildtype MDCK cells. Equal amounts for Cav-1 KD and 100 % wildtype MDCK cell lysates were loaded together with a dilution series of wildtype MDCK cell lysates. Cav-1 KD MDCK cells show significantly diminished expression levels as compared to wildtype MDCK cells. Actin served as protein loading control.

B) Densitometric quantification of Cav-1 protein levels in knock down and wildtype MDCK cells using ImageJ. Results are given in % of 100 % wildtype protein, showing an efficient Cav-1 knock down with 15 % residual protein expression.

C) Cav-1 protein levels were standardized to actin, yielding similar ratios for all wildtype cells and considerably lower values for Cav-1 KD MDCK.

One representative experiment is shown.

Densitometric quantification of the remaining protein levels with ImageJ yielded a reduction in overall Cav-1 expression of 85 % when compared to a dilution series of wildtype MDCK cells (Figure 7 B). Standardization of Cav-1 to actin protein levels gave similar ratios for all wildtype samples with the values for the Cav-1 KD MDCK cells being considerably lower than for wildtype cells (0.5 and 0.6 for Cav-1 KD MDCK as compared to 1.8 – 2.6 for wildtype MDCK cells) (Figure 7 C).

Cav-1 protein levels were quantified for each fatty acid uptake assay carried out with Cav-1 KD MDCK cells in order to verify the stability of the protein knock down (see section 5.3.9).

5.2 CD36 overexpression increases oleate uptake

Initial experiments using CD36 overexpressing MDCK cells showed a moderate increase in fatty acid uptake as compared to control cells. Radioactive oleate uptake assays were performed to analyze whether CD36 mediated fatty acid uptake is modulated by different (free) oleate concentrations.

5.2.1 CD36 mediated oleate uptake is similarly enhanced independent from free oleate concentrations

To vary free oleate concentrations, $CD36_{FLAG}$ overexpressing MDCK cells were incubated with ^{3}H-oleic acid bound to BSA in various proportions, starting from 0.5:1 (50 µM oleate:100 µM BSA) up to 8:1 (800 µM deate: 100 µM BSA) with BSA concentrations fixed at 100 µM.

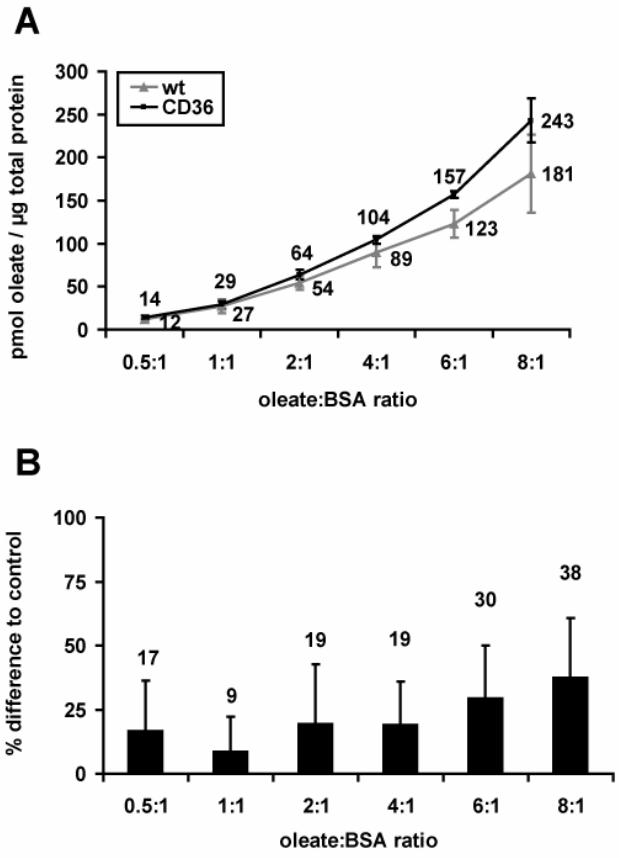

Figure 8: Variation of free oleate concentrations does not significantly influence CD36 mediated fatty acid uptake.

CD36FLAG overexpressing as well as wildtype MDCK cells were incubated with 3H-oleic acid bound to BSA in various ratios (100 µM BSA, oleate changing, 3 Ci/mol specific activity) for 3 h. Although CD36 mediated oleate uptake was increased more at higher oleate:BSA ratios (A) no significant difference was observed in comparison to lower ratios (B).

The assay was performed in triplicates, error bars correspond to standard deviation. n=3

Although CD36 mediated oleate uptake increased with higher oleate:BSA ratios (Figure 8 A) no significant difference to wildtype MDCK cells was evident as compared to lower ratios (Figure 8 B). Hence, for all following assays an oleate:BSA ratio of 2:1 was chosen in accordance with the standard protocols used in our laboratory.

5.2.2 CD36 overexpression increases oleate uptake over a range of different oleate concentrations

Different molar concentrations of oleate were tested in respect to their influence on CD36 mediated oleate uptake. Three different molarities were used ranging from 20 – 600 µM, whereas oleate:BSA ratios remained constant at 2:1. The amount of incorporated oleate increased with rising molarity of the applied ^{3}H-oleic acid (Figure 9 A).

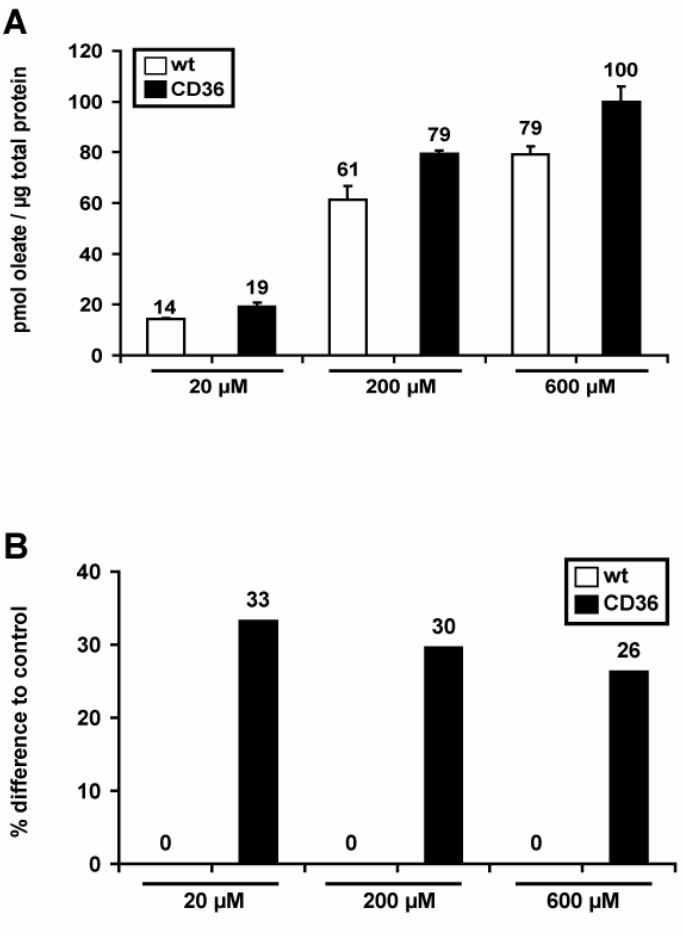

Figure 9: Influence of different oleate concentrations on CD36 mediated fatty acid uptake.

$CD36_{FLAG}$ overexpressing as well as wildtype MDCK cells were incubated with BSA bound oleate (oleate:BSA = 2:1) for 3 h. Different molar concentrations of oleate were used, ranging from 20 µM (5 Ci/mol specific activity) over 200 µM to 600 µM (both 0.5 Ci/mol specific activity).

A) Oleate uptake of $CD36_{FLAG}$ and wildtype MDCK cells at different oleate molarities was determined as pmol oleate/µg total protein. Increasing molar concentrations of oleate caused an enhanced oleate uptake.

B) Effect of CD36 overexpression on oleate uptake shown in % difference to the respective wildtype control. Only slight differences were observed between different samples.

The assay was performed in triplicates (20 µM, 600 µM) or duplicates (200 µM), error bars correspond to standard deviation. n=1

When analyzing the effect of CD36 overexpression on fatty acid uptake in comparison to control cells no significant difference was observed between the various oleate molarities (Figure 9 B). A molar concentration of 200 µM oleate was subsequently chosen for further experiments, thus ensuring a sufficient amount of ^{3}H-oleate uptake for reliable readings of radioactivity.

5.3 Quantification of CD36, FATP4 and ACSL1 protein amounts in correlation to oleate uptake

The main body of this work incorporated 1) the measurement of fatty acid uptake in MDCK cells overexpressing CD36, FATP4 or ACSL1 protein by radioactive oleate uptake assays and 2) the quantification of CD36, FATP4 and ACSL1 protein expression by comparison to a recombinant protein standard.

5.3.1 Preparation of recombinant FATP4$_{FLAG}$ protein standard

A recombinant FLAG-tagged FATP4 protein standard was generated for quantification of CD36, FATP4 and ACSL1 proteins in MDCK cells. Two different variants of FATP4 protein were overexpressed in MDCK cells, which differed in the localization of the FLAG-tag. One protein lacked its membrane anchor to facilitate the purification process. Hence, two different kinds of FATP4 standard were used for subsequent western blotting, running at 72 kDa (C-terminal FLAG = FATP4$_{FLAG}$) and 33 kDa (N-terminal FLAG = $_{FLAG}$ FATP4), respectively.

Quantification of affinity purified FATP4$_{FLAG}$ by western blotting yielded a concentration of 18.7 ng/µl in a total volume of 60 µl. A much higher quantity was obtained for $_{FLAG}$FATP4, with 47.5 ng/µl in overall 120 µl sample volume (Figure 10 A, B).

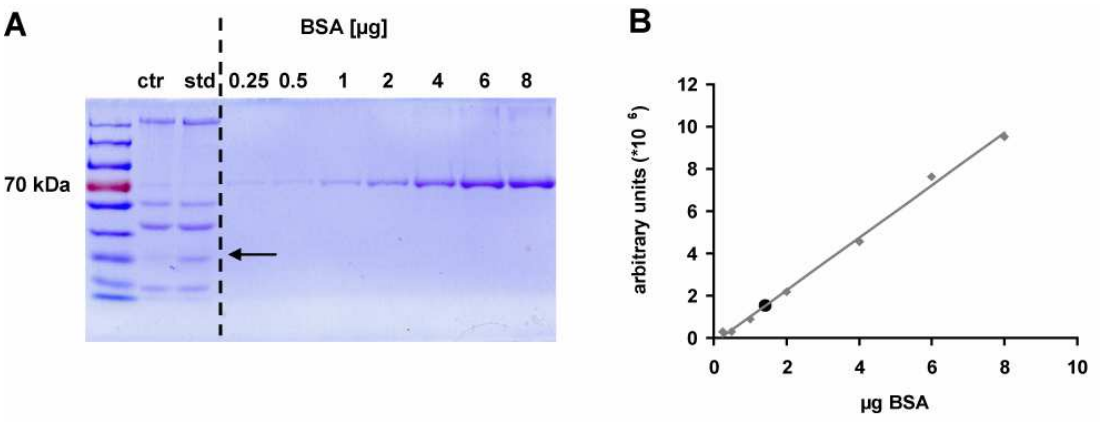

Figure 10: Quantification of purified $_{FLAG}$ FATP4 protein.
$_{FLAG}$FATP4 protein was stably overexpressed in MDCK cells and afterwards purified using a FLAG-tag based gel affinity system. Quantification of the purified protein was performed by SDS PAGE, with sample values being compared to a BSA standard curve. 30 µl of purified protein (= 1/4 of total sample volume) were loaded.
A) SDS gel showing purified $_{FLAG}$FATP4 protein, together with a BSA dilution series and purified wildtype cells serving as negative control. With coomassie brilliant blue staining the $_{FLAG}$FATP4 can be detected at 33 kDa (arrow).
B) Standard curve established from the BSA dilution series. The $_{FLAG}$FATP4 sample loaded on the gel contained 1.4 µg of protein in 30 µl sample (black dot), yielding a final concentration of 47.5 ng/µl.

5.3.2 Oleate uptake is significantly enhanced by FATP4 overexpression and correlates with FATP4 protein quantities

Wildtype MDCK cells were infected with rising amounts of 0.1 – 6 µl FATP4 adenovirus that correlated with an increase in FATP4 protein expression, ranging from 1,699 – 4,223 ng FATP4 protein/sample (Figure 11 A). Oleate uptake was significantly enhanced and correlated with increasing protein levels (Figure 11 B). Correlation of the enhancement in oleate uptake to FATP4 protein was comparable between the various approaches (Figure 11 C). Taken together, FATP4 mediated oleate uptake increased with enhanced protein expression levels while the specific oleate uptake per 1 ng FATP4 protein remained steady.

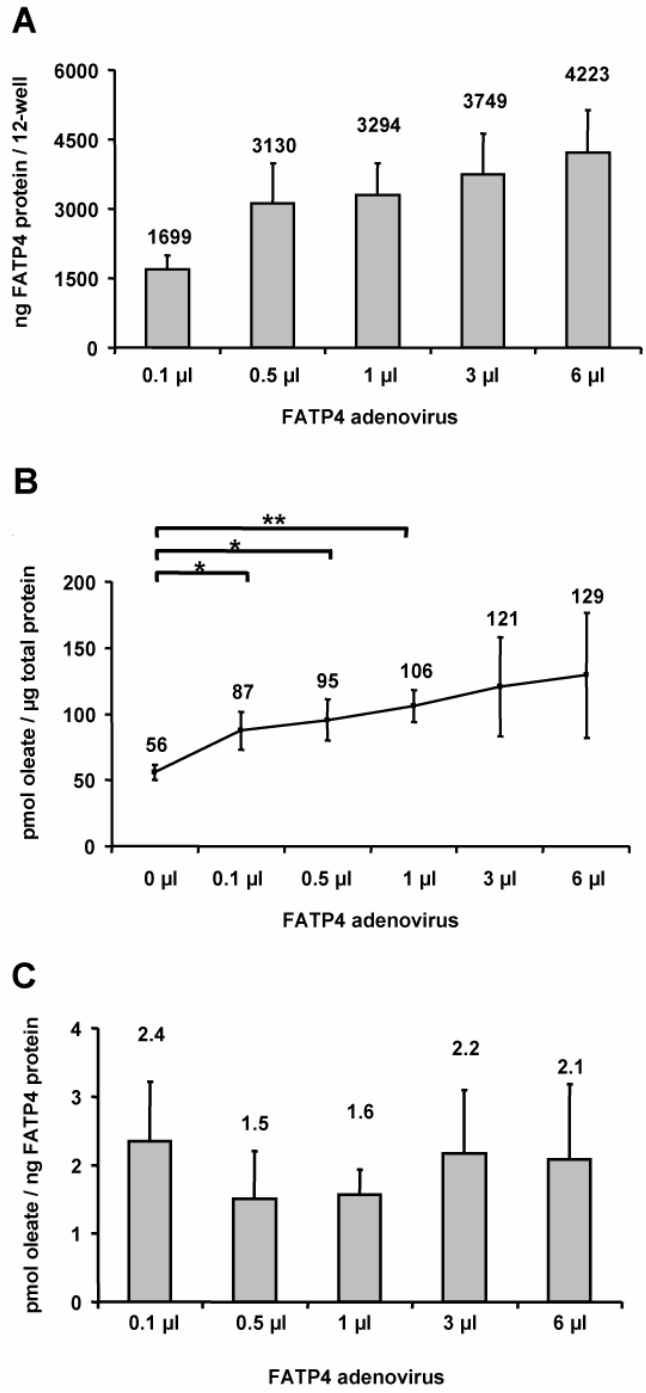

Figure 11: Titration of FATP4 protein levels and its influence on oleate uptake.

For FATP4 overexpression, wildtype MDCK cells were infected with increasing quantities of FATP4 adenovirus.

A) FATP4 protein levels correlated with the quantity of applied FATP4 adenovirus as shown by western blot analysis.

B) Sample analysis by radioactive oleate uptake assays. Cells were incubated with ^{3}H-oleate (200 µM oleate:100 µM BSA, 0.5 Ci/mol specific activity) for 3 h. Oleate uptake increased significantly with enhanced amounts of FATP4 adenovirus used for infection.

C) Referring the increase in oleate uptake to FATP4 protein levels showed similar values for all investigated samples and was independent from FATP4 protein amounts.

All assays were performed in triplicates, error bars correspond to standard deviation. n=3; * $p < 0.05$; ** $p < 0.01$

5.3.3 Oleate uptake increases in correlation to the amount of overexpressed CD36 protein

Wildtype MDCK cells were infected with different quantities of $CD36_{FLAG}$ adenovirus to analyze the influence of overexpressed CD36 protein on fatty acid uptake.

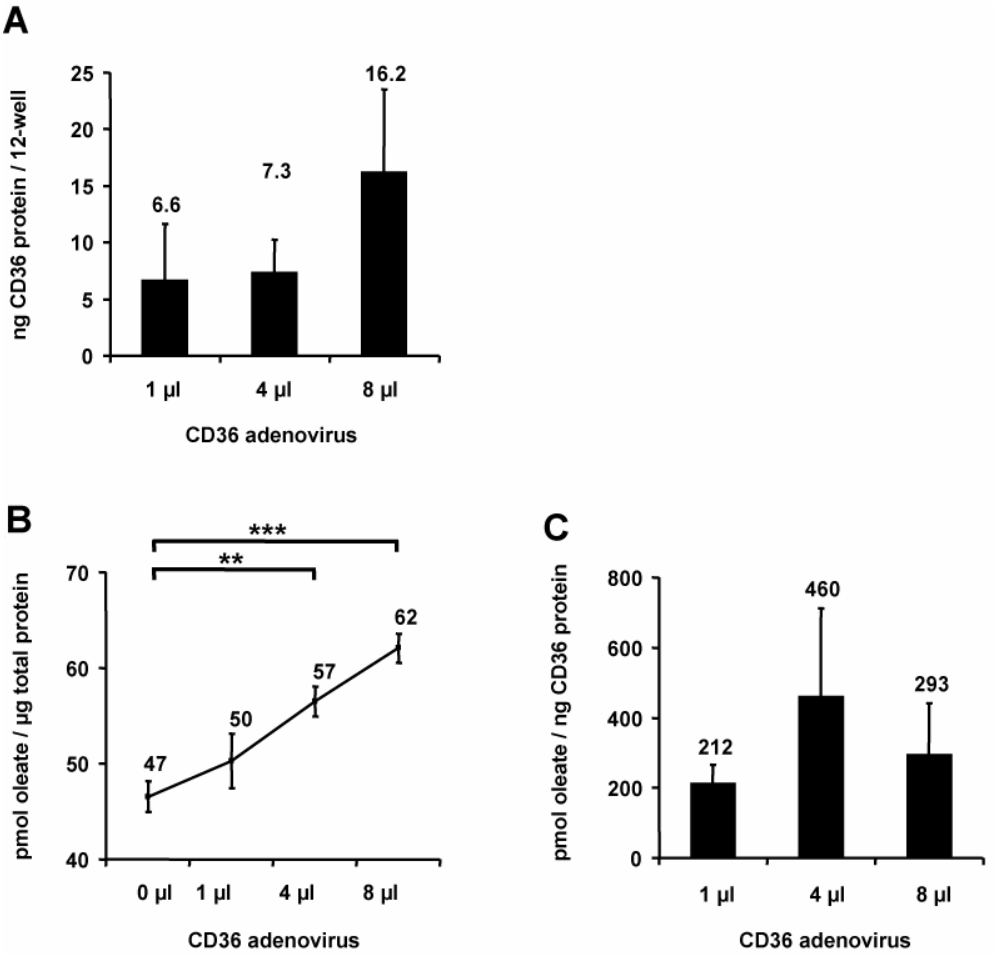

Figure 12: Oleate uptake is enhanced in CD36 overexpressing cells in correlation to the CD36 protein amount.
Wildtype MDCK cells were infected with increasing quantities of $CD36_{FLAG}$ adenovirus and effects analyzed by radioactive oleate uptake assays and western blots.
A) Western blot analysis of protein levels. Samples were measured in duplicates or as single values (1 µl samples). $CD36_{FLAG}$ protein levels increased with rising amounts of $CD36_{FLAG}$ adenovirus.
B) Cells were incubated with ^{3}H-oleate (200 µM oleate:100 µM BSA, 0.5 Ci/mol specific activity) for 3 h to assess oleate uptake. Samples were measured in triplicates. Increasing amounts of $CD36_{FLAG}$ adenovirus used for infection enhanced fatty acid uptake correspondingly.
C) Correlation of oleate uptake to quantities of CD36 protein.
Error bars correspond to standard deviation. n=3; ** $p < 0.01$; *** $p < 0.001$

Corresponding to increasing amounts of adenovirus CD36 protein levels were enhanced. This effect was especially evident for cells infected with 8 µl adenovirus as compared to infections with 1 µl and 4 µl. Measured protein levels ranged from 6.6 – 16.2 ng CD36/sample (Figure 12 A).Oleate uptake was significantly enhanced with rising concentrations of overexpressed CD36 protein as compared to control cells (Figure 12 B). When correlating the increase in oleate uptake to CD36 protein no obvious trend was observed. Calculated values reached from the uptake of 212 – 460 pmol oleate/ng $CD36_{FLAG}$ protein (Figure 12 C).

Quantities of incorporated oleate as well as CD36 protein expression levels were considerably lower than previously observed for FATP4 overexpressing MDCK cells.

In conclusion, infection of wildtype MDCK cells with increasing quantities of $CD36_{FLAG}$ adenovirus resulted in correspondingly enhanced amounts of overexpressed protein that correlated with increased oleate uptake.

5.3.4 At comparable protein expression levels CD36 increases oleate uptake more than FATP4

Comparable amounts of CD36 and FATP4 protein were overexpressed in MDCK cells to quantify the effects on oleate uptake. Wildtype MDCK cells were infected with 6 µl $CD36_{FLAG}$ adenovirus and a dilution series of FATP4 adenovirus, ranging from 0.001 – 0.5 µl. CD36 protein samples obtained from one out of three independently performed oleate uptake assays could not be quantified by western blotting due to too low protein amounts. The lowest concentration of FATP4 yielded similar protein levels as obtained by CD36 overexpression and was subsequently used for radioactive oleate uptake assays (Figure 13 A, B).

CD36 overexpressing cells showed enhancement in fatty acid uptake by 7 pmol oleate/µg total protein (27 %) as compared to control cells. On the contrary, the effect of FATP4 overexpression at similar protein quantities caused a much smaller increase in oleate uptake, corresponding to 1 pmol oleate/µg total protein (4 %) difference to control cells (Figure 13 C).

Results from oleate uptake assays were related to protein quantitites of CD36 and FATP4, thereby confirming a higher impact of CD36 than FATP4 on fatty acid uptake: CD36 overexpression caused a 3 x higher rise in oleate uptake of MDCK cells as observed for FATP4 (Figure 13 D).

Conclusively, overexpression of CD36 and FATP4 at comparable protein quantities in MDCK cells shows a clearly higher increase in oleate uptake for CD36 MDCK than for FATP4 MDCK. This observation confirms a higher potency for CD36 than FATP4 in enhancing fatty acid uptake at low protein quantities.

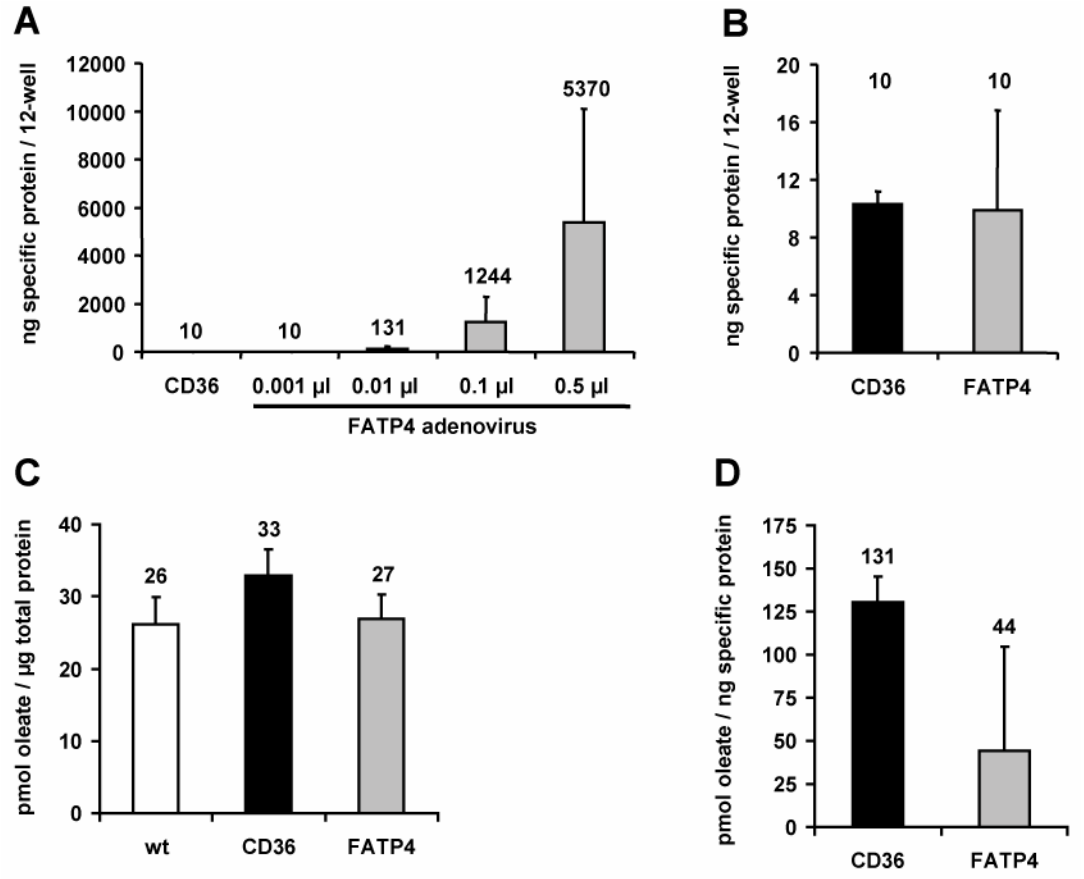

Figure 13: Expression of similar CD36 and FATP4 protein amounts and their influence on oleate uptake.
Wildtype MDCK cells were infected with $CD36_{FLAG}$ and various amounts of FATP4 adenovirus and results analyzed by western blotting and radioactive oleate uptake assays.
A) + B) Quantitative analysis of CD36 and FATP4 protein levels by western blotting. Similar protein levels of CD36 and FATP were achieved at the lowest concentration of FATP4 used for adenoviral infection.
C) Results obtained from radioactive oleate uptake assays. Cells were incubated with ^{3}H-oleate (200 µM oleate:100 µM BSA, 0.5 Ci/mol specific activity) for 3 h. Only CD36 overexpression resulted in a clear increase in fatty acid uptake.
D) When matching the results from oleate uptake assays to protein quantities the oleate uptake per 1 ng protein was 3 x higher for overexpressed CD36 than FATP4 protein.
Assays were performed in triplicates, error bars correspond to standard deviation. n=3, A), B), D): CD36 values n=2

5.3.5 CD36 is expressed at significantly lower quantities than FATP4 but increases oleate uptake more than FATP4 when normalized to protein amounts

In most experiments, FATP4 overexpression typically increased oleate uptake more than CD36. Thus, protein expression levels for both proteins were quantified and related to the respective alterations in fatty acid uptake.

For better comparability, a high concentration of $CD36_{FLAG}$ adenovirus (6 µl) was chosen together with a low amount of FATP4 adenovirus (0.05 µl) for infection of wildtype MDCK cells.

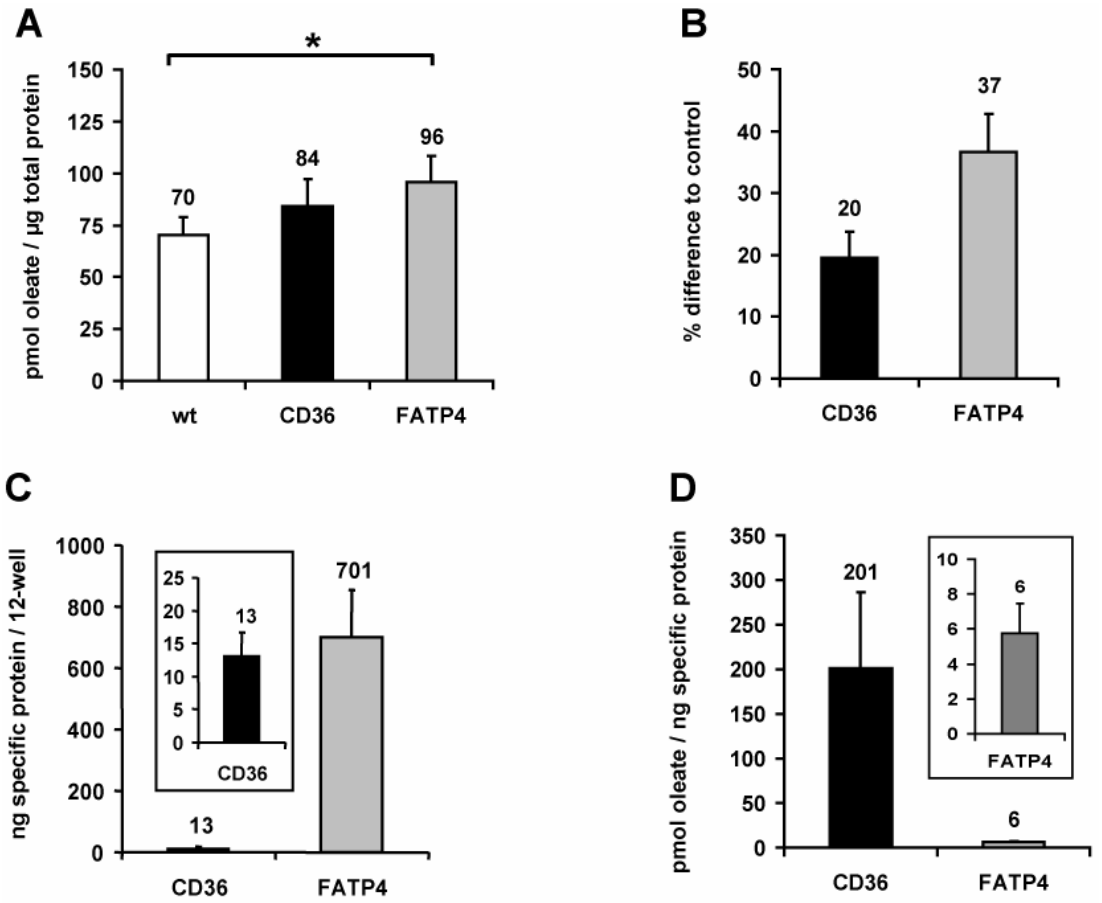

Figure 14: Quantitative comparison of increases in fatty acid uptake as mediated by CD36 or FATP4 protein overexpression.
Wildtype MDCK cells were infected with 6 µl $CD36_{FLAG}$ or 0.05 µl FATP4 adenovirus for protein overexpression.
A) For radioactive oleate uptake assays cells were treated with ^{3}H-oleate (200 µM oleate:100 µM BSA, 0.5 Ci/mol specific activity) for 3 h. CD36 as well as FATP4 overexpression enhanced oleate uptake as compared to control cells.
B) Increases in fatty acid uptake that were mediated by CD36 and FATP4 overexpression are shown in % difference
C) Quantification of protein amounts by western blotting revealed a 54 x higher expression for FATP4 than CD36 protein.
D) The oleate uptake related to ng protein CD36 or FATP4 was 33.5 x higher for overexpressed CD36 than FATP4 protein.
Values shown partially correspond to values depicted in Figures 16 and 17. All assays were performed in triplicates, error bars correspond to standard deviation. n=4; * $p < 0.05$

Oleate uptake was enhanced by CD36 and FATP4 overexpression but only in the case of FATP4 overexpressing cells reached a significant increase when related to controls (Figure 14 A). The increase in fatty acid uptake was 20 % in CD36 overexpressing cells, whereas FATP4 overexpression enhanced oleate uptake by 37 % (Figure 14 B). Although the effects of both proteins on fatty acid uptake were within a comparable dimension, protein amounts for CD36 and FATP4 were significantly apart: protein quantification yielded a quantity of 13 ng CD36 protein as opposed to 701 ng FATP4 protein which corresponds to a 54 x higher expression of

FATP4 protein (Figure 14 C). Accordingly, when the increase in oleate uptake was referred to protein amounts, CD36 mediated the uptake of 201 pmol oleate/ng protein whereas FATP4 had a much smaller effect (6 pmol oleate/ng protein). This corresponds to a 33.5 x enhanced uptake caused by CD36 versus FATP4 (Figure 14 D).

In summary, overexpression of CD36 or FATP4 protein in MDCK cells increases oleate uptake by 20 - 37 % as compared to wildtype cells. Although CD36 protein is expressed in much lower quantities than FATP4 it has a more than 30 x higher effect on oleate uptake when referred to 1 ng of specific protein.

5.3.6 Co-expression of CD36 and FATP4 has a synergistic effect on oleate uptake

Co-expression experiments were performed to investigate whether two differentially localized enzymes, CD36 and FATP4, might cooperate in enhancing fatty acid uptake. Therefore, stable FATP4 MDCK cells were infected with $CD36_{FLAG}$ adenovirus and compared to MDCK cells overexpressing CD36 or FATP4 alone.

Single overexpression of CD36 and FATP4 proteins increased fatty acid uptake in MDCK cells (Figure 15 A). FATP4 overexpression enhanced oleate uptake twice as much as CD36, resulting in 52 % versus 25 % increase as compared to control cells (Figure 15 B). Combined overexpression of both proteins additionally boosted fatty acid uptake and caused an increase that was considerably higher than calculated from single protein overexpression (122 % for CD36 and FATP4 co-expression as opposed to 25 % (CD36) + 52 % (FATP4) = 77 %) as depicted in Figure 15 B.

Protein quantification again confirmed a strong difference in CD36 and FATP4 expression levels, yielding 4.3 ng CD36 protein/sample as opposed to 539 ng FATP4 protein/sample. In CD36 and FATP4 co-expressing MDCK cells, protein quantities were decreased to 42 % for CD36 (1.8 ng/sample) and 63 % for FATP4 (337 ng protein/sample) in comparison to single protein overexpression (Figure 15 C, D). No specific oleate uptake per 1 ng CD36 and FATP4 protein could be calculated in co-expressing MDCK cells because within this experimental setup it was not possible to determine to which proportion every protein contributed to the observed effect.

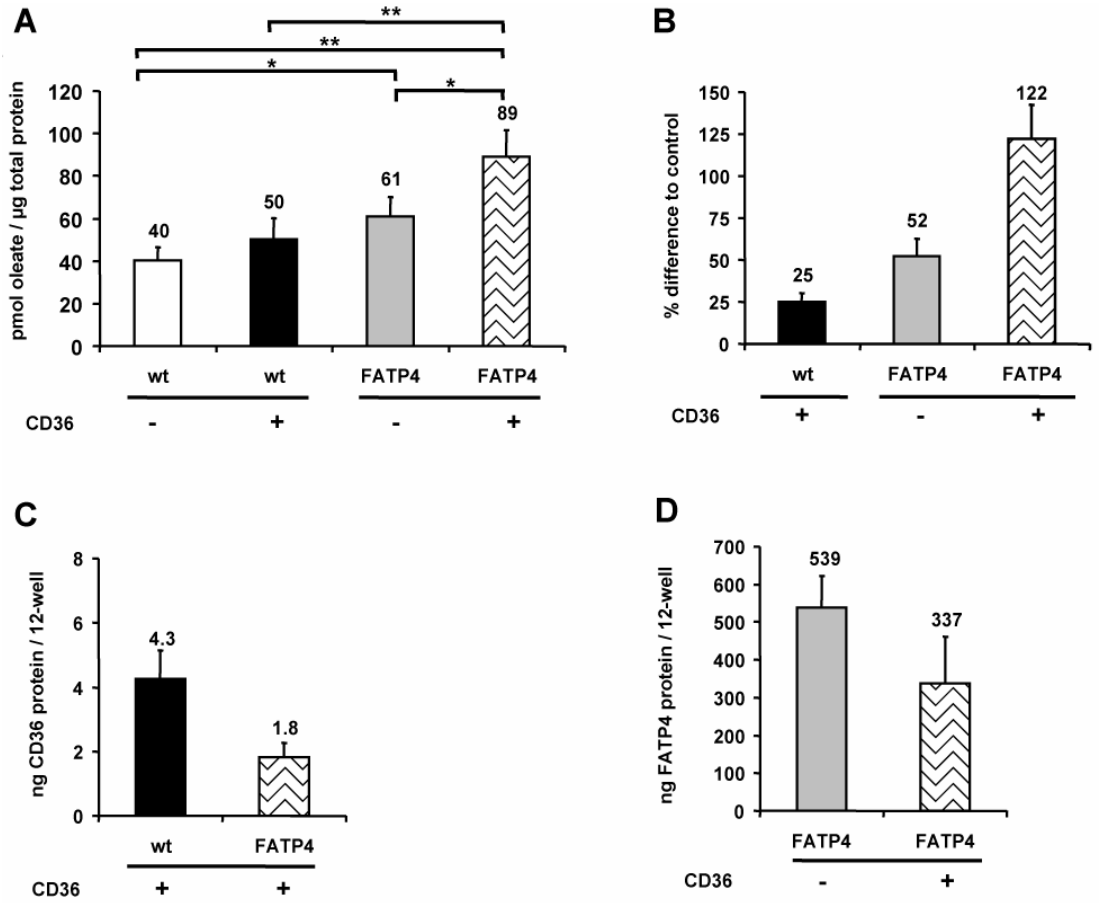

Figure 15: Combined overexpression of CD36 and FATP4 proteins significantly enhances fatty acid uptake.

To study the effect of combined protein overexpression, FATP4 MDCK were infected with 3 µl $CD36_{FLAG}$ adenovirus. Wildtype as well as MDCK cells overexpressing either CD36 or FATP4 served as control.

A) + B) Samples were treated with ^{3}H-oleate (200 µM oleate:100 µM BSA, 0.5 Ci/mol specific activity) for 3 h. Overexpression of CD36 and FATP4 alone increased oleate uptake. Co-expression of both proteins significantly boosted fatty acid uptake, resulting in a higher increase than calculated from data obtained by single protein overexpression.

C) + D) Western blot analysis showed clearly different protein levels for CD36 and FATP4 upon overexpression. Co-expression resulted in reduction of both protein amounts.

Values shown partially correspond to values depicted in Figure 19. Assays were performed in triplicates, error bars correspond to standard deviation. n=4; * $p < 0.05$; ** $p < 0.01$

Nevertheless, it can be concluded that combined overexpression of CD36 and FATP4 protein significantly increases oleate uptake in MDCK cells. This effect is considerably more pronounced than calculated based on data from single protein overexpression.

5.3.7 Simultaneous overexpression of ACSL1 and CD36 significantly increases oleate uptake in comparison to single protein overexpression

$ACSL1_{FLAG}$ MDCK cells were infected with 6 µl $CD36_{FLAG}$ adenovirus to investigate a possible cooperation of plasma membrane localized CD36 and intracellular ACSL1 in facilitating fatty acid uptake. Results were compared to MDCK cells overexpressing either CD36 or ACSL1 alone.

Overexpression of ACSL1 or CD36 alone enhanced fatty acid transport to a comparable amount, resulting in 20 % increased oleate uptake as compared to wildtype control cells (Figure 16 A, B). Again, co-expression of both proteins significantly boosted fatty acid uptake. MDCK cells overexpressing ACSL1 and CD36 accepted 58 % more oleate than control cells, which corresponded to 150 % increase as compared to summation of the effects of single protein overexpression (58 % for CD36 and ACSL1 co-expression as opposed to 20 % (CD36) + 20 % (ACSL1) = 40 %) (Figure 16 A, B).

Quantification of protein amounts by western blotting showed significantly different expression levels for both investigated proteins. ACSL1 MDCK cells contained 1,198 ng ACSL1 protein/sample as opposed to 13 ng of CD36 protein/sample in CD36 overexpressing MDCK, resulting in a 92 x higher amount of ACSL1 versus CD36 protein (Figure 16 C).

Accordingly high differences were observed in the amount of oleate uptake per 1 ng specific protein: 1 ng ACSL1 protein accounted for the uptake of 2 pmol oleate, as opposed to 201 pmol oleate uptake mediated by 1 ng $CD36_{FLAG}$ protein (Figure 16 D).

In summary, CD36 and ACSL1 co-expression in MDCK cells displayed a synergistic influence on increasing oleate uptake. These results were in parallel with previous findings from CD36 and FATP4 co-expression experiments (see section 5.3.6).

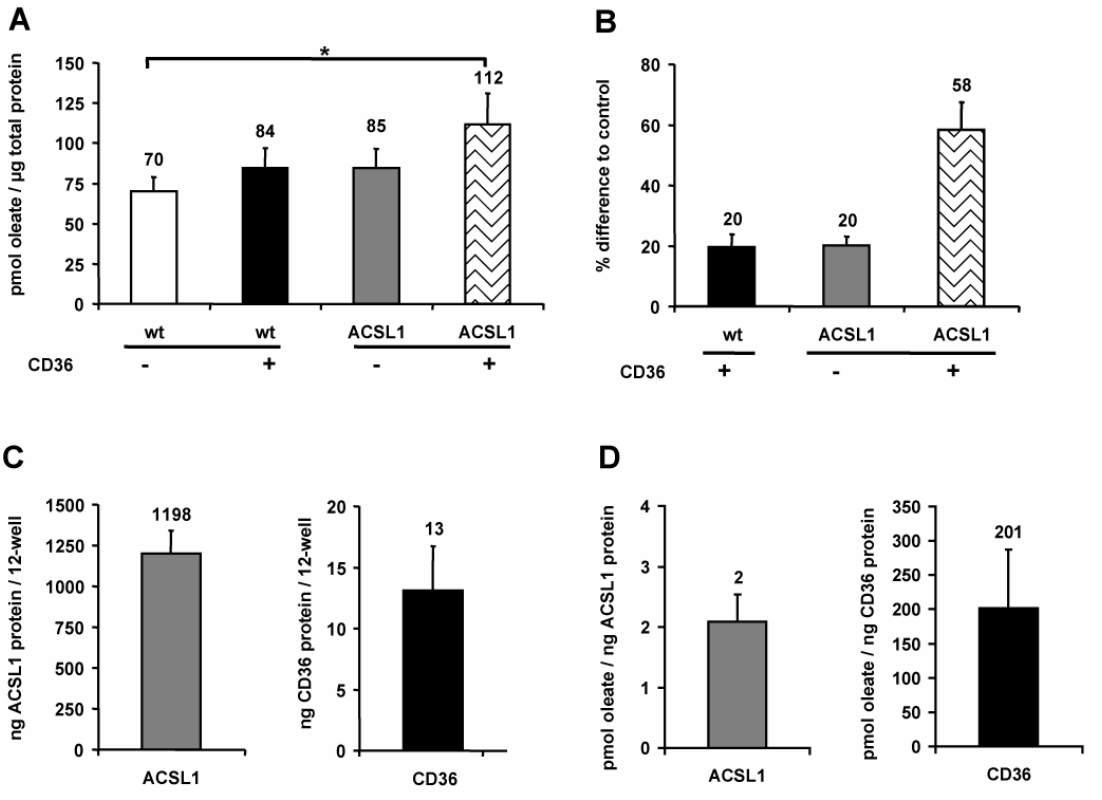

Figure 16: Synergistic effect of ACSL1 and CD36 co-expression on oleate uptake.
Wildtype and $ACSL1_{FLAG}$ MDCK cells were infected with $CD36_{FLAG}$ adenovirus. Samples were analyzed by oleate uptake assays and co-expressing cells compared to $ACSL1_{FLAG}$ MDCK and $CD36_{FLAG}$ MDCK.
A) + B) Cells were incubated with ^{3}H-oleate (200 µM oleate:100 µM BSA, 0.5 Ci/mol specific activity) for 3 h. Overexpression of CD36 and ACSL1 alone equally increased oleate uptake by 20 %. Co-expression of both proteins boosted fatty acid uptake significantly, corresponding to 150 % increase as compared to summation of the effects obtained by single protein overexpression.
C) Protein quantification by western blotting showed great differences between the investigated samples. ACSL1 was expressed 92 x higher than CD36 protein.
D) The specific oleate uptake per 1 ng protein was 100 x higher for CD36 than for ACSL1.
Values shown partially correspond to values depicted in Figures 14 and 17. All assays were performed in triplicates, error bars correspond to standard deviation. n=4; * $p < 0.05$

5.3.8 ACSL1 and FATP4 mediated increases in fatty acid uptake are not additive

Like FATP4, ACSL1 belongs to the family of intracellular acyl-CoA synthetases that activate fatty acids by esterification with coenzyme A. $ACSL1_{FLAG}$ overexpressing cells were infected with 0.05 µl FATP4 adenovirus to study the effect of combined protein overexpression on fatty acid uptake.

Oleate uptake was enhanced by single overexpression of both, ACSL1 and FATP4, with FATP4 having a significantly higher effect. In comparison to control cells, FATP4 enhanced fatty acid uptake by 37 % whereas ACSL1 overexpression caused only 20 % of increase (Figure 17 A, B).

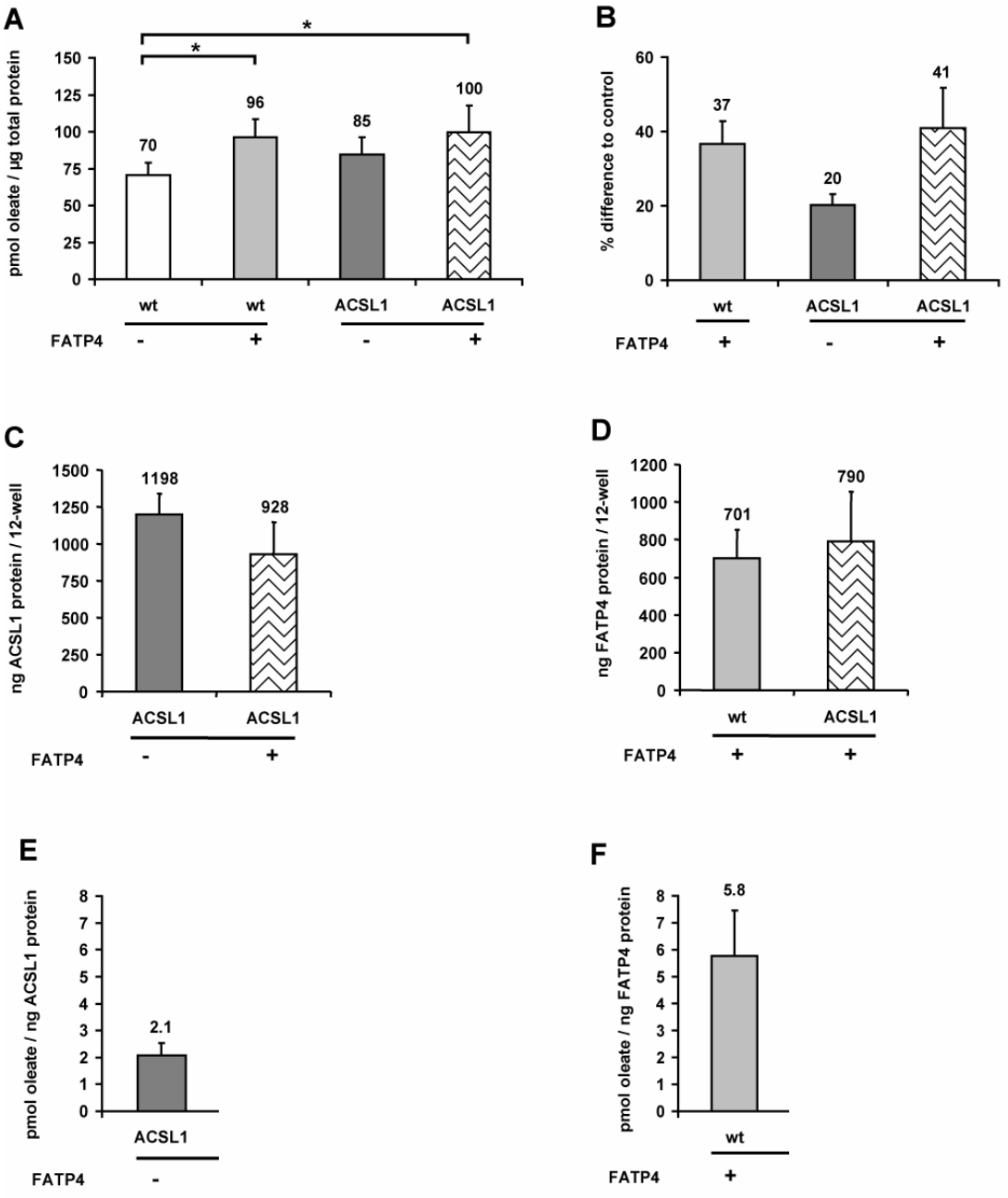

Figure 17: ACSL1 and FATP4 co-expression does not considerably increase oleate uptake.
To study the effect of ACSL1 and FATP4 co-expression $ACSL1_{FLAG}$ MDCK were infected with 0.05 µl FATP4 adenovirus. Samples were compared to stable $ACSL1_{FLAG}$ overexpressing MDCK cells as well as to wildtype cells infected with FATP4 adenovirus.
A) + B) Samples were incubated with ^{3}H-oleate (200 µM oleate:100 µM BSA, 0.5 Ci/mol specific activity) for 3 h. Overexpression of ACSL1 and FATP4 alone increased oleate uptake, with FATP4 overexpression having a more pronounced effect. Co-expression of both proteins did not significantly differ from overexpression of FATP4 alone and was smaller than calculated from single protein overexpression of both proteins.
C) + D) Proteins were quantified by western blotting and yielded expression levels for ACSL1 and FATP4 within the same dimension.
E) + F) The specific oleate uptake per 1 ng protein was in a comparable dimension for both investigated proteins.
Values shown partially correspond to values depicted in Figures 14 and 16. Assays were performed in triplicates, error bars correspond to standard deviation. n=4; * $p < 0.05$

Although co-expression of the two proteins significantly increased oleate uptake as compared to control cells (Figure 17 A) this enhancement differed only slightly from the effect caused by FATP4 overexpression alone and was considerably lower than calculated from single effects (41 % for FATP4 and ACSL1 co-expression as opposed to 37 % (FATP4) + 20 % (ACSL1) = 57 %) (Figure 17 B).
Corresponding protein amounts yielded roughly comparable quantities for single as well as combined overexpression for each candidate protein (Figure 17 C, D). ACSL1 was expressed at higher protein levels than FATP4, with quantities ranging from 928 – 1,198 ng for ACSL1 (Figure 17 C) and 701 – 790 ng for FATP4 per sample (Figure 17 D). Accordingly, when oleate uptake was referred to the specific protein amounts similar results were obtained for both investigated proteins. Overexpression of ACSL1 or FATP4 alone caused an uptake of 2.1 pmol, respectively 5.8 pmol, oleate per 1 ng protein (Figure 17 E, F).
Taken together, co-expression of ACSL1 and FATP4 proteins did not significantly increase oleate uptake in comparison to single protein overexpression.

5.3.9 Knock down of Cav-1 has no effect on oleate uptake independent from CD36 expression

Cav-1 has been suggested as an interaction partner for CD36 in mediating fatty acid transport across the plasma membrane. Hence, Cav-1 KD MDCK were analyzed to investigate whether Cav-1 modulates CD36 facilitated oleate uptake in MDCK cells.
Protein quantities of Cav-1 were assessed by western blotting in all Cav-1 KD samples (Figure 18 A).
Densitometric analysis of protein bands yielded a residual protein expression of 10 – 15 % for the investigated samples, thus verifying a high and stable knock down efficiency (Figure 18 B). Normalization of Cav-1 values to actin showed comparable ratios for all wildtype samples (1.0 – 2.0, 4.2 for the smallest amount of wildtype protein). The values calculated for the Cav-1 KD cells were much more lower (0.2 and 0.3) and confirmed successful reduction of protein expression levels (Figure 18 C).

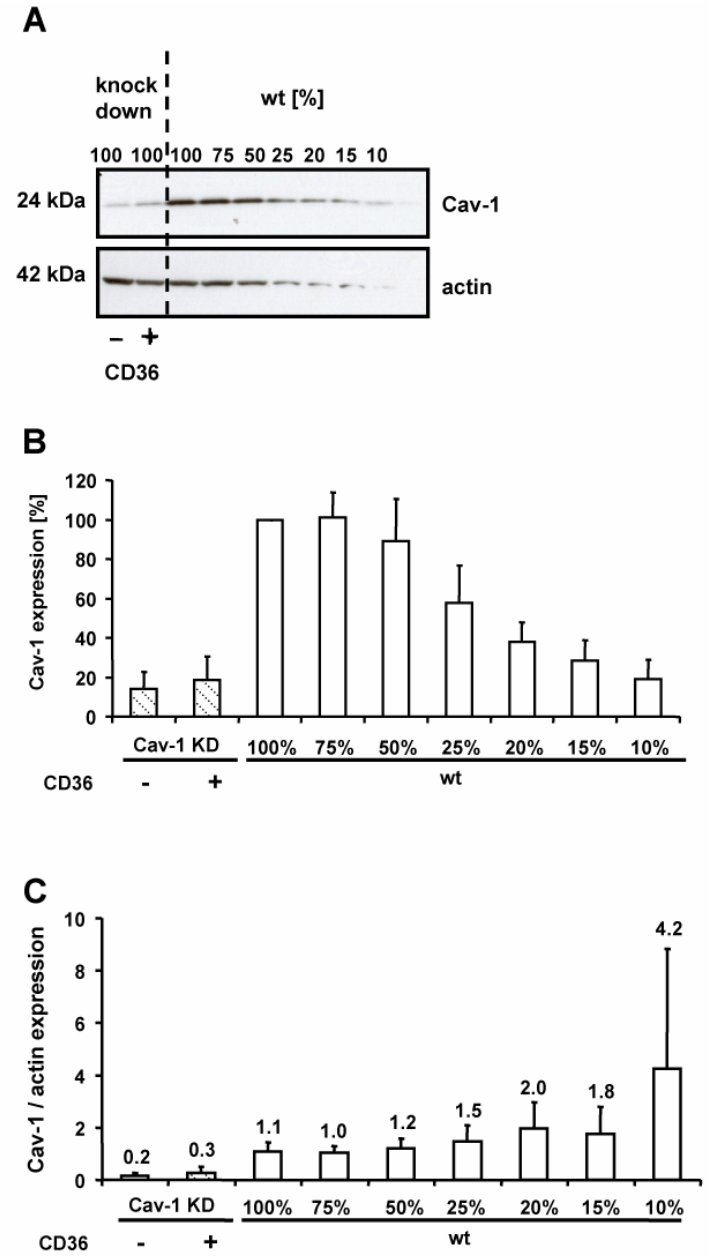

Figure 18: Quantification of Cav-1 knock down in MDCK cells used for oleate uptake assays.

Knock down of Cav-1 in MDCK cells was established by RNAi and cells subsequently infected with CD36FLAG adenovirus.

A) Quantification of Cav-1 protein amounts in wildtype and knock down MDCK cells was performed by western blotting. Equal amounts for Cav-1 KD and 100 % wildtype MDCK cell lysates were loaded together with a dilution series of wildtype MDCK cell lysates. Cav-1 KD MDCK cells display clearly diminished protein expression levels as compared to controls. Actin was used as loading control.

B) Proteins bands were densitometrically quantified with ImageJ. Cav-1 KD cells (uninfected or infected with $CD36_{FLAG}$ adenovirus) showed an efficient knock down with 10 – 15 % residual protein activity. Results are given in % of 100 % wildtype protein.

C) Standardization of Cav-1 protein levels to actin yielded similar ratios for most wildtype cells whereas ratios for Cav-1 KD MDCK were considerably lower.

Error bars correspond to standard deviation. n=4

In radioactive oleate uptake assays, CD36 overexpression increased fatty acid uptake in wildtype and Cav-1 KD MDCK cells. Cav-1 depletion did not alter oleate uptake in wildtype MDCK cells but caused a slight change in $CD36_{FLAG}$ adenovirus infected Cav-1 KD cells that accounted for an 8 % increase as compared to CD36 overexpressing wildtype cells (Figure 19 A).

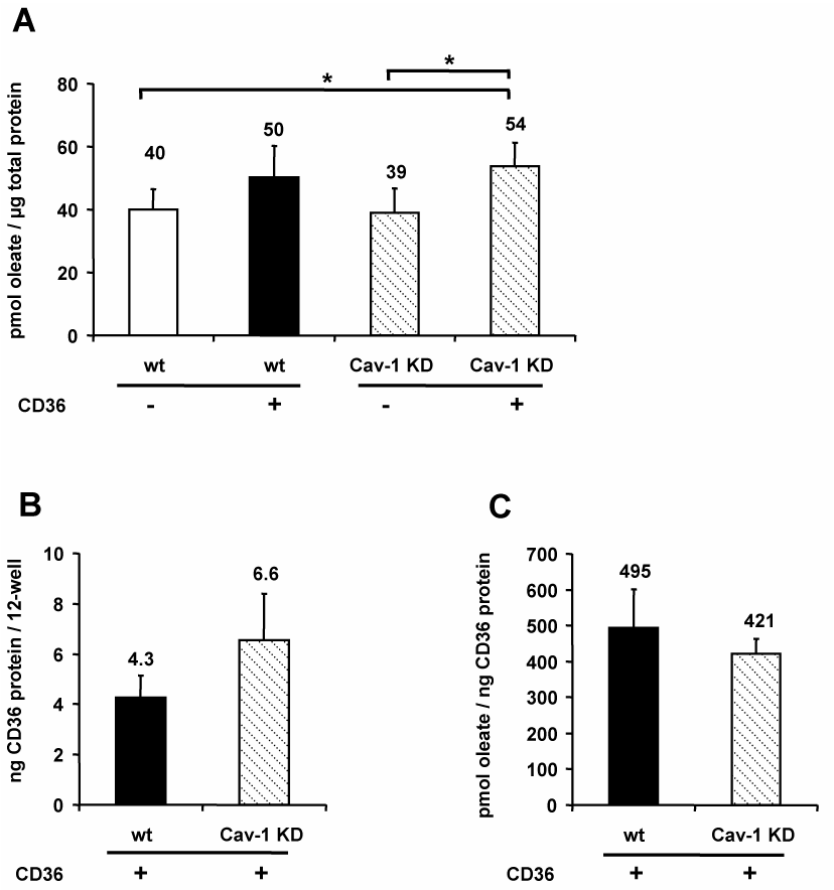

Figure 19: Cav-1 knock down has no effect on CD36 mediated oleate uptake.
Wildtype as well as Cav-1 KD MDCK cells were infected with $CD36_{FLAG}$ adenovirus. The respective uninfected cell lines served as control.
A) For fatty acid uptake assays cells were incubated with ^{3}H-oleate (200 µM oleate:100 µM BSA, 0.5 Ci/mol specific activity) for 3 h. CD36 overexpression increased oleate uptake in both investigated cell lines. Cav-1 knock down had no effect on fatty acid uptake in wildtype MDCK but caused a slight increase in CD36 overexpressing cells.
B) Quantification of protein amounts by western blotting showed an increased CD36 protein level in Cav-1 KD as compared to wildtype cells.
C) The specific increase in oleate uptake per 1 ng protein CD36 was similar for both investigated cell lines.
Values shown partially correspond to values depicted in Figure 15. Assays were performed in triplicates, error bars correspond to standard deviation. n=4; * $p < 0.05$

Quantification of CD36 protein amounts showed a higher expression level of CD36 protein in Cav-1 KD MDCK (6.6 ng/sample) as compared to CD36 overexpressing wildtype MDCK cells (4.3 ng/sample) which correlated to an increase by 53 % (Figure 19 B). When increases in oleate uptake were correlated to CD36 protein levels no significant difference was observed between wildtype and Cav-1 KD MDCK cells (Figure 19 C).

In summary, within this experimental setup knock down of Cav-1 had no significant influence on oleate uptake in wildtype and CD36 overexpressing cells.

5.3.10 Overexpression of CD36 and FATP4 increases short term oleate uptake in correlation to protein amounts

The majority of oleate uptake assays in this study was performed by incubating cells with radiolabeled oleate for 3 h. After this time, the activation of signaling cascades as well as transcriptional regulatory processes might have influenced fatty acid uptake. Thus, assays with a decreased incubation time of 5 min were conducted.

For experiments, wildtype MDCK cells were infected with different amounts of $CD36_{FLAG}$ and FATP4 adenovirus. Protein amounts correlated with increasing quantities of adenovirus: CD36 samples showed an enhanced protein quantity from low (1 µl adenovirus, 8.2 ng CD36 protein/sample) to high (4 µl adenovirus, 27 ng CD36 protein/sample and 6 µl adenovirus, 25.9 ng CD36 protein/sample) virus concentrations (Figure 20 A). FATP4 protein amounts clearly increased with rising quantities of FATP4 adenovirus used for infection (371 ng, 4,715 ng and 7,825 ng, respectively) (Figure 20 B). Again, FATP4 protein was expressed at much higher levels than $CD36_{FLAG}$ protein.

Oleate uptake was enhanced in correlation to rising protein amounts and was more prominent in FATP4 than CD36 overexpressing cells. Whereas $CD36_{FLAG}$ overexpression slightly enhanced fatty acid uptake by 11 – 15 %, FATP4 overexpression increased oleate uptake by 7 - 92 %, respectively (Figure 20 C). Relating the increase in oleate uptake to CD36 and FATP4 protein amounts showed no clear tendency for CD36 samples. Ratios ranged from uptake of 1.1 pmol oleate/1 ng protein (4 µl) to 2.3 pmol oleate/1 ng protein (2 µl) (Figure 20 D). On the contrary, data calculated for FATP4 samples showed a clear trend: ratios of oleate uptake by 1 ng protein decreased with increasing quantities of overexpressed FATP4 (Figure 20 E).

Taken together, overexpressed $CD36_{FLAG}$ as well as FATP4 increase short term oleate uptake in MDCK cells. This effect is more pronounced for FATP4 overexpression, with the rise in fatty acid uptake corresponding to increasing protein amounts.

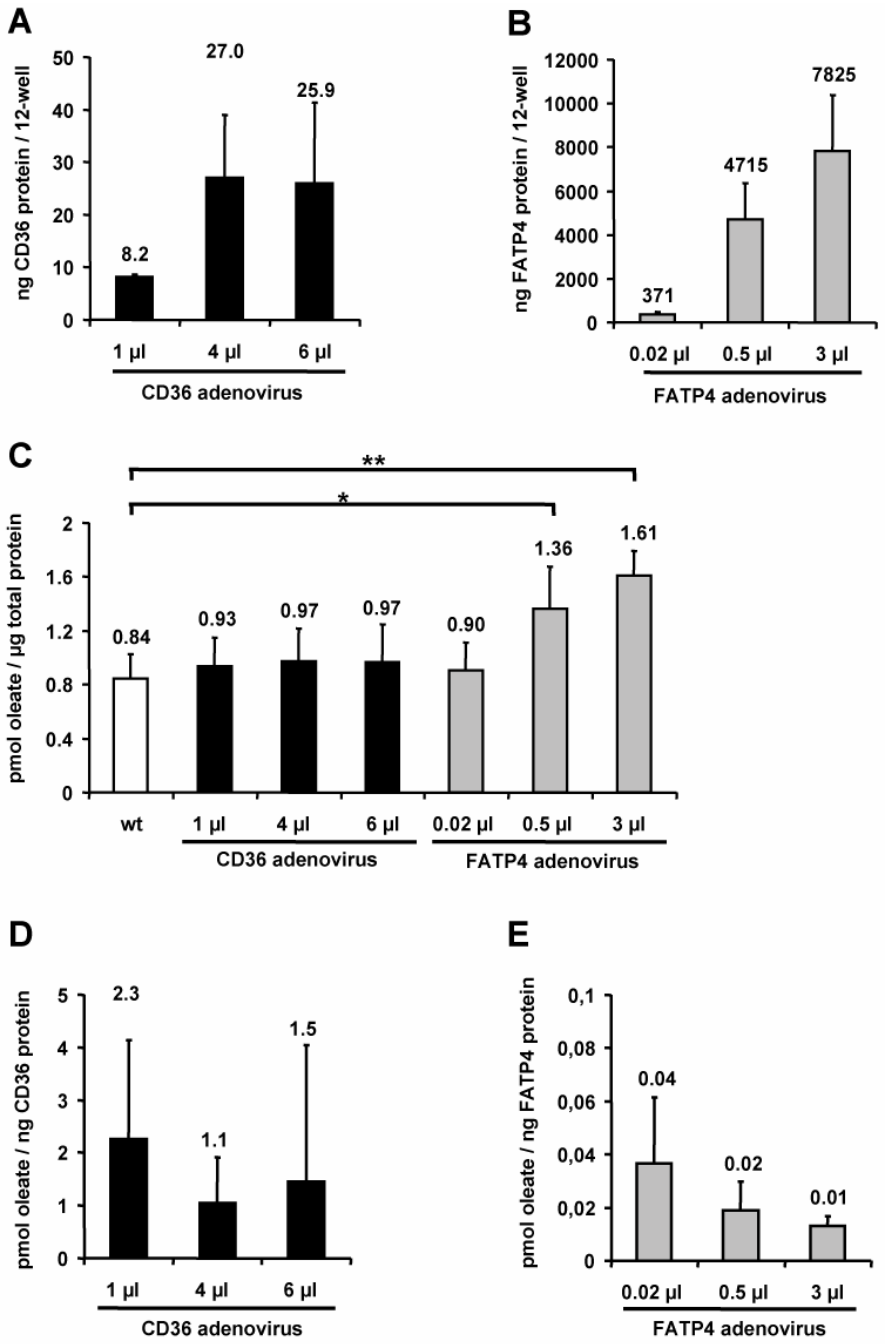

Figure 20: Overexpression of CD36 and FATP4 increases short term oleate uptake.
Wildtype MDCK cells were infected with increasing concentrations of $CD36_{FLAG}$ and FATP4 adenovirus. Uninfected cells served as controls.
A) + B) Western blot analysis of CD36 and FATP4 protein amounts. Protein quantities rise with increasing amount of respective adenovirus used for infection. FATP4 protein is expressed at much higher levels than CD36.
C) Analysis of oleate uptake. Cells were incubated with ^{3}H-oleate (200 µM oleate:100 µM BSA, 2 Ci/mol specific activity) for 5 min. CD36 as well as FATP4 overexpression increased oleate uptake, with FATP4 having a much more prominent effect.
D) + E) Assessment of the specific increase in oleate uptake per 1 ng protein. CD36 overexpression enhances fatty acid uptake more efficiently than FATP4 overexpression. The ratio of oleate uptake per 1 ng protein FATP4 decreases with increasing protein quantities.
All assays were performed in triplicates, error bars correspond to standard deviation. oleate uptake assays: n=4; western blots: FATP4: n=4, $CD36_{FLAG}$ 1 µl adenovirus: n=2, $CD36_{FLAG}$ 4 µl and 6 µl adenovirus: n=3, * $p < 0.05$; ** $p < 0.01$

5.4 Analysis of CD36, FATP4 and ACSL1 localization by immunofluorescence microscopy

In scientific literature, different cellular localizations have been described for CD36, FATP4 and ACSL1. Hence, MDCK cells were analyzed by immunofluorescence to identify the respective localization of each protein. Stable $ACSL1_{FLAG}$ MDCK and FATP4 MDCK as well as $CD36_{FLAG}$ adenovirus infected wildtype MDCK were used for analysis of single protein overexpression. FATP4 and $ACSL1_{FLAG}$ overexpressing cells were infected with $CD36_{FLAG}$ or FATP4 adenovirus to analyze protein localization upon co-expression.

5.4.1 CD36 is expressed at the plasma membrane and intracellularly

For analysis of CD36 localization, $CD36_{FLAG}$ MDCK cells were stained using a ms-α-CD36 antibody and a rb-α-FLAG antibody. Each of the two antibodies detected a differently localized pool of $CD36_{FLAG}$ protein within the same cell: the ms-α-CD36 antibody stained CD36 in the plasma membrane (Figure 21 A) as opposed to the rb-α-FLAG antibody that showed an intracellular signal (Figure 21 B). Overlay of both pictures confirmed the differential localization (Figure 21 C).

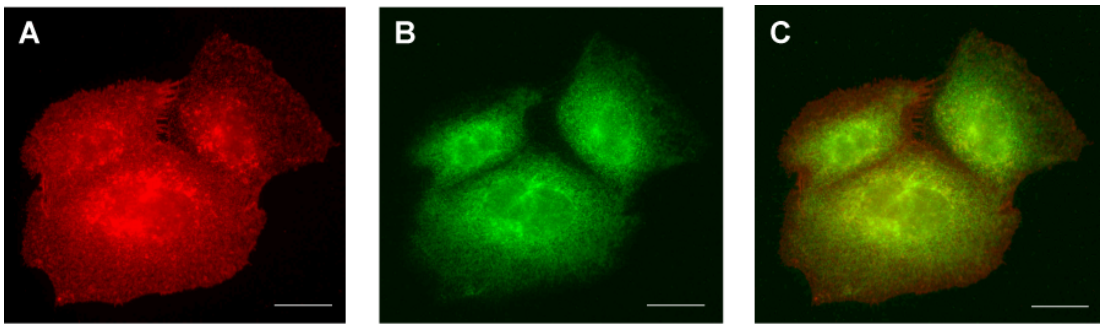

Figure 21: Overexpressed $CD36_{FLAG}$ is found in two differentially localized pools in MDCK cells.
Wildtype MDCK cells were infected with CD36FLAG adenovirus and subsequently stained using a ms-α-CD36 antibody (A) or a rb-α-FLAG antibody (B). Two differently localized pools of CD36FLAG were detected within the same cell, depending on the antibody. The ms-α-CD36 antibody shows a signal for CD36FLAG located in the plasma membrane (A) whereas the rb-α-FLAG antibody detects CD36FLAG in the cytoplasm (B). An overlay of both pictures confirms the different localization (C). Pictures from a representative sample are shown. Dimension bars are 20 µm.

5.4.2 FATP4 is located at the endoplasmic reticulum

To analyze the intracellular expression pattern of FATP4, stably overexpressing retroviral FATP4 MDCK cells as well as FATP4 adenovirus infected wildtype MDCK cells were used.

After staining with an α-FATP4 antibody all samples showed a typical network like structure surrounding the cellular nucleus (Figure 22). This pattern is known to be characteristic for proteins localized to the endoplasmic reticulum and is in accordance with former experimental data from our group (Krammer *et al.*, 2011) (Milger *et al.*, 2006) (Digel *et al.*, 2011). FATP4 localization was the same for retroviral infected, stable overexpressing as well as adenoviral infected, transiently overexpressing MDCK cells.

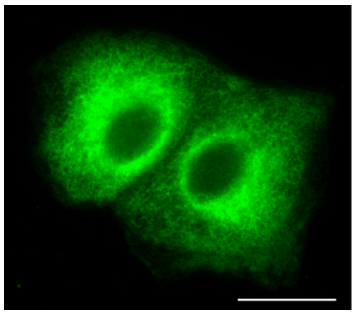

Figure 22: FATP4 localizes to the ER when overexpressed in MDCK cells.
Samples were stained using a rb-α-FATP4 antibody and analyzed by fluorescence microscopy. FATP4 MDCK cells display a characteristic network like structure, typical for proteins localized to the endoplasmic reticulum.
A picture from a representative sample is shown. The dimension bar is 20 µm.

5.4.3 Co-expression of CD36 and FATP4 does not change either protein localization

Stable FATP4 MDCK cells were infected with $CD36_{FLAG}$ adenovirus in order to analyze the localization of each protein when co-expressed. For detection of $CD36_{FLAG}$ protein the ms-α-CD36 antibody was chosen, which before had specifically detected plasma membrane localized CD36.

Immunofluorescence analysis showed that co-expression of CD36 and FATP4 did not change the localization of either protein (Figure 23). FATP4 remained to show a strong signal within the endoplasmic reticulum (Figure 23 A) whereas $CD36_{FLAG}$ was detected at the plasma membrane (Figure 23 B). An overlay of the single pictures confirmed a clearly distinct localization of both proteins within the same cell (Figure 23 C).

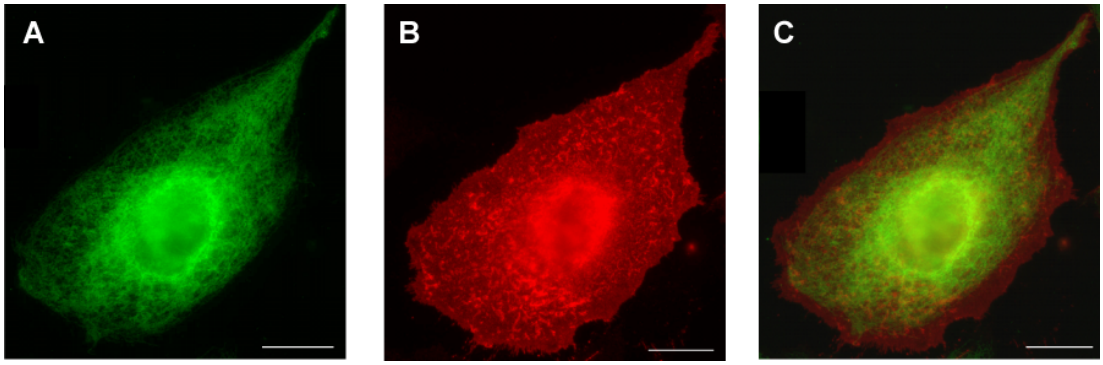

Figure 23: Co-expression of CD36 and FATP4 does not change the localization of either protein. Combined overexpression of CD36 and FATP4 in MDCK cells was achieved by infection of a stably overexpressing FATP4 cell line with $CD36_{FLAG}$ adenovirus. Samples were stained by incubation with a rb-α-FATP4 antibody (FATP4, green) and a ms-α-CD36 antibody ($CD36_{FLAG}$, red).
A) FATP4 protein is found in the network like structures of the endoplasmic reticulum.
B) CD36 localizes to the plasma membrane.
Overlay of the single pictures confirms the distinct localization of the investigated proteins.
Pictures from representative samples are shown. Dimension bars are 20 µm.

5.4.4 ACSL1 is expressed on mitochondria and does not alter the localization of CD36 or FATP4

Stable $ACSL1_{FLAG}$ MDCK were analyzed by immunofluorescence before and after infection with $CD36_{FLAG}$ and FATP4 adenovirus. Overexpressed ACSL1 protein was found on worm like structures in all investigated samples, typical for a localization on mitochondria. This observation is in accordance with previous results from our group, showing a co-localization of $ACSL1_{FLAG}$ with a mitochondrial marker (Milger *et al.*, 2006) (Zhan *et al.*, 2012).

Additional overexpression of either CD36 or FATP4 protein did not change the distribution pattern of $ACSL1_{FLAG}$ within the analyzed cells (Figure 24 A, D). Analysis of CD36 and FATP4 proteins in the respective samples also displayed no alterations in localization: CD36 was expressed at the plasma membrane (Figure 24 B) whereas FATP4 was still found on the endoplasmic reticulum (Figure 24 E). As overexpressed $CD36_{FLAG}$ and $ACSL1_{FLAG}$ both possessed a FLAG-tag, co-staining of the two proteins occured (Figure 24 A). Due to the lack of an ACSL1 antibody for immunofluorescence this drawback could not be avoided. An overlay of the single pictures of ACSL1 and CD36 or FATP4 confirmed a clearly distinct localization for ACSL1 and CD36 (Figure 24 C) as well as for ACSL1 and FATP4 (Figure 24 F) within the same cell.

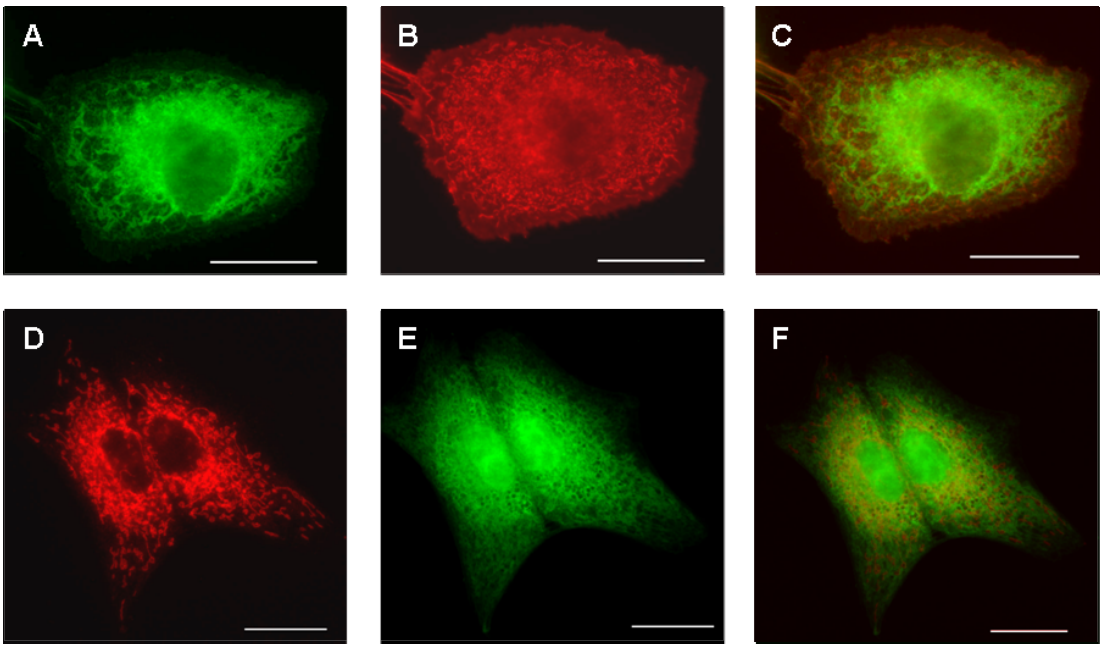

Figure 24: Co-expression of ACSL1 with CD36 or FATP4 has no influence on intracellular protein localization.
Stable $ACSL1_{FLAG}$ MDCK cells were either infected with $CD36_{FLAG}$ or FATP4 adenovirus in order to achieve a combined overexpression. Samples were stained by incubation with ms-α-FLAG ($ACSL1_{FLAG}$), rb-α-FLAG ($ASCL1_{FLAG}$), ms-α-CD36 ($CD36_{FLAG}$) or rb-α-FATP4 (FATP4) antibodies and anlyzed by fluorescence microscopy. Co-expression of ACSL1 and CD36 or ACSL1 and FATP4 did not influence the localization of either protein.
A) ACSL1 localizes to worm like structures representing mitochondria.
B) CD36 protein is detected in the plasma membrane.
C) ACSL1 and CD36 show a clearly distinct localization within the same cells.
D) Mitochondrial expression pattern of ACSL1 in MDCK cells co-expressing FATP4.
E) FATP4 is located on the endoplasmic reticulum.
F) Overlay of single sections shows a distinct localization for ACSL1 and FATP4 proteins.
Pictures from representative samples are shown. Dimension bars are 20 µm.

5.4.5 Cav-1 knock down does not change CD36 localization

For immunofluorescence, wildtype and Cav-1 KD MDCK cells were infected with $CD36_{FLAG}$ adenovirus to analyze the cellular localization of CD36. Successful knock down of Cav-1 was verified by a diminished number of stained cells in Cav-1 KD MDCK as compared to controls (Figure 25 A, D). CD36 protein was localized to the plasma membrane, with no obvious alterations in expression pattern in Cav-1 KD MDCK as opposed to wildtype MDCK cells (Figure 25 B, E).

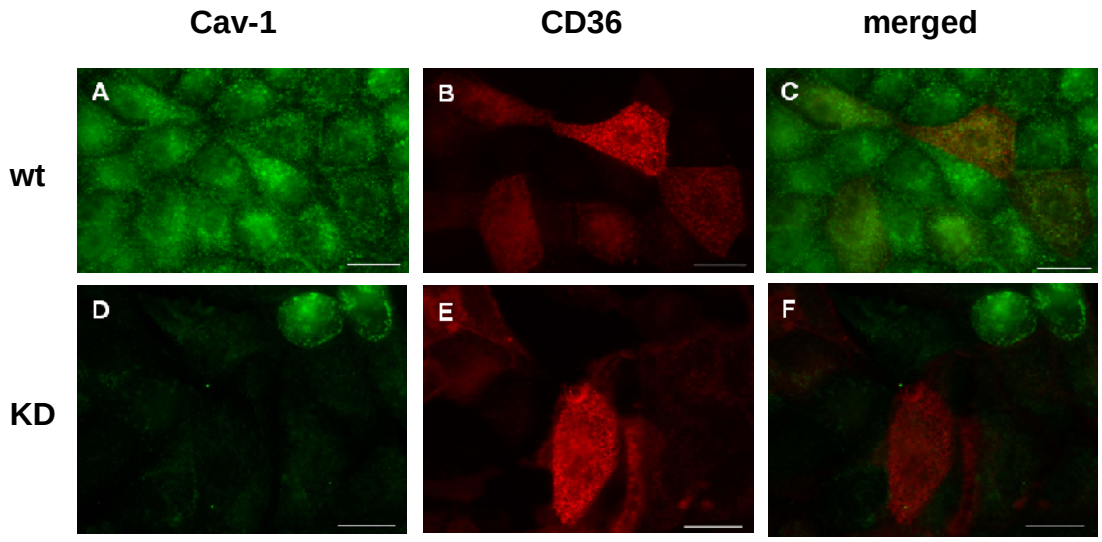

Figure 25: CD36 localization is not influenced by Cav-1 KD in MDCK cells.
Wildtype and Cav-1 KD MDCK cells were infected with $CD36_{FLAG}$ adenovirus and stained for Cav-1 (green) and CD36 (red).
A-C) Wildtype MDCK cells show Cav-1 expression together with plasma membrane localized CD36 protein.
D-F) Cav-1 KD MDCK cells show a diminished number of stained cells as compared to controls. Localization of CD36 is uneffected, with CD36 still visible at the plasma membrane.
Pictures from representative samples are shown. Dimension bars are 20 µm.

6. Discussion

Regulation of fatty acid uptake is essential for maintaining lipid homeostasis and for prevention of diseases. Two mechanism are considered for fatty acid uptake: passive diffusion across the plasma membrane and protein facilitated transport. Proteins that have been implicated in fatty acid uptake include the fatty acid translocase CD36 as well as the acyl-CoA synthetases FATP4 and ACSL1. It has been shown that all three proteins enhance fatty acid uptake upon overexpression but there is an ongoing debate about their localization and mode of action. To gain a better understanding of how each protein may contribute to cellular fatty acid uptake, this study correlated molar amounts of overexpressed CD36, FATP4 and ACSL1 to the increase in fatty acid uptake. MDCK cells allowed a generalized analysis and unbiased quantification of this process, because they are not specialized in fatty acid uptake.

6.1 FATP4 overexpression increases fatty acid uptake more than CD36 overexpression – due to higher expression levels

Various studies previously verified a role for CD36 and FATP4 in fatty acid uptake. The transmembrane glycoprotein CD36 binds long chain fatty acids (Baillie *et al.*, 1996) and mediates fatty acid uptake (Ibrahimi *et al.*, 1996). Its overexpression increased palmitate uptake in C2C12 muscle cells (Bastie *et al.*, 2004) and enhanced fatty acid transport in rat skeletal muscle (Nickerson *et al.*, 2009). These findings correlate with results from our own group that evidenced an increase in fatty acid uptake upon CD36 overexpression in COS cells (Ehehalt *et al.*, 2008) and human hepatoma cells (Krammer *et al.*, 2011).

The acyl-CoA synthetase FATP4 has also been implicated in the regulation of fatty acid uptake. Although its localization and mode of action remain a matter of discussion, FATP4 overexpression was shown to increase fatty acid uptake in Hek293 cells (Stahl *et al.*, 1999) and rat skeletal muscle (Nickerson *et al.*, 2009). Again, theses findings correlate with previous data from our group that showed an increase in fatty acid uptake upon FATP4 overexpression in COS cells (Milger *et al.*, 2006), C2C12 cells (Digel *et al.*, 2011) and 3T3-L1 adipocates (Zhan *et al.*, 2012).

Fatty acid uptake in MDCK cells was consistently increased more by FATP4 than CD36 overexpression. During this study, the comparison of oleate uptake in CD36 and FATP4 overexpressing MDCK cells confirmed a higher increase for FATP4 than CD36 cells as related to controls. It seemed conclusive that FATP4 had a higher impact on fatty acid uptake than CD36. Surprisingly, when protein levels were quantified CD36 was expressed at much lower levels than FATP4. Although FATP4 increased oleate uptake nearly twice as much as CD36, calculation of the oleate quantity taken up by 1 ng overexpressed protein revealed a more than 30 x higher efficiency for CD36. This finding reversed the assumption that FATP4 is more potent in mediating intracellular fatty acid uptake than CD36. However, it has to be taken in account that CD36 and FATP4 differ in their molecular weights (55 kDa for $CD36_{FLAG}$ versus 72 kDa for FATP4). Correspondingly, for example similar protein amounts of CD36 and FATP4 would equal about one third more CD36 than FATP4 molecules. Although the difference in oleate uptake calculated for 1 ng protein would then be reduced by a fraction CD36 still would be more considerably efficient than FATP4 in facilitating fatty acid uptake.

Yet, it had to be considered that the striking difference in protein amounts might at least partially influence the analytical outcome. If CD36 and/or FATP4 mediate fatty acid uptake by a saturable process it would be likely that at low protein amounts the increase in fatty acid uptake would be higher than at high protein amounts. With increasing protein quantities the process would come close to saturation, leading to a proportionally smaller rise in fatty acid uptake. To test this hypothesis, CD36 and FATP4 were overexpressed at comparable low protein amounts. This time, CD36 increased oleate uptake considerably more than FATP4 (27 % versus 4 %) with FATP4 overexpressing cells barely showing a difference in fatty acid uptake as compared to control cells. Comparing the effect of FATP4 on fatty acid uptake at low and high protein expression levels revealed a striking difference: at 10 ng FATP4 protein/sample oleate uptake was enhanced by 44 pmol oleate/ng protein whereas at 701 ng FATP4 protein/sample the increase in fatty acid uptake was 6 pmol oletae/ng protein. Again, these findings would indicate a saturable process for both, CD36 and FATP4 mediated fatty acid uptake.

When MDCK cells were infected with increasing amounts of CD36 and FATP4 fatty acid uptake was increased in correlation to rising CD36 and FATP4 protein levels. Interestingly, expression levels of FATP4 could be easily varied within a broad range whereas CD36 expression rates were limited to low concentrations of several ng per 12-well and sample. Higher dilutions of adenovirus used for infection allowed for the expression of very small protein quantities which no longer effected oleate uptake whereas high amounts of adenovirus killed the infected cells.

As protein overexpression was achieved by adenoviral infection in both cases it seems unlikely that methodical restrictions might be the cause that CD36 and FATP4 proteins were expressed at such different levels. Even if adenoviral titres would have been much higher for FATP4 than CD36 (which was not indicated by immunfluorescence experiments) they could not have accounted for such a big difference in expression levels. The best explanation at this point seems that cells tolerated FATP4 overexpression better and over a broader range than CD36 overexpression. The reasons for this remain speculative but spatial restriction could come in mind. As shown before, we suggested a model that places CD36 at the plasma membrane for mediating fatty acid transport. The plasma membrane is limited in space and might therefore prevent high amounts of CD36 overexpression, thereby limiting the expression rates of functionally active CD36 protein. A distinct half-life of both proteins might also contribute to the observed differences in protein quantities but was not tested in our model.

6.2 Cav-1 does not influence CD36 mediated fatty acid uptake

Cav-1 is a membrane protein that contributes to the formation of cell membrane invaginations (caveolae) that serve as signaling platforms. It was suggested that Cav-1 is involved in fatty acid uptake via its lipid binding site (Trigatti *et al.*, 1999) in accordance with its high expression rate in adipocytes. The role of Cav-1 in CD36 facilitated fatty acid transport is still a matter of debate as there are conflicting opinions stating or denying an interaction of CD36 and Cav-1. Evidence for a regulation of CD36 function in fatty acid uptake by Cav-1 was obtained from experiments with Cav-1 knock out mouse embryonic fibroblasts. In wildtype cells, CD36 was localized intracellularly and at the plasma membrane, whereas in Cav-1 knock out cells the surface expression of CD36 was abolished. The altered

localization of CD36 resulted in decreased fatty acid uptake, indicating that Cav-1 is needed for proper plasma membrane localization and function of CD36 (Ring *et al.*, 2006). Controversially, a former study conducted in CHO cells and C32 cells stated that CD36 was localized to the plasma membrane but not found in caveolae (Zeng *et al.*, 2003). Another group overexpressed various amounts of Cav-1 in Hek293 cells and concluded that fatty acid transport was modulated by Cav-1. As results were obtained in absence of CD36, it was suggested that Cav-1 mediated fatty acid transport occurred independent from CD36 expression (Meshulam *et al.*, 2006). Controversially, in chinese hamster ovary cells CD36 was expressed in detergent-resistant membranes together with Cav-1 but failed to enhance oleate uptake independent from protein expression levels (Eyre *et al.*, 2008).

In this study, a knock down of Cav-1 in MDCK cells was performed to shed some light on a potential interaction of CD36 and Cav-1 in fatty acid uptake. Residual protein levels ranged from 10 - 15 %, confirming an efficient and stable reduction in protein quantities. In our model system, Cav-1 knock down did not change the CD36 localization at the plasma membrane of wildtype and Cav-1 KD cells. A slight increase in fatty acid uptake was observed in Cav-1 KD MDCK cells overexpressing CD36 as compared to CD36 overexpressing wildtype cells. The Cav-1 KD cells showed higher CD36 protein expression levels thus indicating that increase in fatty acid uptake was due to the higher protein quantity.

Contradictory to results obtained by other groups, we could not confirm a regulation of CD36 by Cav-1 expression with reference to localization or function in fatty acid uptake. Previous studies had stated that Cav-1 knock down impaired CD36 mediated fatty acid transport, however this was not the case in Cav-1 KD cells overexpressing adenoviral CD36. Based on the observation that CD36 protein expression was slightly enhanced in Cav-1 KD cells, it could be speculated that knock down of Cav-1 facilitates adenoviral infection thereby increasing CD36 protein expression levels. In conclusion, Cav-1 knock down did neither change the localisation nor the functions of CD36 in fatty acid uptake in MDCK cells. As reviewed by Glatz *et al.* (Glatz *et al.*, 2010), controversial results for the interaction of CD36 and Cav-1 might result from tissue- or cell type-specific differences in CD36 function.

6.3 CD36 and FATP4 are differentially localized and enhance fatty acid uptake by distinct mechanisms

Different models have been suggested for enhancing fatty acid transport, involving intracellular as well as plasma membrane localized proteins. CD36 has been described as a plasma membrane glycoprotein (reviewed by (Silverstein and Febbraio, 2009)) that can be translocated from intracellular sites to the PM where it enhances FA uptake (Bonen *et al.*, 2000).

During this study, the cellular localisation of overexpressed $CD36_{FLAG}$ was analyzed by immunofluorescence. Two different antibodies were used, one targeting the CD36 protein whereas the second antibody bound to the C-terminal FLAG-tag. A plasma membrane localisation was confirmed for CD36 but interestingly the two antibodies detected different pool of $CD36_{FLAG}$ protein within the same cell. The α-CD36 antibody stained CD36 in the plasma membrane whereas the α-FLAG antibody showed an intracellular signal.

The phenomenon of two diverse antibodies targeting the same protein but detecting differently localized pools has been detected before, such as for Cav-1 (Luetterforst *et al.*, 1999). A possible explanation might be that antibody accessibility could be blocked depending on the protein localization. Furthermore, glycosylation is likely to be involved in trafficking of CD36 to the plasma membrane (Hoosdally *et al.*, 2009) and might influence proper antibody binding.. Accordingly, inappropriately glycosylated CD36 would be found at a cytoplasmic localization and could only be recognized by an α-FLAG antibody. However, no CD36 was detected in the endoplasmic reticulum

We assume, that only plasma membrane localized CD36 is functionally active in mediating fatty acid uptake. This is in accordance with other studies that verified a plasma membrane localization of CD36 in combination with increased fatty acid uptake. Exemplarily, plasma membrane localization of CD36 was required for enhancing oleate uptake in rat hepatoma cells (Eyre *et al.*, 2007) and insulin mediated translocation of CD36 from an intracellular localization to the sarcolemma of cardiac myocytes increased fatty acid uptake (Luiken *et al.*, 2002). CD36 can be inhibited by treatment with sulfo-*N*-succinimidyl oleate (SSO), leading to decreased fatty acid uptake in adipocates (Pohl *et al.*, 2005). As SSO is not membrane permeable, only plasma membrane localized CD36 is blocked, indicating that CD36 facilitates fatty acid uptake directly at the plasma membrane. It is therefore likely,

that the effect of CD36 on oleate uptake has rather been underestimated in this study as protein quantification by western blotting did not differentiate between intracellular and plasma membrane localized CD36. A reliable quantification of plasma membrane localized CD36 alone would require a subcellular fractionation, with subsequent western blotting.

In the case of FATP4, different localizations and functions are discussed. On the one hand, FATP4 has been described as fatty acid transport protein which is localized in the plasma membrane (Stahl *et al.*, 2001; Doege and Stahl, 2006) but controversial studies indicated an intracellular localization at the endoplasmic reticulum (Jia *et al.*, 2007; Lobo *et al.*, 2007). This would imply an indirect effect for FATP4 on fatty acid uptake, mediated by its enzymatic activity.

During this study, we have consistently detected overexpressed FATP4 at the endoplasmic reticulum of MDCK cells. This finding is in accordance with previous observations from our group that equally showed FATP4 localized to the endoplasmic reticulum of MDCK cells (Milger *et al.*, 2006). It seems reasonable to conclude, that in our model system FATP4 is located intracellularly at the endoplasmic reticulum and enhances fatty acid uptake indirectly by its enzymatic activity. Free fatty acids are metabolically trapped by esterification with coenzyme A, causing a concentration gradient of extra- to intracellular free fatty acids that drives fatty acid uptake.

The majority of fatty acid uptake assays in this study was performed by incubation of the respective samples with radioactive oleate for 3 h. After this time, in addition to the overexpressed proteins also signaling processes, transcriptional regulation and energy storage in lipid droplets influence fatty acid uptake. This situation probably mirrors metabolic conditions better than short term oleate but might also complicate the evaluation of CD36 and FATP4 effect on fatty acid transport. Additionally, proteins might facilitated fatty acid uptake differently at different time points.

Hence, experiments with an incubation time of 5 min were performed in MDCK cells that overexpressed increasing amounts of CD36 and FATP4 protein. In accordance with oleate uptake measured after 3 h fatty acid uptake increased with rising amounts of FATP4 protein. CD36 overexpressing MDCK cells showed the similar tendency but effects were very small, probably due to the overall low increase of fatty acid uptake.

In summary, CD36 and FATP4 are differentially localized and enhance fatty acid uptake by different mechanisms: CD36 is located in the plasma membrane where it enhances fatty acid transport whereas FATP4 is localized at the endoplasmic reticulum and metabolically traps intracellular fatty acids by esterification with coenzyme A. CD36 and FATP4 mediated oleate uptake plays a role in initial transport as well as in long-term uptake.

6.4 Transport and metabolic trapping act synergistically to increase fatty acid uptake

After assigning different localizations and modes of action to CD36 and FATP4 we wondered whether these proteins might act in cooperation for enhancing fatty acid uptake. One model for fatty acid uptake is the vectorial acylation hypothesis that proposes a cooperation of fatty acid transport across the plasma membrane with subsequent activation (Black and DiRusso, 2003).

This model could nicely be applied to our system, with CD36 acting as transport protein and FATP4 and ACSL1 catalyzing fatty acid activation. In our system, fatty acid transport and activation would be only functionally coupled whereas vectorial acylation is often associated with additional spatial coupling (Zou *et al.*, 2003; Doege and Stahl, 2006).

Combined overexpression of CD36 and FATP4 did not change either protein localization , suggesting that also the functional mechanisms would be unaltered. Co-expression of CD36 and FATP4 increased oleate uptake significantly more than calculated from results obtained by single protein overexpression.

Remarkably, the respective protein quantities of CD36 and FATP4 were lower in co-expressing cells as compared to single overexpression, thus making the synergistic increase in fatty acid uptake even more pronounced. These results strengthen our hypothesis that CD36 and FATP4 might act together in increasing fatty acid uptake. If this assumption was correct, CD36 would show a similar behaviour in combination with other acyl-CoA synthetases, such as ACSL1. Contrarily, co-expression of two enzymes acting in the same manner, like the two acyl-CoA synthetases FATP4 and ACSL1, would enhance fatty acid uptake to a smaller extent.

Co-expression experiments were performed for CD36 and ACSL1 as well as for FATP4 and ACSL1. Initial immunofluorescence analysis confirmed the intracellular localization of ACSL1 on mitochondria. As previously observed for CD36 and FATP4, neither protein localization was altered upon combined overexpression. As predicted, CD36 and ACSL1 co-expression in MDCK cells displayed a synergistic influence on increasing oleate uptake in agreement with our data from CD36 and FATP4 co-expression experiments. On the contrary, co-expression of ACSL1 and FATP4 proteins caused a smaller increase in fatty acid uptake than calculated by summation of the effects caused by single protein overexpression.

It seems evident, that oleate uptake mediated by intracellular enzymes targets only one metabolic mechanism and is limited by the transport rate of fatty acids across the plasma membrane and their intracellular accumulation. Co-expresssion of CD36 and FATP4 or ACSL1 on the other hand enhances fatty acid uptake by pushing two different mechanisms (fatty acid transport and activation).

6.5 Conclusion

Cellular fatty acid uptake can be facilitated by plasma membrane localized as well as intracellular proteins through different mechanisms. CD36 is a transmembrane glycoprotein that can be translocated from an intracellular pool to the plasma membrane where it binds fatty acids and mediates their transport across the lipid bilayer. FATP4 and ACSL1 are intracellular enzymes that activate fatty acids by esterification with coenzyme A, leading to metabolic trapping.

In MDCK cells, overexpressed CD36 was detected at the plasma membrane as well as at an intracellular localization. Based on previous data we assumed only the plasma membrane localized CD36 to be functionally active in facilitating fatty acid uptake. FATP4 and ACSL1 were expressed intracellularly at the endoplasmic reticulum (FATP4) and on mitochondria (ACSL1). Co-expression of CD36 and FATP4 or ACSL1 with CD36 or FATP4 did not alter either protein localization. Knock down of Cav-1 did neither change CD36 localization nor influence fatty acid uptake in wildtype or CD36 overexpressing cells, concluding that Cav-1 is not required for CD36 mediated fatty acid uptake in MDCK cells.

CD36 was expressed at much lower protein levels than FATP4 and limited in its maximal protein quantity, maybe due to spatial limitations at the plasma membrane.

It showed a considerably higher potency for increasing fatty acid uptake than FATP4. Low protein amounts of FATP4 led to a greater increase in oleate uptake per 1 ng protein when contrasted with high expression levels. This hints at a saturable process of protein mediated fatty acid uptake that might also apply to CD36. Increasing quantities of overexpressed CD36 or FATP4 protein correlated with enhanced oleate uptake after 3 h of oleate incubation. A similar tendency was shown in short term oleate uptake after 5 min, indicating that CD36 and FATP4 play a role in short as well as long term fatty acid uptake.

Co-expression of CD36 with either acyl-CoA synthetase, FATP4 or ACSL1, resulted in enhanced fatty acid uptake that was higher than could be expected from single protein overexpression. On the contrary, combined overexpression of FATP4 and ACSL1 resulted in only a slight increase of fatty acid uptake. It seems conclusive, that CD36 interacts with the acyl-CoA synthetases FATP4 and ACSL1 to enhance fatty acid uptake according to the concept of vectorial acylation: a fatty acid transport protein (CD36) ccoperates with an intracellular enzyme (FATP4, ACSL1) that activates fatty acids for downstream metabolism. In the case of CD36 and FATP4 or ACSL1, there would be a functional but no spatial coupling. No cooperation is possible between FATP4 and ACSL1 because they act in the same manner and target the same pathways when increasing fatty acid uptake. As both proteins are assumed to work near their maximum capacity their action is limited by the diffusion rate of fatty acids into the cell as well as by the accumulation of intracellular fatty acids. By interaction with the fatty acid transporter CD36 fatty acid uptake is not longer restricted by the diffusion rate, resulting in a much higher efficiency.

6.6 Suggestion of a model for facilitated fatty acid uptake involving CD36, FATP4 and ACSL1

We suggest a model for facilitated fatty acid uptake with CD36 localized at the plasma membrane and an intracellular localization for FATP4 (endoplasmic reticulum) and ACSL1 (mitochondria). Fatty acid uptake is mediated by two different mechanisms depending on the respective protein localization: facilitated transport across the plasma membrane by CD36 and intracelluar activation of fatty acids by FATP4 and ACSL1.

The glycoprotein CD36 is localized to the plasma membrane where it directly facilitates fatty acid transport into the cell, for example by lowering the activation energy that is necessary for a fatty acid carboxyl group to transverse through an apolar lipid bilayer (Abumrad *et al.*, 1999) or by binding of fatty acids close to the extracellular side of the plasma membrane.

For intracellular acyl-CoA synthetases, like FATP4 and ACSL1, it was suggested that they enhance fatty acid uptake indirectly by metabolic trapping (Mashek and Coleman, 2006). The activation of intracellular fatty acids is mediated by esterification with coenzyme A, consequently preventing fatty acids from diffusing back out of the cell and simultaneously decreasing the amount of free fatty acids in the cytoplasm. The gradient from extra- and intracellular free fatty acid concentration subsequently enhances fatty acid uptake (Figure 26 A).

As CD36 mediates fatty acid uptake by a different mechanism than FATP4 and ACSL1 it seems a reasonable assumption that CD36 and the acyl-CoA synthetases may act in cooperation. In this model, co-expression of CD36 with FATP4 or ACSL1 would increase fatty acid uptake more than single protein overexpression due to an increased fatty acid translocation across the plasma membrane (CD36) followed by immediate activation by acyl-CoA synthetases (FATP4, ACSL1). Co-expression of FATP4 and ACSL1 on the other hand would not significantly alter fatty acid uptake in comparison to single overexpression of either protein as both enzymes are expected to work close to their maximum capacity. Therefore, the effect of a combined protein overexpression of FATP4 and ACSL1 on fatty acid uptake would be limited by the transport rate of fatty aids into the cell. (Figure 26 B).

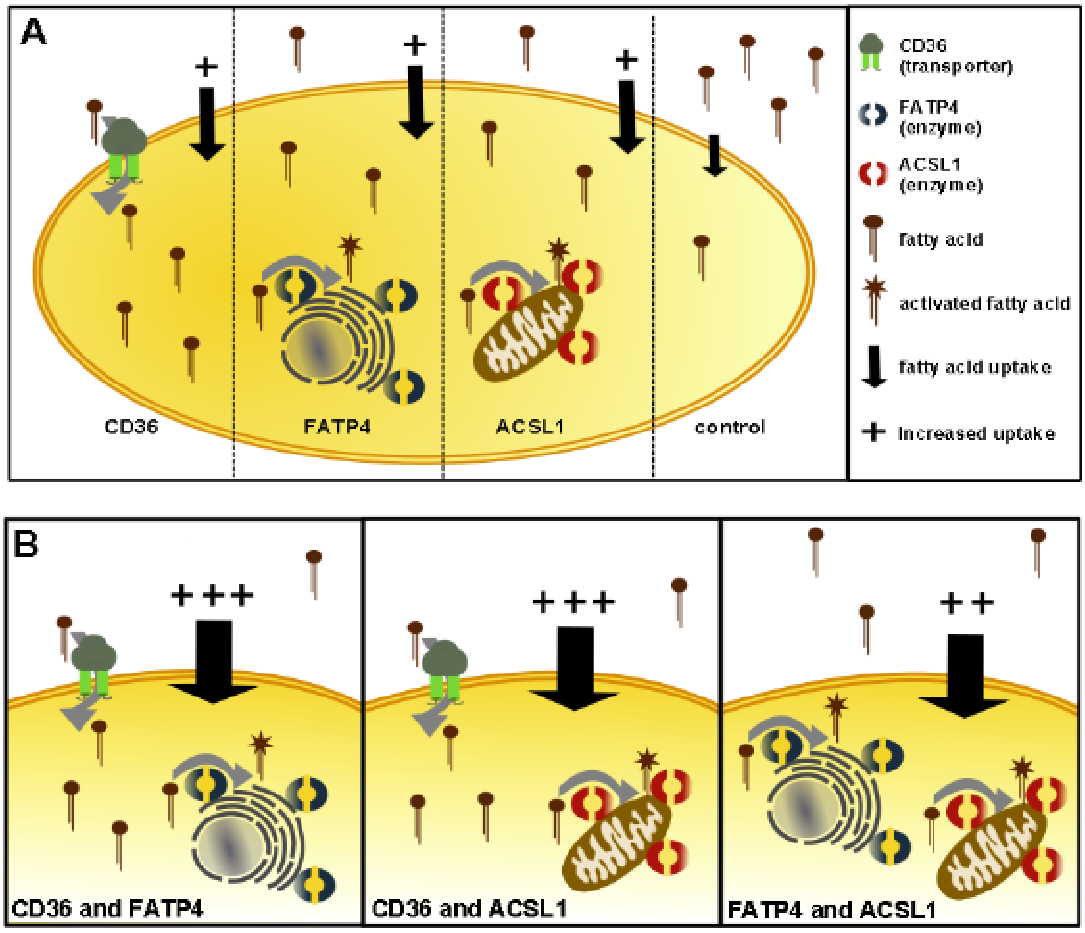

Figure 26: Model for facilitated fatty acid uptake mediated by CD36, FATP4 and ACSL1.
A) Cellular fatty acid uptake is increased by the single overexpression of either CD36 (plasma membrane), FATP4 (endoplasmic reticulum) or ACSL1 (mitochondria) as compared to control cells. CD36 directly facilitates fatty acid uptake over the plasma membrane whereas the acyl-CoA synthetases FATP4 and ACSL1 activate intracellular free fatty acids to make them available for further downstream metabolism.
B) The combined overexpression of CD36 with FATP4 or CD36 with ACSL1 enhances fatty acid uptake more than expected from summation of the single effects of both proteins. On the contrary, the overexpression of FATP4 with ACSL1 increases fatty acid uptake more than single expression of either protein but less than summation of the respective single effects.

7. References

Abumrad N, Coburn C, Ibrahimi A (1999) Membrane proteins implicated in long-chain fatty acid uptake by mammalian cells: CD36, FATP and FABPm. Biochim Biophys Acta **1441:** 4-13

Abumrad N, Harmon C, Ibrahimi A (1998) Membrane transport of long-chain fatty acids: evidence for a facilitated process. J Lipid Res **39:** 2309-2318

Abumrad NA (2005) CD36 may determine our desire for dietary fats. J Clin Invest **115:** 2965-2967

Baillie AG, Coburn CT, Abumrad NA (1996) Reversible binding of long-chain fatty acids to purified FAT, the adipose CD36 homolog. J Membr Biol **153:** 75-81

Bastie CC, Hajri T, Drover VA, Grimaldi PA, Abumrad NA (2004) CD36 in myocytes channels fatty acids to a lipase-accessible triglyceride pool that is related to cell lipid and insulin responsiveness. Diabetes **53:** 2209-2216

Bechmann LP, Gieseler RK, Sowa JP, Kahraman A, Erhard J, Wedemeyer I, Emons B, Jochum C, Feldkamp T, Gerken G, Canbay A (2010) Apoptosis is associated with CD36/fatty acid translocase upregulation in non-alcoholic steatohepatitis. Liver Int **30:** 850-859

Berg JM TJ, Stryer L. (2003) Biochemie, Ed 5. Spektrum Akademischer Verlag GmbH Heidelberg, Berlin

Black PN, DiRusso CC (2003) Transmembrane movement of exogenous long-chain fatty acids: proteins, enzymes, and vectorial esterification. Microbiol Mol Biol Rev **67:** 454-472

Bonen A, Luiken JJ, Arumugam Y, Glatz JF, Tandon NN (2000) Acute regulation of fatty acid uptake involves the cellular redistribution of fatty acid translocase. J Biol Chem **275:** 14501-14508

Bradford MM (1976) A rapid and sensitive method for the quantitation of microgram quantities of protein utilizing the principle of protein-dye binding. Anal Biochem **72:** 248-254

Brinkmann JF, Abumrad NA, Ibrahimi A, van der Vusse GJ, Glatz JF (2002) New insights into long-chain fatty acid uptake by heart muscle: a crucial role for fatty acid translocase/CD36. Biochem J **367:** 561-570

Chidlow JH, Jr., Sessa WC (2010) Caveolae, caveolins, and cavins: complex control of cellular signalling and inflammation. Cardiovasc Res **86:** 219-225

Coburn CT, Knapp FF, Jr., Febbraio M, Beets AL, Silverstein RL, Abumrad NA (2000) Defective uptake and utilization of long chain fatty acids in muscle and adipose tissues of CD36 knockout mice. J Biol Chem **275:** 32523-32529

Cohen AW, Razani B, Wang XB, Combs TP, Williams TM, Scherer PE, Lisanti MP (2003) Caveolin-1-deficient mice show insulin resistance and defective insulin receptor protein expression in adipose tissue. Am J Physiol Cell Physiol **285:** C222-235

Digel M, Staffer S, Ehehalt F, Stremmel W, Ehehalt R, Fullekrug J (2011) FATP4 contributes as an enzyme to the basal and insulin mediated fatty acid uptake of C2C12 muscle cells. Am J Physiol Endocrinol Metab **301:**E785-796

Doege H, Stahl A (2006) Protein-mediated fatty acid uptake: novel insights from in vivo models. Physiology (Bethesda) **21:** 259-268

Drover VA, Nguyen DV, Bastie CC, Darlington YF, Abumrad NA, Pessin JE, London E, Sahoo D, Phillips MC (2008) CD36 mediates both cellular uptake of very long chain fatty acids and their intestinal absorption in mice. J Biol Chem **283:** 13108-13115

Ducharme NA, Bickel PE (2008) Lipid droplets in lipogenesis and lipolysis. Endocrinology **149:** 942-949

Ehehalt R, Fullekrug J, Pohl J, Ring A, Herrmann T, Stremmel W (2006) Translocation of long chain fatty acids across the plasma membrane--lipid rafts and fatty acid transport proteins. Mol Cell Biochem **284:** 135-140

Ehehalt R, Sparla R, Kulaksiz H, Herrmann T, Fullekrug J, Stremmel W (2008) Uptake of long chain fatty acids is regulated by dynamic interaction of FAT/CD36 with cholesterol/sphingolipid enriched microdomains (lipid rafts). BMC Cell Biol **9:** 45

Ellis JM, Li LO, Wu PC, Koves TR, Ilkayeva O, Stevens RD, Watkins SM, Muoio DM, Coleman RA (2010) Adipose acyl-CoA synthetase-1 directs fatty acids toward beta-oxidation and is required for cold thermogenesis. Cell Metab **12:** 53-64

Eyre NS, Cleland LG, Mayrhofer G (2008) FAT/CD36 expression alone is insufficient to enhance cellular uptake of oleate. Biochem Biophys Res Commun **370:** 404-409

Eyre NS, Cleland LG, Tandon NN, Mayrhofer G (2007) Importance of the carboxyl terminus of FAT/CD36 for plasma membrane localization and function in long-chain fatty acid uptake. J Lipid Res **48:** 528-542

Forneris F, Mattevi A (2008) Enzymes without borders: mobilizing substrates, delivering products. Science **321:** 213-216

Fullekrug J, Ehehalt R, Poppelreuther M (2012) Outlook: membrane junctions enable the metabolic trapping of fatty acids by intracellular acyl-CoA synthetases. Front Physiol **3:** 401

Funk CD (2001) Prostaglandins and leukotrienes: advances in eicosanoid biology. Science **294:** 1871-1875

Gimeno RE (2007) Fatty acid transport proteins. Curr Opin Lipidol **18:** 271-276

Glatz JF, Luiken JJ, Bonen A (2010) Membrane fatty acid transporters as regulators of lipid metabolism: implications for metabolic disease. Physiol Rev **90:** 367-417

Hamilton JA, Guo W, Kamp F (2002) Mechanism of cellular uptake of long-chain fatty acids: Do we need cellular proteins? Mol Cell Biochem **239:** 17-23

He TC, Zhou S, da Costa LT, Yu J, Kinzler KW, Vogelstein B (1998) A simplified system for generating recombinant adenoviruses. Proc Natl Acad Sci U S A **95:** 2509-2514

Hoosdally SJ, Andress EJ, Wooding C, Martin CA, Linton KJ (2009) The Human Scavenger Receptor CD36: glycosylation status and its role in trafficking and function. J Biol Chem **284:** 16277-16288

Ibrahimi A, Sfeir Z, Magharaie H, Amri EZ, Grimaldi P, Abumrad NA (1996) Expression of the CD36 homolog (FAT) in fibroblast cells: effects on fatty acid transport. Proc Natl Acad Sci U S A **93:** 2646-2651

Inoue H, Nojima H, Okayama H (1990) High efficiency transformation of Escherichia coli with plasmids. Gene **96:** 23-28

Jia Z, Moulson CL, Pei Z, Miner JH, Watkins PA (2007) Fatty acid transport protein 4 is the principal very long chain fatty acyl-CoA synthetase in skin fibroblasts. J Biol Chem **282:** 20573-20583

Kampf JP, Kleinfeld AM (2007) Is membrane transport of FFA mediated by lipid, protein, or both? An unknown protein mediates free fatty acid transport across the adipocyte plasma membrane. Physiology (Bethesda) **22:** 7-14

Koonen DP, Jacobs RL, Febbraio M, Young ME, Soltys CL, Ong H, Vance DE, Dyck JR (2007) Increased hepatic CD36 expression contributes to dyslipidemia associated with diet-induced obesity. Diabetes **56:** 2863-2871

Krammer J, Digel M, Ehehalt F, Stremmel W, Fullekrug J, Ehehalt R (2011) Overexpression of CD36 and Acyl-CoA Synthetases FATP2, FATP4 and ACSL1 Increases Fatty Acid Uptake in Human Hepatoma Cells. Int J Med Sci **8:** 599-614

Li LO, Ellis JM, Paich HA, Wang S, Gong N, Altshuller G, Thresher RJ, Koves TR, Watkins SM, Muoio DM, Cline GW, Shulman GI, Coleman RA (2009) Liver-specific loss of long chain acyl-CoA synthetase-1 decreases triacylglycerol synthesis and beta-oxidation and alters phospholipid fatty acid composition. J Biol Chem **284:** 27816-27826

Li LO, Klett EL, Coleman RA (2010) Acyl-CoA synthesis, lipid metabolism and lipotoxicity. Biochim Biophys Acta **1801:** 246-251

Li LO, Mashek DG, An J, Doughman SD, Newgard CB, Coleman RA (2006) Overexpression of rat long chain acyl-coa synthetase 1 alters fatty acid metabolism in rat primary hepatocytes. J Biol Chem **281:** 37246-37255

Lingwood D, Simons K (2010) Lipid rafts as a membrane-organizing principle. Science **327:** 46-50

Liu P, Rudick M, Anderson RG (2002) Multiple functions of caveolin-1. J Biol Chem **277:** 41295-41298

Lobo S, Wiczer BM, Smith AJ, Hall AM, Bernlohr DA (2007) Fatty acid metabolism in adipocytes: functional analysis of fatty acid transport proteins 1 and 4. J Lipid Res **48:** 609-620

Love-Gregory L, Sherva R, Sun L, Wasson J, Schappe T, Doria A, Rao DC, Hunt SC, Klein S, Neuman RJ, Permutt MA, Abumrad NA (2008) Variants in the CD36 gene associate with the metabolic syndrome and high-density lipoprotein cholesterol. Hum Mol Genet **17:** 1695-1704

Luetterforst R, Stang E, Zorzi N, Carozzi A, Way M, Parton RG (1999) Molecular characterization of caveolin association with the Golgi complex: identification of a cis-Golgi targeting domain in the caveolin molecule. J Cell Biol **145:** 1443-1459

Luiken JJ, Koonen DP, Willems J, Zorzano A, Becker C, Fischer Y, Tandon NN, Van Der Vusse GJ, Bonen A, Glatz JF (2002) Insulin stimulates long-chain fatty acid utilization by rat cardiac myocytes through cellular redistribution of FAT/CD36. Diabetes **51:** 3113-3119

Luo J, Deng ZL, Luo X, Tang N, Song WX, Chen J, Sharff KA, Luu HH, Haydon RC, Kinzler KW, Vogelstein B, He TC (2007) A protocol for rapid generation of recombinant adenoviruses using the AdEasy system. Nat Protoc **2:** 1236-1247

Mashek DG, Bornfeldt KE, Coleman RA, Berger J, Bernlohr DA, Black P, DiRusso CC, Farber SA, Guo W, Hashimoto N, Khodiyar V, Kuypers FA, Maltais LJ, Nebert DW, Renieri A, Schaffer JE, Stahl A, Watkins PA, Vasiliou V, Yamamoto TT (2004) Revised nomenclature for the mammalian long-chain acyl-CoA synthetase gene family. J Lipid Res **45:** 1958-1961

Mashek DG, Coleman RA (2006) Cellular fatty acid uptake: the contribution of metabolism. Curr Opin Lipidol **17:** 274-278

Meshulam T, Simard JR, Wharton J, Hamilton JA, Pilch PF (2006) Role of caveolin-1 and cholesterol in transmembrane fatty acid movement. Biochemistry **45:** 2882-2893

Milger K, Herrmann T, Becker C, Gotthardt D, Zickwolf J, Ehehalt R, Watkins PA, Stremmel W, Fullekrug J (2006) Cellular uptake of fatty acids driven by the ER-localized acyl-CoA synthetase FATP4. J Cell Sci **119:** 4678-4688

Mullis K, Faloona F, Scharf S, Saiki R, Horn G, Erlich H (1986) Specific enzymatic amplification of DNA in vitro: the polymerase chain reaction. Cold Spring Harb Symp Quant Biol **51 Pt 1:** 263-273

Nickerson JG, Alkhateeb H, Benton CR, Lally J, Nickerson J, Han XX, Wilson MH, Jain SS, Snook LA, Glatz JF, Chabowski A, Luiken JJ, Bonen A (2009) Greater transport efficiencies of the membrane fatty acid transporters FAT/CD36 and FATP4 compared with FABPpm and FATP1 and differential effects on fatty acid esterification and oxidation in rat skeletal muscle. J Biol Chem **284:** 16522-16530

Pohl J, Ring A, Korkmaz U, Ehehalt R, Stremmel W (2005) FAT/CD36-mediated long-chain fatty acid uptake in adipocytes requires plasma membrane rafts. Mol Biol Cell **16:** 24-31

Razani B, Combs TP, Wang XB, Frank PG, Park DS, Russell RG, Li M, Tang B, Jelicks LA, Scherer PE, Lisanti MP (2002) Caveolin-1-deficient mice are lean, resistant to diet-induced obesity, and show hypertriglyceridemia with adipocyte abnormalities. J Biol Chem **277:** 8635-8647

Ring A, Le Lay S, Pohl J, Verkade P, Stremmel W (2006) Caveolin-1 is required for fatty acid translocase (FAT/CD36) localization and function at the plasma membrane of mouse embryonic fibroblasts. Biochim Biophys Acta **1761:** 416-423

Schaffer JE, Lodish HF (1994) Expression cloning and characterization of a novel adipocyte long chain fatty acid transport protein. Cell **79:** 427-436

Schuck S, Manninen A, Honsho M, Fullekrug J, Simons K (2004) Generation of single and double knockdowns in polarized epithelial cells by retrovirus-mediated RNA interference. Proc Natl Acad Sci U S A **101:** 4912-4917

Silverstein RL, Febbraio M (2009) CD36, a scavenger receptor involved in immunity, metabolism, angiogenesis, and behavior. Sci Signal **2:** re3

Soupene E, Kuypers FA (2008) Mammalian long-chain acyl-CoA synthetases. Exp Biol Med (Maywood) **233:** 507-521

Stahl A, Gimeno RE, Tartaglia LA, Lodish HF (2001) Fatty acid transport proteins: a current view of a growing family. Trends Endocrinol Metab **12:** 266-273

Stahl A, Hirsch DJ, Gimeno RE, Punreddy S, Ge P, Watson N, Patel S, Kotler M, Raimondi A, Tartaglia LA, Lodish HF (1999) Identification of the major intestinal fatty acid transport protein. Mol Cell **4:** 299-308

Stremmel W, Strohmeyer G, Berk PD (1986) Hepatocellular uptake of oleate is energy dependent, sodium linked, and inhibited by an antibody to a hepatocyte plasma membrane fatty acid binding protein. Proc Natl Acad Sci U S A **83:** 3584-3588

Su X, Abumrad NA (2009) Cellular fatty acid uptake: a pathway under construction. Trends Endocrinol Metab **20:** 72-77

Suzuki H, Kawarabayasi Y, Kondo J, Abe T, Nishikawa K, Kimura S, Hashimoto T, Yamamoto T (1990) Structure and regulation of rat long-chain acyl-CoA synthetase. J Biol Chem **265:** 8681-8685

Thorne RF, Ralston KJ, de Bock CE, Mhaidat NM, Zhang XD, Boyd AW, Burns GF (2010) Palmitoylation of CD36/FAT regulates the rate of its post-transcriptional processing in the endoplasmic reticulum. Biochim Biophys Acta **1803:** 1298-1307

Tran TT, Poirier H, Clement L, Nassir F, Pelsers MM, Petit V, Degrace P, Monnot MC, Glatz JF, Abumrad NA, Besnard P, Niot I (2011) Luminal lipid regulates CD36 levels and downstream signaling to stimulate chylomicron synthesis. J Biol Chem **286:**25201-25210

Trigatti BL, Anderson RG, Gerber GE (1999) Identification of caveolin-1 as a fatty acid binding protein. Biochem Biophys Res Commun **255:** 34-39

van Meer G, Voelker DR, Feigenson GW (2008) Membrane lipids: where they are and how they behave. Nat Rev Mol Cell Biol **9:** 112-124

Watkins PA (2008) Very-long-chain acyl-CoA synthetases. J Biol Chem **283:** 1773-1777

Wong JM, de Souza R, Kendall CW, Emam A, Jenkins DJ (2006) Colonic health: fermentation and short chain fatty acids. J Clin Gastroenterol **40:** 235-243

Zeng Y, Tao N, Chung KN, Heuser JE, Lublin DM (2003) Endocytosis of oxidized low density lipoprotein through scavenger receptor CD36 utilizes a lipid raft pathway that does not require caveolin-1. J Biol Chem **278:** 45931-45936

Zhan T, Poppelreuther M, Ehehalt R, Fullekrug J (2012) Overexpressed FATP1, ACSVL4/FATP4 and ACSL1 Increase the Cellular Fatty Acid Uptake of 3T3-L1 Adipocytes but Are Localized on Intracellular Membranes. PLoS One **7:** e45087

Zou Z, Tong F, Faergeman NJ, Borsting C, Black PN, DiRusso CC (2003) Vectorial acylation in Saccharomyces cerevisiae. Fat1p and fatty acyl-CoA synthetase are interacting components of a fatty acid import complex. J Biol Chem **278:** 16414-16422

8. Appendix

8.1 List of Figures

Figure 1: Model of fatty acid uptake. 8
Figure 2: Structure of CD36 10
Figure 3: Activation of fatty acids by esterification with coenzyme A. 13
Figure 4: Mechanism of fatty acid activation by the bacterial acyl-CoA synthetase FACS. 14
Figure 5: Quantification of western blot signals by using ImageJ. 43
Figure 6: Quantification of FATP4 protein amounts by western blotting. 46
Figure 7: Quantification of Cav-1 knock down in MDCK cells. 59
Figure 8: Variation of free oleate concentrations does not significantly influence CD36 mediated fatty acid uptake. 60
Figure 9: Influence of different oleate concentrations on CD36 mediated fatty acid uptake. 61
Figure 10: Quantification of purified $_{FLAG}$ FATP4 protein. 63
Figure 11: Titration of FATP4 protein levels and its influence on oleate uptake. 64
Figure 12: Oleate uptake is enhanced in CD36 overexpressing cells in correlation to the CD36 protein amount. 65
Figure 13: Expression of similar CD36 and FATP4 protein amounts and their influence on oleate uptake. 67
Figure 14: Quantitative comparison of increases in fatty acid uptake as mediated by CD36 or FATP4 protein overexpression. 68
Figure 15: Combined overexpression of CD36 and FATP4 proteins significantly enhances fatty acid uptake. 70
Figure 16: Synergistic effect of ACSL1 and CD36 co-expression on oleate uptake. 72
Figure 17: ACSL1 and FATP4 co-expression does not considerably increase oleate uptake. 73
Figure 18: Quantification of Cav-1 knock down in MDCK cells used for oleate uptake assays. 75
Figure 19: Cav-1 knock down has no effect on CD36 mediated oleate uptake. 76
Figure 20: Overexpression of CD36 and FATP4 increases short term oleate uptake. 78

Figure 21: Overexpressed $CD36_{FLAG}$ is found in two differentially localized pools in MDCK cells. 79
Figure 22: FATP4 localizes to the ER when overexpressed in MDCK cells. 80
Figure 23: Co-expression of CD36 and FATP4 does not change the localization of either protein. 81
Figure 24: Co-expression of ACSL1 with CD36 or FATP4 has no influence on intracellular protein localization. 82
Figure 25: CD36 localization is not influenced by Cav-1 KD in MDCK cells. 83
Figure 26: Model for facilitated fatty acid uptake mediated by CD36, FATP4 and ACSL1. 94

8.2 List of Tables

Table 1: Molecular biology equipment used in this study. 19
Table 2: Protein biochemistry equipment used in this study. 20
Table 3: Radioactive work equipment used in this study. 20
Table 4: Cell culture equipment used in this study. 20
Table 5: Molecular biology chemicals used in this study. 21
Table 6: Protein biochemistry chemicals used in this study. 21
Table 7: Radioactive work chemicals used in this study. 21
Table 8: Cell culture chemicals used in this study. 22
Table 9: Kits used in this study. 22
Table 10: Molecular weight standards used in this study. 23
Table 11: Antibodies used in this study. 23
Table 12: Enzymes used in this study. 24
Table 13: Oligonucleotides used in this study. 24
Table 14: Plasmids for cloning used in this study. 25
Table 15: Retroviral plasmids used in this study. 25
Table 16: Adenoviral plasmids used in this study. 26
Table 17: Media used in this study. 26
Table 18: Buffers used in this study. 27
Table 19: Cells used in this study. 28
Table 20: Viruses used in this study. 29
Table 21: Bacteria used in this study. 30
Table 22: Software used in this study. 30
Table 23: Standard conditions for performing a preparative PCR. 35
Table 24: Reaction mixtures and conditions for standard ligation procedures. 36
Table 25: Composition of stacking and resolving gels as used in SDS-PAGE. 40
Table 26: Composition of a labeling mix as used in radioactive uptake assays. 47
Table 27: Culture conditions for immortalized, adherently growing cell lines. 49
Table 28: Master mix preparation for Lipofectamine transfection. 50
Table 29: Master mix preparation for $CaPO_4$ transfection. 52
Table 30: Linearization of adenoviral plasmid DNA. 53
Table 31: Lipofection of Hek293 packaging cells using adenoviral plasmid DNA. 54

8.3 Publication and Oral Presentations

Publication

Schneider H., Braun A., Füllekrug J., Stremmel W., Ehehalt R.: Lipid Based Therapy for Ulcerative Colitis - Modulation of Intestinal Mucus Membrane Phospholipids as a Tool to Influence Inflammation.
International Journal of Molecular Sciences. 2010; 11(10):4149-4164.

Oral Presentations

01/2012
”Fatty acid transport in polarized cells – role of CD36 and FATP4“
Dijon, 21st Lipid binding protein (LBP) workshop

03/2012
“Role of CD36 and FATP4 in fatty acid transport of polarized cells”
Lohrbach, DGVS Arbeitsgruppentreffen – Transport und Barriere

09/2012
”Regulatory effects of CD36, FATP4 and ACSL1 on fatty acid uptake – a quantitative analysis”
Hamburg, Viszeralmedizin 2012 – DGVS Jahrestagung

9. Affirmation

I hereby declare that my dissertation "*Quantitative analysis of proteins facilitating fatty acid uptake: CD36, Caveolin-1, FATP4 and ACSL1*" has been written independently and with no other sources and aids than quoted. I clearly marked any ideas borrowed from other sources as not my own and documented their sources.
I furthermore declare that this dissertation has not been submitted in the same or any altered form to this or any other university for obtaining an equivalent degree and will not be used for such purpose in the future.

Heidelberg, the 6th November 2012

10. Acknowledgements

This study would not have been possible without the contribution of several people whom I would like to thank.

First of all, I want to thank my supervisor Prof. Dr. Robert Ehehalt for his continuous support over the last years while giving me the freedom to try many things on my own. Thank you also Robert for introducing me to the research field of ulcerative colitis.

Many thanks go to PD Dr. Joachim Füllekrug, my unofficial supervisor, for his help with lab work and writing – through topics 1, 2A and 2B. I learnt a lot from you!

I thank Prof. Dr. Wolfgang Stremmel for giving me the opportunity to conduct this thesis in his department. Thanks also go to Prof. Dr. Fricker for acting as first referee and to Prof. Dr. Bartenschlager and PD Dr. Seedorf for taking part in my defense as examiners.

I would also like to thank Simone Staffer for continuous support with (not only) radioactive assays and for providing a very nice working environment (not only) in our radioactive lab. Thanks also to Dr. Margarete Poppelreuther and Sabine Tuma-Kellner for helping me with the lab work.

Many thanks go to Dr. Eva-Maria Küch – thank you so much for many nice working hours, for helping and explaining and for my thesis correction. We had a great time in and outside of the lab!

Thanks also to everyone who contributed to a nice atmosphere and kept the labs in 345 alive and running: Sarah, Friedrich, Fadil, Ingrid, Jessica, Annika.....

Schlussendlich gilt mein größter Dank meiner Familie: Simon und Hannes und meinem Schwesterlein – Danke, Sarah! Mein allergrößter Dank aber gilt meinen Eltern. Mama, Papa, Goethe hat einmal gesagt “Zwei Dinge sollten Eltern ihren Kindern mitgeben: Wurzeln und Flügel.“ Ihr habt mir beides im Übermaß gegeben und noch Vieles mehr – ich danke euch sehr für euren Beitrag. Dies ist nicht nur meine Arbeit – es ist auch eure.